UNIVERSITAT POLITÈCNICA DE CATALUNYA

Photonic Devices for Next Generation Fiber-to-the-Home Access Network

Author

Guang Yong Chu

Advisor

Prof. Dr. Josep Prat

A thesis submitted in fulfillment for the
degree of Doctor of Philosophy

At the
OPTICAL COMMUNICATIONS GROUP (GCO)
Signal Theory and Communications Department (TSC)

December 2015

The work described in this thesis was performed at the Signal Theory and Communications department of the Universitat Politècnica de Catalunya / BarcelonaTech. It was supported in part by the European Comission through the FP7 ICT COCONUT Project.

Guang Yong Chu
Photonic Devices for Next Generation Fiber-to-the-Home Access Network
Subject headings: *Optical fiber communication*

Printed in Barcelona, Spain.

ISBN:

Reg:

The greatest test of courage on earth is to bear defeat without losing heart...

Abstract

It would be unaffordable if the WDM-PON technologies were directly applied for massive deployment. Hence, the potential WDM-PON is to be integrated and improved in order to adapt it for NGPON and the future 5G. The UDWDM-PON can be considered as an ultimate solution for the next-generation access network capable of providing unlimited bandwidth for each user, thanks to the coherent detection.

Plenty of scientists have believed that it is crucial to increase the operating speed and maximum reach of WDM-PON, while it has no sense if people achieve them without affordable cost.

In order to apply them cost-efficiently, the system should require colorless ONUs and bidirectional systems. It is desired that the whole system use modulators on a low bias consumption, even limit the number of amplifiers.

However, for bidirectional transmission the backscattering effects would limit the performance if we want to reuse the carrier from OLT. So, we should design a method to separate the wavelength between upstream and downstream.

The traditional UDWDM-PON uses 2 laser at ONU, in this thesis, the single-DFB based ONUs are presented with integrated devices.

What is the most plausible configuration? The photonic devices such as RSOA, DEML, FML with advanced configurations are presented in this thesis with different applications.

The thesis includes these parts: key devices for WDM-PON and the chirp parameters of these integrated photonic devices are measured, the polarization independent RSOA with different applications is also included, demonstration of dual output DEML with bidirectional coherent UDWDM-PON transmission, mitigating residual AM of DEML for phase modulation, and fast tuning for the UDWDM channel via FML are described.

Key words: Optical fiber communications, fiber to the home, passive optical networks, photonics, optical network units.

Acknowledgements

Time is like a fleeting show, tones of memories come into my mind. During the three years of my Ph.D. study, there have been frustration of failure as well as the joy of success. In this most important journey of my life, I would like to say it is the people around me that make the journey worth taking.

First of all, I would like to express my deepest gratitude towards my supervisor Prof. Dr. Josep Prat for giving me the opportunity to join his team to pursue my doctoral studies. His excellent supervision, constant guidance, valuable advice as well as his encouragement and patients throughout my doctoral research helped me accomplish this great task. His passion for science made me push harder each day and complete my work with pure dedication. I could not have imagined having a better advisor and mentor for my PhD study. If it was not Prof. Prat, I even wouldn't be here, learning, working, and fighting for the future.

Dr. Victor Polo, did his job as lab chief well during all the years, received many questions for many times and always had an open ear for all the PhD students. I still remember that, day and night, the time is spent with him on calculating and designing the mechanics for assembling the photonic devices, the high speed mini-circuit board for supporting the high speed RF line, and the stuff on controlling temperature with less wavelength drifts of integrated lasers. Besides, I also want to thank Dr. Polo for buying the lab stuff with the quickly response of *Yes, we can!*.

A special thank would be given to Dr. Ivan Cano, for his kind support during my doctoral period and the enthusiastic revision on papers. Furthermore, I would like to express my heartfelt thanks to Jeison Alejandro Tabares, Juan Camilo Velasquez who are currently doing their PhD for sharing the friendly moments with me. Many thanks to Fabio Bottoni from *Scuola Superiore Sant'Anna University-Italy*, for making an enjoyable atmosphere as well as sharing the bored Sunday at lab during his PhD visit. I would like to thank Adolfo Lerín, Xavier Escanoy, Saeed Ghasemi, and Javi Martnez for the fruitiful discussions during my PhD period, especially for the friendly memory. In particular, I am grateful to Mr. Pau Borotau Bosser for enlightening me the first glance of lab research. Also, many thanks to Joaquim Giner and Rubén Tardío López for their kind helps on circuit fabrication for high speed RF.

Here, special thanks to Prof. Christophe Kazmierski, for his clear explanations such as the phase shifter on multi-drived photonic devices, multi function on integrated chips when I was in Paris at *Alcatel-Lucent Bell Labs*. Also, I give my gratitude to Prof. Romain Brenot for his suggestions, device supports as well as constructive remarks

and revisions on papers. Prof. Helene Debregeas from *Alcatel-Lucent III-V Labs* who provides us the photonic devices, especially the high backfacet output power with EML-SOA and the excellent explanations and advices. I would like to say, without their advices and supports, it would be impossible for me to finish the main tasks in this thesis.

I want to thank the China Scholarship Council for providing me the fellowship. It would be impossible for me to dedicate myself to the research work without this support. Special thanks are given to the education office of the embassy of China in Spain for the enthusiastic supports and concern.

Last by no means the least, I would like to express my thanks to my parents and sister, who give their supports during all the years of my PhD study and my academic career development during the years before. They give me the most selfless and greatest love, no matter where I am and whatever difficulties I endure. Their smile and encouragement are always my most motivation to move on.

Contents

List of Figures

List of Tables

Abbreviations

AON	**A**ctive **O**ptical **N**etwork
APD	**A**valanche **P**hoto **D**iode
AR	**A**nti-**R**eflection
ASE	Amplified Spontaneous Emission
ASK	Amplitude Shift Keying
AWG	Arrayed Waveguide Grating
BER	Bit Error Ratio
DCF	Dispersion Compensating Fiber
DoS	Density of State
DS	Downstream
EAM	Electro-absorption Modulator
EDF	Erbium-Doped Fiber
EDFA	Erbium-Doped Fiber Amplifier
EML	Electro-absorption Modulated Laser
ER	Extinction Ratio
FBG	Fiber Bragg Grating
FEC	Forward Error Correction
FPF	Fabry Perot Filter
FSK	Frequency Shift Keying
FSR	Free Spectral Range
FWM	Four-Wave Mixing
GPON	Gigabit PON
ITU	International Telecommunication Unit

Symbols

$\Delta\nu$	laser linewith
c	speed of light
ER	modulation extintion ratio of optical signal
F	finesse of filter
G	gain of optical amplifier
$h_{e/o}$	electro-optical transfer function
I	electrical injection current
I_{dc}	DC component of injection current
I_{ff}	feed-forward component of injection current
i_{mod}	injected modulation current
k	integer
L	length of filter
n	refractive index of filter medium
$\delta\nu$	filter bandwidth
p, P	optical power
π	logical bit pattern
R	facet reflectivity
R_b	data rate
$t, \delta t$	time and timespan, respectively
τ	decay time
T_{max}	maximal transmission
T_{rtt}	round trip time
z	number of consecutive identical bits

To my parents...

Chapter 1

The rise of access network

Fiber-to-the-home (FTTH) technologies are required to enable universal communication with an improvement of capacity and distance, as well as enhanced security, scalability and other vital functionalities [1]-[3]. For implementing this, ultra dense WDM-PON (UDWDM-PON) [2], [4] has advantages of increased capacity per user, inherent optical spectrum selectivity, providing a promising option of each user one wavelength. Hence, the UDWDM-PON becomes an interesting candidate for next generation PONs recently. This chapter provides an overview about ongoing research and standardization , as well as the different architectures and components used for the access networks.

1.1 Introduction

Optical communications have evolved from being an entelechy to a reality that sustains and makes possible the information society, since Charles K. Kao [5] publicly demonstrated the posibility of transmitting via optical fibers. Nowadays, the optical fiber communication is one of the drivers to enable broadband services for the final users of networks, which will then also be able to spread over a geographic field. In fact, the concept of optical access networks is very wide, including many approaches.

1.2 State of the art

1.2.1 Active and passive optical networks

Generally, two vital types of architectures that make FTTH broadband implementation, active optical networks (AONs) and passive optical networks (PONs). The traffic on AON and PON are shown in Figure 1.1.

AONs use electrically powered switching equipment, such as a router or a switch aggregator and take advantage of repeaters based on $O/E/O$ regenerators for reach extension to have additional intelligence located closer to the subscriber that can reduce latency, flexibly add bandwidth, isolate faults, switch and maximize bandwidth utilization between the switch aggregator and Central Office (CO) [5]-[12].

PONs has not included electrically powered switching equipment and no active components are deployed in the optical distribution network. PONs use optical splitters to separate and collect optical signals as they move through the network. Under this way, cost and energy efficiency would be their advantages. That is why PONs attracts a lot of passion from scientists and network providers.

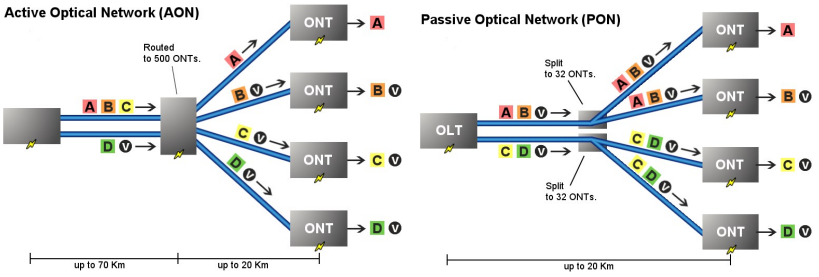

(a) (b)

FIGURE 1.1: Traffic on AON and PON (The icon A means data for single customer, V means video for multiple customers) .

TDMA-PON is the current trend of FTTH [7]. The main characteristics of TDMA-PON are that the downstream uses broadcast mode, and upstream uses TDMA mode. The advantage is low cost and transparency. unfortunately, the bandwidth would be shared, not independent.

1.2.2 TDM-PON

This architecture implements a topology to share the fiber plant among a higher number of customers using a power signal splitting. Therefore, several ONUs are connected to a single fiber. This sharing scheme leads a reduction in the data per customer. However,

considering the statistical nature of internet traffic, a mechanism based on dynamic bandwidth allocation (DBA), can partially compensate for the disadvantage. In TDM, the maximization of the common fiber link leads to a higher share of infrastructure. The implementation based on one-fiber/one wavelength for a completely passive PON allows higher cost efficiency and is desirable also for a green field deployment [8].

Physical layer network innovations both drive and are driven by advancements in enabling component and subsystem technologies. By the end of the 1970s, the development of low-loss optical fiber, laser transmitters, and receivers had set the stage for transmission system and optical networking innovations in the decades to come, among which were the first proposals and demonstrations of todays most widely deployed optical access networks.

XG-PON has already the standard of NGPON1. From ITU Standard, the main PON specifications are as following Table 1.1:

Characteristics	BPON	GPON	XGPON	NGPON2
Standard	ITU-T G.983	ITU-T G.984	ITU-T G.987	ITU-T G.989
Split ratio	32	64	256	256

TABLE 1.1: Major PON technology

1.2.3 WDM-PON

A more recently commercialized class of multiuser optical access networks is the WDM-PON.

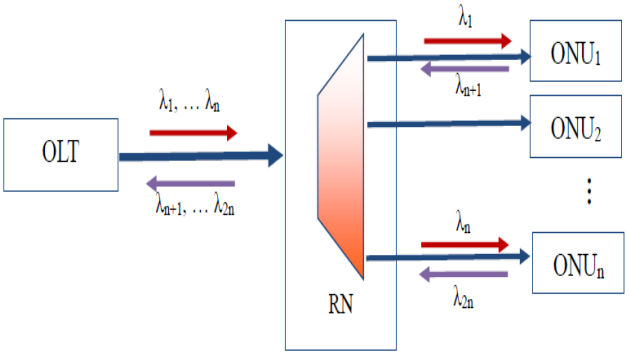

FIGURE 1.2: WDM-PON structure.

Based on an architectural concept that takes advantage of the unique properties of the arrayed waveguide grating (AWG) and employs colorless identical transceivers at each user premise to avoid the costs and inventory complexities associated with distinct

WDM transceivers, these systems are available commercially, but have not yet been widely deployed for residential access [9]. The WDM-PON structure is shown in Figure 1.2.

1.2.4 Hybrid WDM/TDM-PON

Hybrid PON architecture maximizes the customer density by incorporating WDM/TDM techniques.

The loss budget of hybrid PONs is typically extended to far beyond the budget of a TDM-PON, since a metro-access convergence is targeted at the same time. Due to the highly non-centric loss distribution, meaning a placement of the TDM splitting stage (i.e. in general the largest concentrated loss element) very close to the ONU, problems are very likely to arise due to Rayleigh backscattering in the feeding fibers when a single wavelength is reused for down- and upstream transmission. The junction between the WDM and the TDM segment is often used to incorporate some network intelligence or means of amplification. While in networks that contain electrically powered equipment these so-called remote nodes include routers [11]-[14] or protocol terminators [14], other approaches, which provide optical amplification by remotely pumping rare-earth doped fibers, exist [14-16].

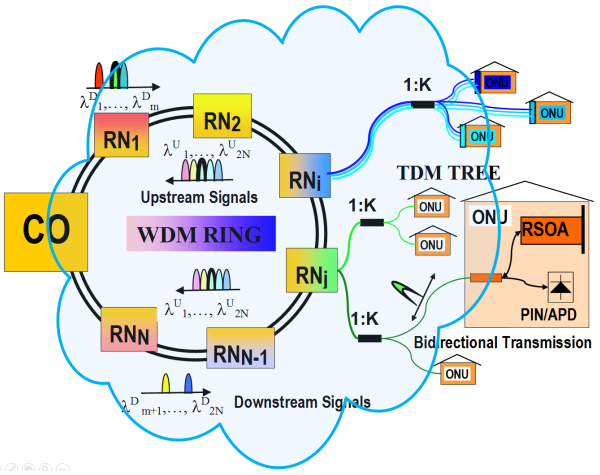

FIGURE 1.3: An example of WDM/TDM-PON architecture .

Nowadays, NG-PON scheme is desired for every company. The hybrid WDM/TDM architecture based on a WDM ring and a TDM tree from European FP7 ICT-Sardana Project is shown at Figure 1.3 [2].

1.2.5 Optical OFDM-PON

Orthogonal frequency-division multiplexing (OFDM) was first demonstrated is a bandwidth efficient transmission technology. At first, OFDM was proposed as a mobile radio technology with superior performance in a fading environment, and has been successfully incorporated into various systems including high-speed DSL access over twisted copper wires as well as over-the-air broadcast. In retrospect, it may seem obvious that OFDM would eventually be applied to optical communications, but only recently have the underlying high-speed signal processing technologies improved to the point that optical OFDM systems could rival the performance of more conventional WDM systems. In fact, although high-capacity long-haul OFDM systems have been demonstrated in the lab, they have not yet been commercialized.

Optical OFDM can be considered a highly spectrally efficient version of optical subcarrier multiplexing, which is not only the underlying technology in the previously discussed hybrid fiber coax networks, but was under serious consideration as a future multi-user PON technology during the years before the emergence of TDM PON [10]-[14]. Recent demonstrations of OFDM PON, although utilizing optical subcarrier, are entirely based on digital signal processing (DSP) rather than analog RF techniques, so are much more closely related to the present generation of experimental long-haul OFDM systems rather than old-fashioned subcarrier PONs [14]. While, it is not a low cost scheme for the cost efficient access network. Even though, Coherent system also can be a good proposal for upgrading an access network.

1.2.6 UDWDM-PON

Ultra-Dense WDM-PONs is an emerging type of access network that allows increasing the customer density of the PON and avoids narrow-band classical WDM multiplexers, via placing passive splitters as signal distribution elements, as it is the case in TDM-PONs, and in turn coherent detection to overcome the introduced high loss budget of the network [9], [10].

UDWDM increases the spectral efficiency with respect to current optical success systems (WDM/TDM) that make poor use of the transmission capacity of optical fiber [11].

Recent advances in optic-electronic and DSP technologies have re-awakened interest in coherent optical communications. Coherent long-haul systems have already been released commercially, so it is not surprising that researchers are re-applying this technique to optical access systems. Ironically, much of the early work on optical coherent systems was focused on optical access, since the tunable local oscillator can be used as the basis

of a tunable receiver. In addition to added flexibility, coherent detection substantially improves receiver sensitivity, which can be applied to increasing the PONs splitting ratio and increasing reach [12]-[16].

A summary with different access technologies are shown in Figure 1.4(a), and the UDWDM-PON solution are now being implemented in the European FP7 ICT CO-CONUT Project. The Figure 1.4(b) shows the different bit rates for different ONU solutions. The UDWDM-PON provides the highest number of the wavelengths, making the 'wavelength-to-the-user' concept to be achieved.

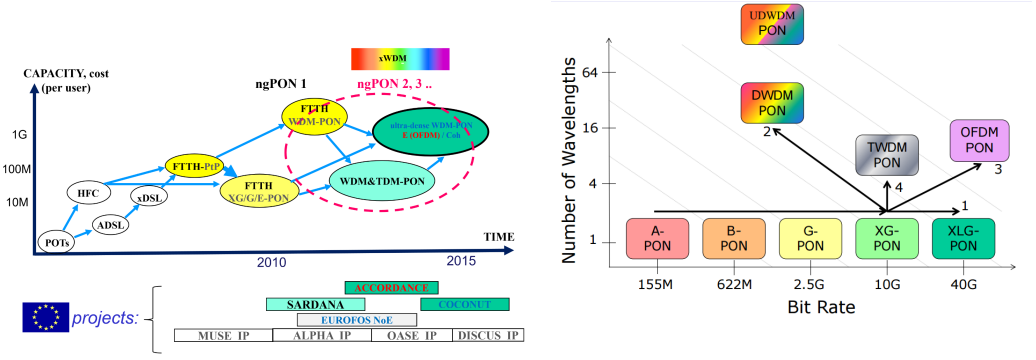

FIGURE 1.4: (a) Evolution of access technologies (b) ONU solutions and corresponding wavelength and bit rates.

1.3 Thesis objectives

This dissertation was realized during a crucial period in the telecommunication industry. Groundbreaking innovations from the research need to address real customer issues and define the future on access network. It describes several strategies to apply low footprint integrated photonics devices into the ONU for ultra dense channel spaced networks (UDCSN). According to discussions presented beforehand, the main idea of is to make the ONU footprint lower and cost-efficiently. In order to fulfill the main objective of this thesis, a set of specific objectives are formulated as follows:

- Optimizing RSOA in phase modulation instead of the traditional intensity modulation for long reach solution.
- Design a bidirectional ultra dense access network for adapting the transparent coherent UDWDM-PON.
- Applying new application with monolithically integrated DEML and exploiting it for bidirectional coherent transmission.

- Demonstrating and mitigating the residual AM produced by DFB, through a integrated DEML.
- Demonstrating A bidirectional performance for UDCSN by applying polarization independent RSOA at single laser ONU.
- Demonstrating fast wavelength jumping for access network by monolithically integrated devices.

1.4 Thesis outline

All the presented objectives and concepts will be explored and analyzed in this document, the rest of the dissertation is organized as follows.

Chapter 2 introduces the method to optimize the RSOA for phase modulation through the measured characterization and operate it at the best condition for phase modulation with the purpose of minimizing the unwanted residual IM (for better BER) and polarization dependency (for long reach ONU), with validating tests with small signal and large signal measurements. The limited bandwidth of 0.4 GHz is overcomed and operated at the speed for each user up to 3.125 Gb/s.

In chapter 3, an efficient bidirectional DPSK-DPSK transmission for UDWDM-PON is proposed. Single DFB at ONU is used both as the local laser for downlink coherent detection and the optical carrier for uplink. A polarization independent RSOA chip is applied at ONU and with the maximum bandwidth of 4.7 GHz.

Chapter 4 first demonstrates a dual output DEML as TRx in an UDWDM-PON ONU. A bidirectional DPSK-ASK transmission is demonstrated and tested.

Chapter 5 first demonstrates mitigating the residual AM of DFB, by means of EAM. An integrated DEML is applied and analyzed.

Chapter 6 first demonstrates a bidirectional coherent DPSK-DPSK transmission with single laser ONU. Besides, there is a novelty on the coupler based ONU, which could be easily integrated in near future. Furthermore, the channel spacing are analyzed here, providing an optimal channel separation between downlink and uplink.

Chapter 7 first demonstrates a fast wavelength jumping and ultra fast wavelength adjustment, using an integrated two section frequency modulated laser (FML).

In chapter 8, a short summary and a prospective future research line conclude the thesis with a list of published contribution to scientific congreses and archival journals.

1.5 Reference

[1] I Tomkos,et al., "Guest editorial: Spatially and spectrally flexible elastic optical networking," in Communications Magazine, IEEE, vol.53, no.2, pp.20-22, Feb. 2015

[2] J. Prat, Technologies for a Cost-effective Coherent udWDM-PON, Proc. OFC, Th3I, Los Angeles, 2015.

[3] Y. C. Chung, Future optical access networks, Proc. SPPC, JW1A.1, Colorado, 2012.

[4] H. Rohde, et al., Digital multi-wavelength generation and real time video transmission in a coherent ultra-dense WDM PON, Proc. OFC, OM3H3, Anaheim, 2013.

[5] K. C. Kao, et al., Dielectric-fibre surface waveguides for optical frequencies. Proceedings of the IEE, 13(7), 1966.

[6] A. Girard. FTTx PON Technology and Testing. EXFO Electrical Eng., 2005.

[7] J. M. Fabrega, J.Prat, Homodyne receiver prototype with time-switching phase diversity and feedforward analog processing, Optics Letters, vol. 32, no. 5, Mar. 2007.

[8] C. Bock, et al., Ultra-Dense WDM PON based on Homodyne Detection and Local Oscillator Reuse for Upstream Transmission, in Proc. ECOC06, We3.P.168, Cannes, France, Sept. 2006.

[9] J. Prat, et al., Simple intradyne PSK system for udWDM-PON, Opt. Exp. 20, 2012.

[10] J. A. Lzaro, et al., Hybrid Dual-Fibre-Ring with Single-Fibre-Trees Dense Access Network Architecture Using RSOA-ONU, Proc. OFC, OTuG2, Anaheim, 2007.

[11] S.Y.Kim, et al., Enhanced Performance of RSOA based WDM-PON using Manchester coding, J. Optical Networking, vol.6, pp. 624-630, 2007.

[12] $http://en.wikipedia.org/wiki/Passive_optical_network$

[13] Grobe, Klaus et al., PON in Adolescence: From TDMA to WDM-PON, IEEE Applications Practice: Topics in optical communications, January 2008, Pages: 26-34

[14] Eduardo T. Lopez, UPC-doctoral thesis, chapter 1, Barcelona, 2013.

[15] J. Prat, et al. Optical network unit based on a bidirectional reflective semiconductor optical amplifier for fiber-to-the-home networks, Photon. Technol. Lett., vol. 17, 2005.

[16] J. Prat, et al. Results from EU Project SARDANA on 10G extended reach WDM PONs, OSA, OFC/ NFOEC, 2010.

Chapter 2

RSOA based UDWDM-PON ONU

2.1 Introduction

The wavelength-division-multiplexed passive optical network (WDM-PON) has been considered as an ultimate solution for the next-generation access network capable of providing unlimited bandwidth to each user [1]. However, if WDM-PON technologies are directly applied for massive deployment, it would be extremely complex, and the potential WDM-PON is to be integrated and improved [2]. Plenty of scientists have believed that it is crucial to increase the operating speed and maximum reach of WDM-PON, while it has no sense if people achieve them without affordable cost [1-3]. In order to apply them cost-efficiently, the system should require colorless optical network units (ONUs). It is desired that the whole system use modulators of low consumption, even limit the number of amplifiers [2,3]. For bidirectional transmission the Rayleigh backscattering (RB) would limit the performance if we want to reuse the carrier from optical line terminal (OLT) [4].

On one side, some researches on reusing the wavelength from OLT via semiconductor optical amplifier (SOA), reflective SOA (RSOA), and SOA integrated with reflective electro-absorption modulator (SOA-REAM) [5-8] have been done, while power penalty is the serious problem for these applications. Hence, there is an idea for limiting the power penalty to put the laser at ONU side, such as tunable laser at ONU [10], however, it is too expensive to deploy at each ONU. It is to be expected the laser at ONU is effectively used. Both downstream and upstream, using phase modulation, present better performances than that of intensity modulation for upstream. On the other side, coherent detection is used at the receiver side to achieve a link budget of beyond 40 dB, which is superior to any existing direct detection based technology, and which can be utilized either for long reach or splitting factors extensions [9-11]. Coherent detection has been confirmed that it can improve the sensitivity and the spectrum efficiency in access network [12,13]. Compared with homodyne detection, heterodyne detection presents inherent image frequency interference, and as a result homodyne/intradyne reception is considered a better solution [14].

With this aim, first we simplify the hardware by applying the laser at ONU with the functions of both uplinks carrier and downlinks local oscillator laser (LO). These components can be integrated in a low footprint monolithic chip at ONU for each user.

This chapter is organized as follows: a bidirectional schematics with single distributed feedback laser (DFB) based ONU is brought forward in section 2.2, and optimization of operating condition for phase modulation is given in section 2.3, validating tests both for small signal and large signal are demonstrated in section 2.4 and 2.5, respectively. A conclusion is given in section 2.6.

2.2 Bidirectional UDWDM Subsystem and Structure

Traditional intensity or phase modulator is based on $LiNbO_3$ architecture, but it presents the issues of large footprint, high optical losses, high-power consumption and integration compatibility with the laser, thus not being suited for fiber-to-the-home (FTTH) ONUs. Semiconductor integration, like InP RSOA, is a way to facilitate the design of complex photonic circuits with multiple photonic functions [15].

A comparison between the traditional phase modulator ($LiNbO_3$) and the RSOA is given in Table 2.1, the parameters are from the references [16-18]. The RSOA presents the benefits both on the size and the injected driving signal.

We propose the network schematic as shown in Figure 2.1. The upstream data use the RSOA as a phase modulator for reducing the power consumption, and it is expected

TABLE 2.1: Comparison between traditional $LiNbO_3$ modulator and RSOA

	$LiNbO_3$	RSOA
Modulator length (L)	[5, 10]cm	[0.3, 1.6]cm
Modulator width (W)	[2, 5]cm	[0.2, 0.5]cm
RF driving signal ($V_o or I_o$)	[4, 6] V	[10, 70]mA

that the laser will be integrated for both RSOA (as the upstream carrier) and receiver (as the LO) at ONU. At OLT side, in order to receive the upstream data, coherent detection is also used for improving the sensitivity of the receiver. The advantage of additional sensitivity can be used for power splitting losses and longer reach ultra-dense WDM-PON (UDWDM-PON). We focus on the upstream direction in this paper.

As previous explanation, the RSOA could be a low cost solution, while, it is not an easy goal to increase its maximum reach and operating speed. To improve these, we generate differential phase shift keying (DPSK) signal by directly modulating the RSOA. Once the RSOA is directly modulated, both the amplitude and phase of the output signal are modulated at the same time [19]. However, the undesired residual Amplitude Modulation (AM) and polarization dependency distort the signal and degrade the sensitivity of the receiver, which will be described in next section. Based on these reasons, the optimal operation region should be found in order to operate it efficiently.

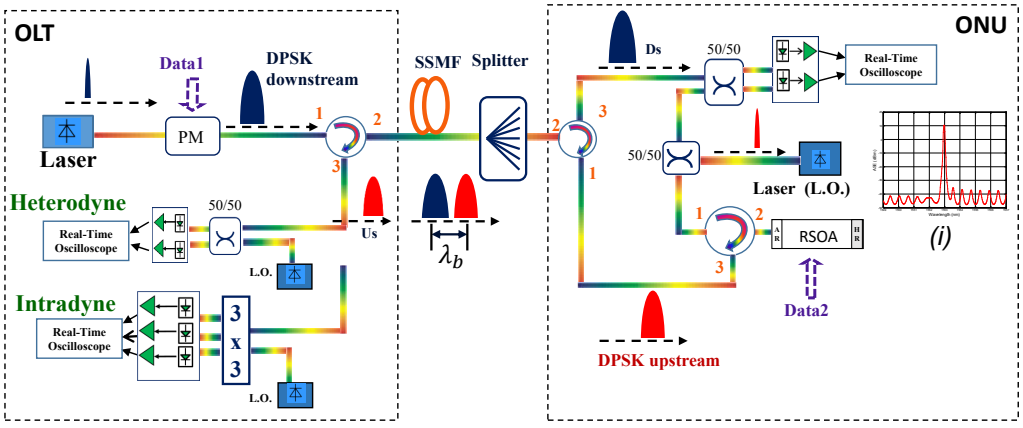

FIGURE 2.1: Proposed subsystem of DPSK-DPSK bidirectional UDWDM-PON

2.3 Optimization of RSOA for phase modulation

In order to be operated at the best condition for the phase modulation, the gain, the optical-signal-to-noise-ratio (OSNR), amplified spontaneous emission (ASE) noise and the polarization dependent factors are required to be considered. The method for optimizing phase region consists of tuning both input power and bias current to achieve

the minimum residual AM component and the polarization sensitivity. The optimal condition should have a better performance of phase modulating efficiency (PME). The equation for gain measurement is as follows [19]:

$$G = 10lg\,\frac{P^s_{out}}{P^s_{in}} = 10lg\,\frac{P_{out} - P_N}{P_{in} - P_{sse}} \tag{2.1}$$

where P^s_{out} and P^s_{in} are the pure output power and input power of RSOA, respectively. P_{out} and P_{in} are the measured output and input powers, P_N represents the noise power, P_{sse} is the source spontaneous emission power of the laser in the experiment.

The room temperature of the RSOA is around 27 °C. Measured gain and OSNR are shown in Figure 2.2. The maximum gain of the RSOA is about 21 dB, and the modulation region is between -10 dBm and 0 dBm. OSNR factor would be increased by injecting more optical power. The output power of the RSOA influences the signal quality at the receiver side, the increasing power goes to the linear region from -30 dBm to -10 dBm, and nearly flat region between -10 dBm and 0 dBm. The output power which directly influences the received performance of modulation, is increased by the input power and the injected current as shown in Figure 2.2(a). At the same time, with a laser after amplifier, the ASE power (PASE) of RSOA is the main noise for RSOA [19]. From Figure 2.2(b), the ASE would be limited by increasing the input power [20,21].

$$P_{ASE} = P_N - G \cdot P_{sse} \tag{2.2}$$

Considering both the noise and output power of the RSOA, 0 dBm presents the optimal condition that minimizes the residual AM. While, for higher than 0 dBm of input power, the laser has a high consumption and it is not suitable for low cost ONU. It is because that we need the laser at ONU, and split the power both for RSOA and coherent detection at ONU for colorless ONU, all the component is required monolithic integrated chip.

As previously mentioned, when directly modulating the RSOA, the AM component would degrade the performance of DPSK detection. Hence, besides input power, we also need to select the bias current for RSOA in order to limit the tiresome AM component. The measured output power under different bias condition is shown in Figure 2.3. Clearly, the 70 mA current is the ideal condition for phase modulation which the amplitude component would maintain the same value, and it would give a stable performance when the signal is introduced to the RSOA.

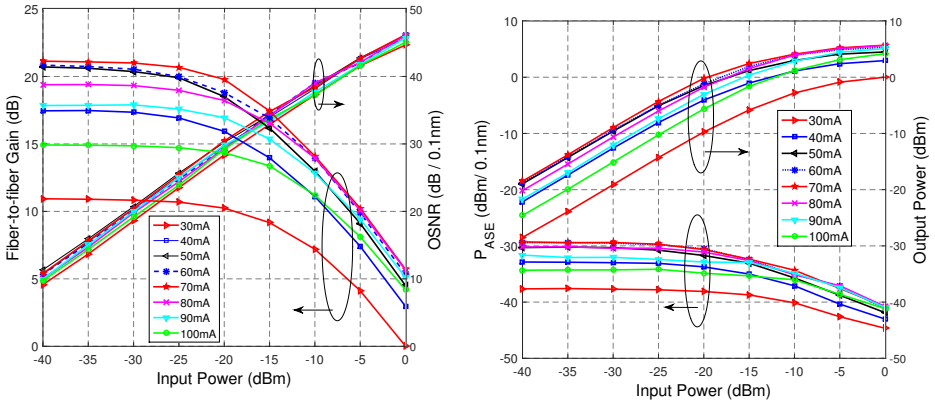

(a) (b)

FIGURE 2.2: (a) Measured Gain and OSNR versus optical input power (b) Measured ASE power spectral density and output power versus optical input power.

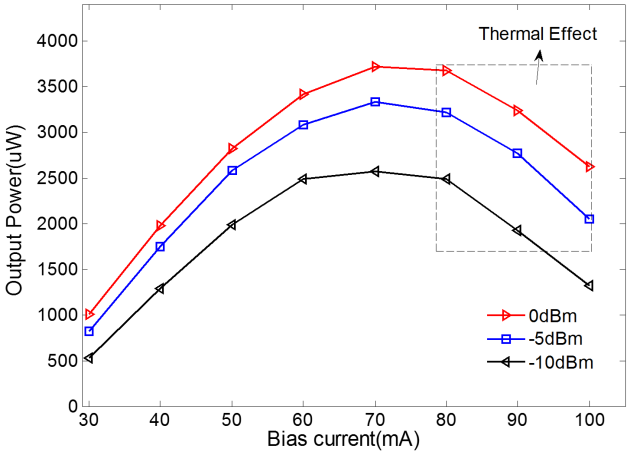

FIGURE 2.3: Measured Output Power versus bias current under different input power (0 dBm, -5 dBm, -10 dBm).

Another important physical issue in coherent detection is the fast polarization changes at the input of the receiver that influences not only the sensitivity but also the demodulation performance. Polarization changes originate both from the signals propagation along the fiber as well as the RSOA structure. In this case, we can limit the RSOA's polarization influences for available To-can packaged RSOA via characterizations measurement (at some region, RSOA is sensitivity for polarization) for the purpose of obtaining the polarization mitigation on the whole link. As we explained previously, the AM component influences the performance of phase modulation, we have found the best operation point at 70 mA with input power of 0 dBm. However, when the component is modulated in phase with coherent detection, the polarization deviation of the RSOA would influence the phase modulation. It is because that the RSOA's polarization dependent gain (PDG) would be different, which would make the AM component always changing. The deviation of the AM component changing by time can cause degradation

on the system performance seriously.

The origin of PDG in RSOA is due to the fact that bulk active material has much larger transverse electric (TE) amplification than transverse magnetic (TM), on account of the different confinement factors [21,22]. To compensate for the birefringence, the strain [23] in the active material enhances the gain of TM with respect to TE, making the RSOA's less polarization dependent. However, this balance does not entirely mitigate PDG [24] and depends on input power, gain, bias current, and wavelength. The wavelength for UDWDM-PON is selected by the structure, for previous results, we have selected the bias current (70 mA) for phase modulation with the advantage of minimizing residual AM component, however both the residual AM and polarization dependent output power are dependent by the optical input power. Based on previous measurements (Figure 2.2), higher input power in saturation region can limit the residual AM, then the polarization insensitivity region is required to be selected.

The measured polarization dependent results are shown at Figure 2.4. Figure 2.4(a) shows the Gain at TE mode and TM mode at the same bias condition (70 mA). Figure 2.4(b) shows the polarization dependent gain influenced by the input power of RSOA. The PDG is the lowest (around 0.1) when the input power is around -5 dBm. The PDG is 0.3 at the input power of 0 dBm.

In summary, balancing between minimizing the residual AM and polarization dependency, the condition of P_{in}=0 dBm, I_{bias} =70 mA is considered as the optimal operating points.

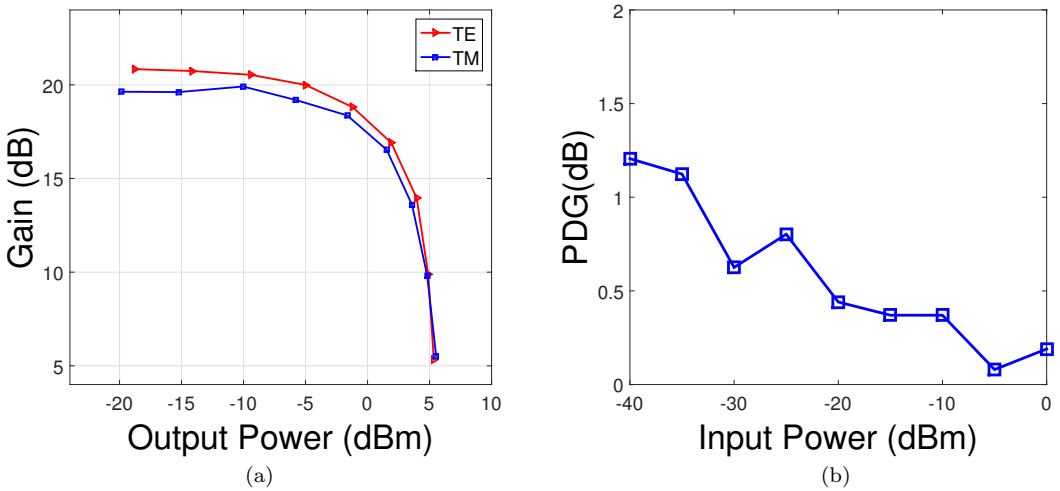

(a) (b)

FIGURE 2.4: (a)Gain versus output power at different polarization mode (b) PDG against input power at 70 mA, 0 dBm.

2.4 Validating for small signal measurement

In order to validate the performance, the RSOA is tested in small signal response via network analyzer. The measurement of Frequency Modulating Efficiency (FME) and PM Efficiency (PME) use the linear transfer function of an optical filter as shown in Figure 2.5(a). It is assumed that the filter transfer function (Figure 2.5(b)) is linear to the frequency (ω_p) around the carrier frequency (ω_0) [25].

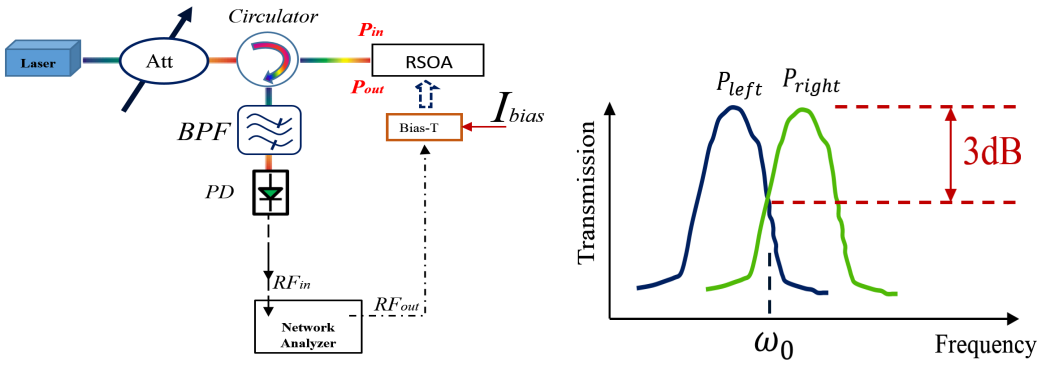

FIGURE 2.5: (a) Experimental setup for FME and PME measurement using a band-pass-filter (BPF), and BPF is controlled by electrical voltage which can be maintain the stable measurement. (b) Explanation of measured transmission characteristics of a BPF, the transmission represents the square root of power loss.

The transfer function can be represented as [25]

$$H(\omega_p) = T_0\,[1 + c_1(\omega_p - \omega_0)] \tag{2.3}$$

where, T_0 is the amplitude transmission and c_1 is the differential coefficient at around ω_0. Based on Fourier analysis, the approximated optical-power waveforms after propagation through the filter can be derived as

$$P_{left} \approx T_0^2\,P_{in}(1 - 2c_1\frac{d\phi}{dt}), P_{right} \approx T_0^2\,P_{in}(1 + 2c_1\frac{d\phi}{dt}) \tag{2.4}$$

here, P_{left} is the output power when the filter slope is at the left side, and P_{right} is the output power when the filter slope is at the right side. Then,

$$P_{AM} = \frac{P_{left} + P_{right}}{2} = T_0^2\,P_{in}, P_{FM} = \frac{P_{left} - P_{right}}{2} = 2\,T_0^2\,P_{in}\,c_1\,\frac{d\phi}{dt} \tag{2.5}$$

FM/AM has the relation with the phase shift component,

$$\frac{P_{FM}}{P_{AM}} = 2c_1 \cdot \frac{d\phi}{dt} \tag{2.6}$$

and the frequency deviation is as follow:

$$\Delta\upsilon = \frac{1}{2\pi} \cdot \frac{d\phi}{dt} = \frac{1}{2\pi} \cdot \frac{1}{2c_1} \cdot \frac{P_{FM}}{P_{AM}} \tag{2.7}$$

For small signal modulation, FM Efficiency is given by

$$\delta\upsilon(\omega) \equiv \delta\bar{\upsilon}(\omega) \approx \frac{1}{2\pi} \cdot \frac{1}{2c_1} \cdot \frac{\delta P_{FM}(\omega)}{P_0} \tag{2.8}$$

and $\delta\upsilon$ has the relationship with $\delta\phi$,

$$\delta\phi = 2\pi \int \delta\upsilon \, dt \tag{2.9}$$

Based on Fourier Transform, PM Efficiency is

$$\delta\phi(\omega) = \frac{2\pi}{j\omega}\delta\upsilon(\omega) \tag{2.10}$$

The frequency responses are measured at the bias condition from 40 mA to 70 mA; and the input power for the RSOA is now maintained at 0 dBm. The AM response and the FM Efficiency are shown in Figure 2.6(a). It shows that the limited 3-dB bandwidth (BW) is limited to around 0.4 GHz, increasing from 40 mA to 70 mA; the FM Efficiency is measured in frequency domain with maximum at 500MHz/mA when the bias current is 70 mA. The PM Efficiency, shown in Figure 2.6(b), is calculated by the FM Efficiency from equation 2.10, presenting a flat and smooth curve appears at low frequency range at 70 mA.

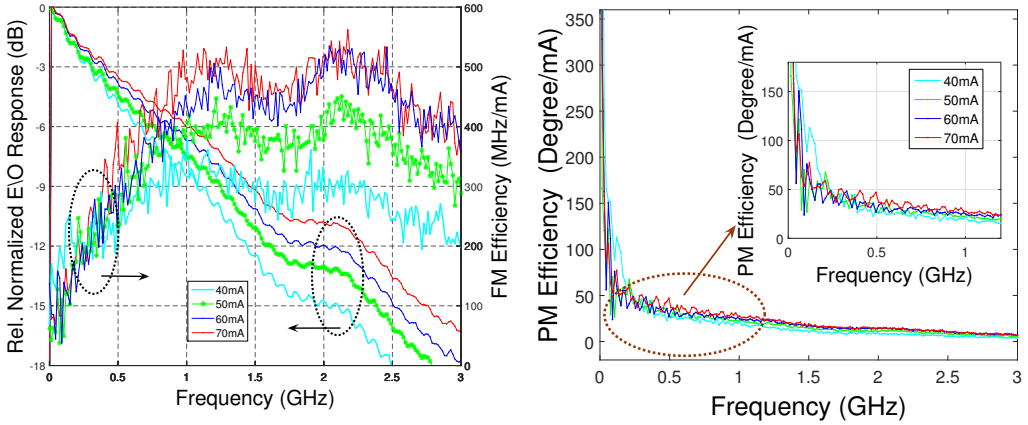

(a) (b)

FIGURE 2.6: (a)Normalized AM response and FM Efficiency at frequency domain (b) PM Efficiency at frequency domain.

In order to obtain accurate results for small signal chirp parameter, fiber dispersion should be accurately and independently measured [26]. The chirp parameter is obtained by measuring the electro-optic (EO) response by inserting dispersive fibers between the modulator and the light-wave component analyzer (LCA) [26-28]. The interaction between fiber dispersion and modulator chirp results in resonance dips in the spectrum. The equation describing the resonance points and the chirp is written as [26]:

$$f_k^2 L = \frac{c}{2D\lambda^2}(1 + 2k - \frac{2}{\pi} arctan\alpha) \tag{2.11}$$

$$\alpha = tan[2\pi(1 - \frac{2f_0^2 DL\lambda^2}{c})] \tag{2.12}$$

where, α is the chirp parameter, f_k is the k-th order of resonance, D is the fiber dispersion, c is the speed of light and λ is the wavelength.

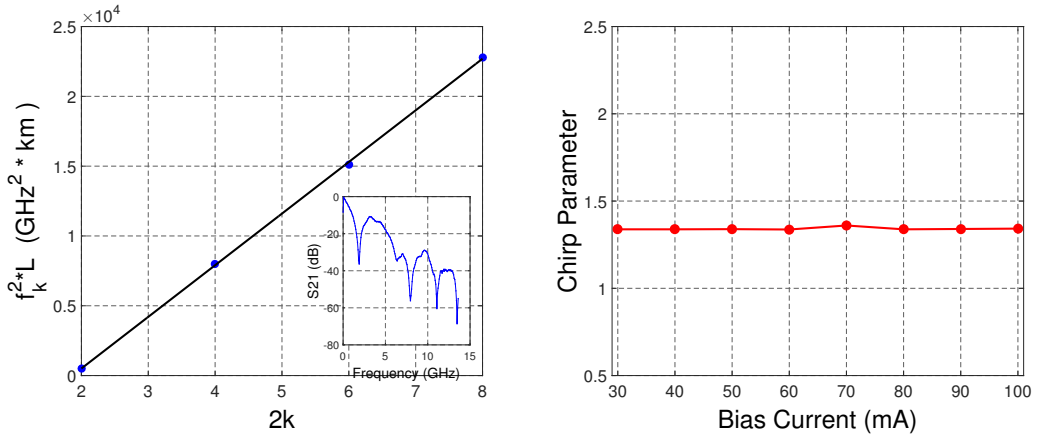

(a) (b)

FIGURE 2.7: (a) Measured resonant frequency at 70 mA bias condition for RSOA, where k is the k-th resonant position. Inset: measured chirp spectrum with 125 km SMF (b) chirp parameters at different bias conditions.

An experimental curve of equation 2.11 is illustrated in Figure 2.7(a). By fitting the experimental resonance points, the chirp under different bias conditions is calculated and the result is shown in Figure 2.7(b). It indicates that the chirp parameter is around 1.34 under different bias currents.

2.5 Validating for large signal measurement with coherent detection

In order to give a clear evidence of the method effectiveness to search for the optimal phase modulating condition (Ibias=70 mA, Pin=0 dBm), we test the RSOA with 2x2 heterodyne detection and 3x3 intradyne detection (without phase lock loop) as shown in Figure 2.8 (a) and 2.8(b).

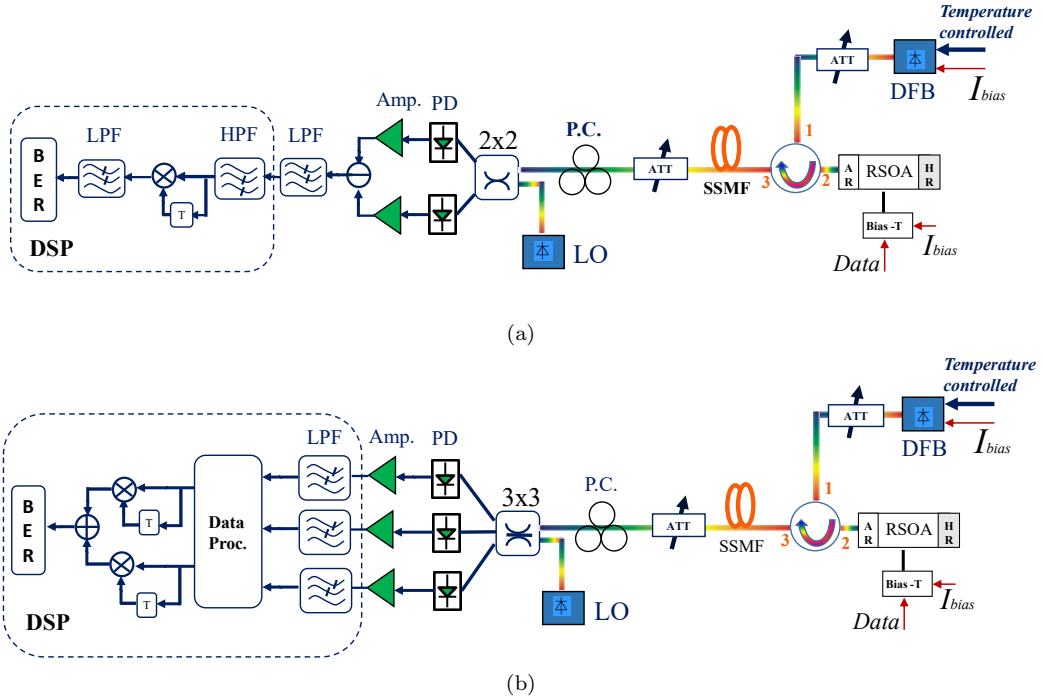

FIGURE 2.8: Experimental setup for coherentdetection.(a)Modulating RSOA in phase for balanced-PDs heterodyne detection.(b) Modulating RSOA in phase for intradyne detection.

Based on the structure we proposed in Figure 2.1 for UDWDM-PON, the DFB is biased at 90 mA under the temperature of 25C, the linewidth is 4MHz [29]. As shown in 2.8(a), the attenuator is used to provide the correct input power (0 dBm) for the RSOA after the circulator, the transmitted data consisted of a non-return-to-zero (NRZ) pseudo random binary sequence (PRBS), which is grouped and stored in an arbitrary waveform generator (AWG) operating at different bit rates. The optical signal is then launched through 50 km of standard single-mode fiber (SSMF). The polarization controller (PC) compensated signal fluctuations due to state of polarization (SOP) changes in the fiber [30]. The received optical signal is converted to the electrical domain via photo-detectors (PD). Low noise amplifiers are used after PDs. The real-time oscilloscope resamples the electrical signal that is further digitally post-processed. The Uncooled To-can Packaged RSOA is tested at 1.25 Gb/s, 2.5 Gb/s, 3.125 Gb/s, respectively.

The heterodyne receiver implemented is shown in Figure 2.8(a). The electrical signal at the output of the photodiodes after amplifying is sampled with a 50 GSa/s real-time oscilloscope at 12.5 GSa/s with 10, 5, 4 samples per bit, respectively [12]. The intermediate frequency is selected at twice the bit rate. At digital signal processing (DSP), the electrical signal passes through a 1-bit delay and multiply block for differential demodulating after filtering. Before bit decision, the signal is filtered again with a 4 order butterworth low-pass filter (LPF). Finally, the bit error ratio (BER) is computed. The BER is also measured with 3x3 intradyne detection as Figure 2.8(b). Unlike the 2x2 heterodyne detection, we use 3 PDs to detect the received signal and obtain the I and Q components, and then use electrical amplifier (Amp.) to amplify the signal before DSP. 3 LPFs are used before data processing, then passed through a 1-bit delay and multiply block for differential demodulating, BER is tested after demodulating.

For heterodyne detection, the BER and the eye diagram are shown in Figure 2.9. An input power of 3 dBm is provided by the ECL as LO. The results present the Rx sensitivities of -44.4 dBm, -40.3 dBm, and -34.3 dBm for back to back (BtB) transmission (after 50km fiber, the sensitivity arrives at -44.2 dBm, -39.7 dBm and -33.6 dBm) at BER=10-3 for 1.25 Gb/s, 2.5 Gb/s, 3.125 Gb/s, respectively. At BER=10-3, there are 4.1 dB power penalty between 2.5 Gb/s and 1.25 Gb/s, and 6 dB between 3.125 Gb/s and 2.5 Gb/s. The RSOA can be operated at the maximum bit rate of 3.125 Gb/s. The improved sensitivity can be used either for extended reach ONU or increased power splitting ratios in UDWDM-PON. Besides, the signal spectrum is also captured from the electrical spectrum analyzer (ESA) at different bit rates and intermediate frequencies as shown in the inset figure of Figure 2.9.

The BER and the eye diagram are also tested via 3x3 intradyne detection (Figure 2.9). Compared to 2x2 heterodyne detection or single-PD coherent detection, 3x3 intradyne detection has the theoretical 3-dB advantage of the sensitivity [12, 30-33]. The RSOA is maintained at the same conditions compared with 2x2 heterodyne detection (PLO=3 dBm). The results from the figure show that the sensitivity arrives at -48.2 dBm, -43.9 dBm, and -38.8 dBm for back to back (BtB) transmission (-48 dBm, -43.6 dBm and -37.4 dBm for 50km fiber transmission) at BER=10-3 for 1.25 Gb/s, 2.5 Gb/s, 3.125 Gb/s, respectively. The figure also shows that the power penalties are 4.4 dB and 5.1 dB at BER=10-3 when increasing the bit rate1.25 Gb/s to 2.5 Gb/s, and from 2.5 Gb/s to 3.125 Gb/s, respectively. It shows that the RSOA, which has the limitation of the modulating bandwidth of 400MHz, is successfully tested at 3.125 Gb/s, with the advantage of optimizing the RSOA in phase modulation region.

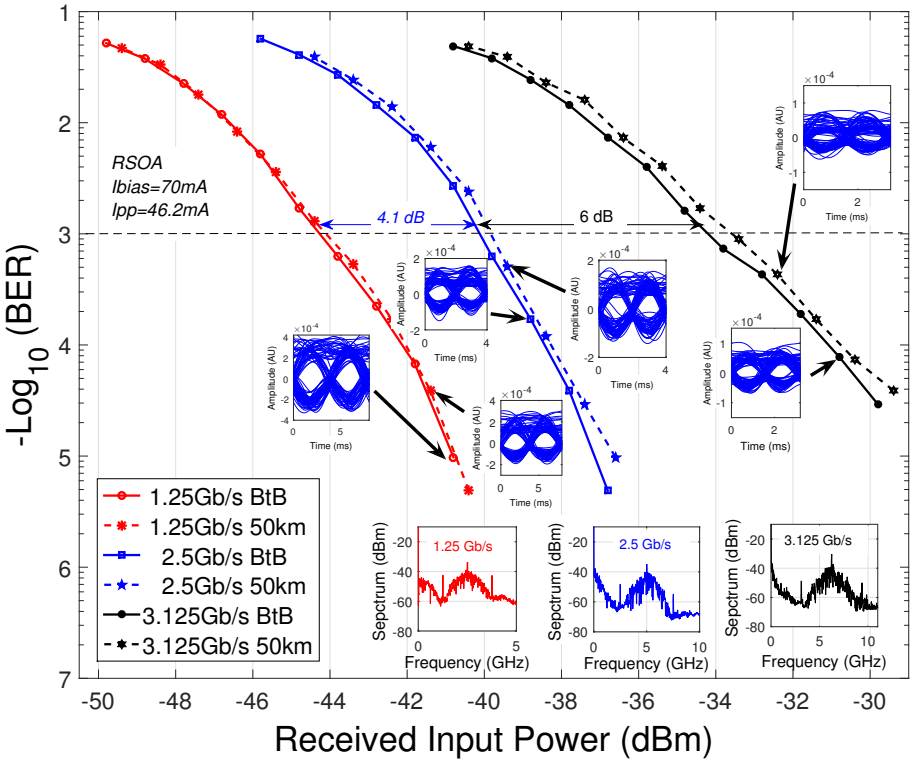

FIGURE 2.9: BER versus optical received input power with heterodyne detection.

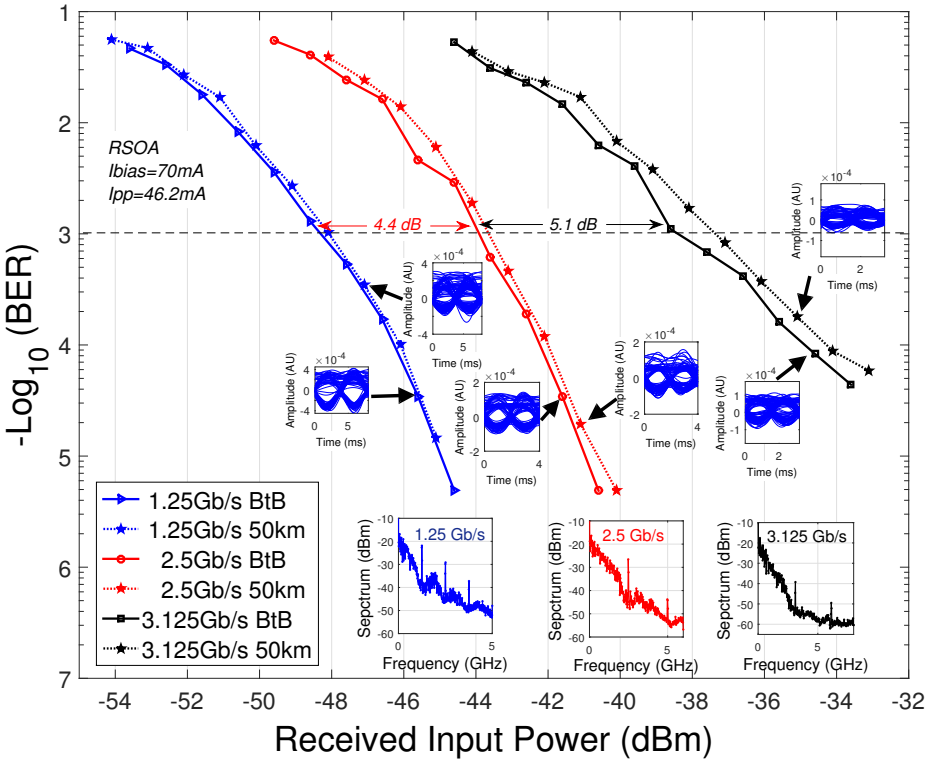

FIGURE 2.10: BER versus optical received input power with intradyne detection.

2.6 Conclusion

We demonstrate an effective optimization of the RSOA for phase modulation through the measured characterization and best condition operation, with the purpose of minimizing the unwanted residual AM (for better BER) and polarization dependency (for long reach ONU). As validating tests with small signal measurements, we test that the FM Efficiency reaches 500MHz/mA at the optimal bias of 70 mA. The results show that we could implement a long-reach UDWDM-PON operating at the speed for each user up to 3.125 Gb/s (using very low cost 0.4 GHz uncooled To-can RSOA), via coherent detection using 2x2 heterodyne and 3x3 intradyne receivers at the OLT, and digital signal processing techniques. Additionally, the downstream carrier and upstream carrier work at the same wavelength range, hence, it constitutes a simplified enabling technique towards Ultra Dense WDM-PON.

2.7 References

[1] J. Prat, Technologies for a Cost-effective Coherent udWDM-PON, Proc. OFC, Th3I, Los Angeles, 2015.

[2] Y. C. Chung, Future optical access networks, Proc. Signal Processing in Photonic Communications, JW1A.1, Colorado, 2012.

[3] M. Milosavljevic, P. Kourtessis and J. M. Senior, Wireless Convergence over Next Generation OFDMA-PONs, Proc. ANIC, AWB3, Toronto, 2011.

[4] B. Schrenk, G. de Valicourt, J.A. Lazaro, R. Brenot, J. Prat, Rayleigh Scattering Tolerant PON Assisted by Four-Wave Mixing in SOA-based ONUs, IEEE J. Lightwave Technol. 28, (2010) 3364-3371.

[5] G. de Valicourt, D. Make, J. Landreau, M. Lamponi, G. H. Duan, P. Chanclou, and R. Brenot, High gain (30 dB) and high saturation power (11 dBm) RSOA devices as colourless ONU sources in long reach hybrid WDM/TDM -PON architecture, IEEE Photon. Technol. Lett., 22(3) (2010) 191-194.

[6] U. H. Hong, K. Y. Cho, H. G. Choi, and Y. C. Chung, A Simple Carrier-Phase Estimation Technique for High Speed RSOA-based Coherent WDM PON, Proc. OFC, OM2A.2, Anaheim, 2013.

[7] B. Schrenk, S. Dris, P. Bakopoulos, I. Lazarou, K. Voigt, L. Zimmermann, and H. Avramopoulos, Flexible quadrature amplitude modulation with semiconductor optical amplifier and electroabsorption modulator, Opt. Letters 37, (2012) 3222-3224.

[8] A. Naughton, C. Antony, P. Ossieur, S. Porto, G. Talli, and P. D. Townsend, Optimisation of SOA-REAMs for Hybrid DWDM-TDMA PON Applications, Optics Express, 19(26), (2011) B722-B727.

[9] F. Saliou, B. Le Guyader, L. Guillo, G. Simon, P. Chanclou, for G-PON , XG-PON1 and TWDM-PON Co-existing on the Same ODN, Proc. ECOC, Mo.4.1.2, Cannes, 2014.

[10] S. Smolorz, H. Rohde, E. Gottwald, D. W. Smith, and A. Poustie, Demonstration of a coherent UDWDM-PON with real-time processing, Proc. OFC, PDPD4, Los Angeles, 2011.

[11] M. Morant, T. Quinlan, S. Walker, R. Llorente, Complete mitigation of brillouin scattering effects in reflective passive optical networks using triple-format OFDM radio signals, Proc. OFC, JWA072, Los Angeles, 2011.

[12] J. Prat, V. Polo, P. Zakynthinos, I. Cano, J. A. Tabares, J. M. Fbrega, D. Klonidis, and I. Tomkos, Simple intradyne PSK system for udWDM-PON, Opt. Express 20(27), (2012) 28758-28763.

[13] M. Presi, F. Bottoni, R. Corsini, G. Cossu, E. Ciaramella, Low Cost Coherent Receivers for UD-WDM NRZ Systems in Access Networks, Proc. ICTON, MoC31, Graz, 2014.

[14] J.M. Fabrega and J. Prat, Homodyne receiver prototype with time-switching phase diversity and feedforward analog processing, Opt. Letters, 32(5), (2007) 463-465.

[15] C. Kazmierski, D. Carrara, K. Lawniczuk, G. Aubin, J. Provost, and R. Guillamet, 12.5GB Operation of a Novel Monolithic 1.55m BPSK Source Based on Prefixed Optical Phase Switching, Proc. OFC, OW4J8, Anaheim, 2013.

[16] X. Zhang, Amir Hosseini, X. Lin, H. Subbaraman, and Ray T. Chen, Polymer-Based Hybrid-Integrated Photonic Devices for Silicon On-Chip Modulation and Board-Level Optical Interconnects, IEEE J. Sel. Topics Quantum Electron., 19(6), (2013) 3401115.

[17] T. Kawanishi, T. Sakamoto, and M. Izutsu, High Speed Control of Lightwave Amplitude, Phase, and Frequency by use of Electro-optic Effect, IEEE J. Sel. Topics Quantum Electron., 13(1), (2007) 79-91.

[18] A. Meehan and M. J. Connelly, Experimental Characterization and Modeling of the Improved Low Frequency Response of a Current Modulated Bulk RSOA Slow Light based Microwave Phase Shifter, Optics Comm., 341, (2015) 241-244.

[19] S. P. Jung, Y. Takushima, and Y. C. Chung, Transmission of 1.25-Gb/s PSK signal generated by using RSOA in 110-km coherent WDM PON, Opt. Express, 18(14), (2009) 14871-14877.

[20] S. Jain, T. C. May-Smith, A. Dhar, A. S. Webb, M. Belal, D. J. Richardson, J. K. Sahu, and D. N. Payne, Erbium-doped multi-element fiber amplifiers for space-division multiplexing operations, Opt. Letters 38(4), (2013) 582-584.

[21] J. C. Ribierre, G. Tsiminis, S. Richardson, G. A. Turnbull, and I. D. W. Samuel, Amplified spontaneous emission and lasing properties of bisfluorene-cored dendrimers, Appl. Phys. Lett. 91, (2007) 081108.

[22] P. H. Lim, S. Park, Y. Ishikawa, and K. Wada, Enhanced direct bandgap emission in germanium by micromechanical strain engineering, Opt. Express, 17(18), (2009) 16358-16365.

[23] M. J. Connelly, Theoretical calculations of the carrier induced refractive index change in tensile-strained InGaAsP for use in 1550 nm semiconductor optical amplifiers, Appl. Phys. Lett. 93, (2008) 181111.

[24] O. L. Ladouceur, K. Bergman, M. Boroditsky, and M. Brodsky, Polarization-Dependent Gain in SOA-Based Optical Multistage Interconnection Networks, IEEE J. Lightwave Technol. 24(11), (2006) 3959-3967.

[25] K. Sato, S. Kuwahara, and Y. Miyamoto, Chirp Characteristics of 40-Gb/s Directly Modulated Distributed-Feedback Laser Diodes, IEEE J. Lightwave Technol. 23(11), (2005) 3790 3797.

[26] F. Devaux, Y. Sorel, J. F. Kerdiles, Simple Measurement of Fiber Dispersion and of Chirp Parameter of Intensity Modulated Light Emitter, IEEE J. Lightwave Technol. 11, (1993) 1937-1940.

[27] N. Courjal and J. M. Dudley, Extinction-ratio-independent method for chirp measurements of Mach-Zehnder modulators, Opt. Express, 12(3), (2004) 442-448.

[28] H. W. Chen, J. D. Peters, and J. E. Bowers, Forty Gb/s hybrid silicon Mach-Zehnder modulator with low chirp, Opt. Express 19(2), (2011) 1455-1460.

[29] H. W. Chen, Y. H. Kuo, and J. E. Bowers, A Hybrid Silicon-AlGaInAs Phase Modulator, IEEE Photon. Technol. Lett. 20(23), (2008) 19201922.

[30] I. N. Cano, A. Lern, V. Polo, J. Tabares, J. Prat, Simple ONU transmitter based on direct-phase modulated DFB laser with heterodyne detection for udWDM-PON, Proc. ECOC, We.2.F.4., London, 2013.

[31] I. N. Cano, A. Lern, M. Presi, V. Polo, E. Ciaramella, J. Prat, 6.25 Gb/s Differential Duobinary Transmission in 2 GHz BW Limited Direct Phase Modulated DFB for udWDM-PONs, Proc. ECOC, P.7.2, Cannes, 2014.

[32] V. Polo, P. Borotau, A. Lern, J. Prat, DFB laser reallocation by thermal wavelength control for statistical udWDM in PONs, Proc. ECOC, P.4.13., Cannes, 2014.

[33] V. Sales, J. Segarra, V. Polo, and J. Prat, Statistical UDWDM-PONs Operating With ONU Lasers Under Limited Tunability, IEEE Photon. Technol. Lett., 27(3), (2015) 257-260.

Chapter 3

Polarization indepdent RSOA chip based ONU

3.1 Introduction

The rapid growth in global telecommunications, in particular optical fiber communications, has continued to fuel the deployment of fiber access networks that are located closer and closer to the end-users [1-3]. Unfortunately, the cost and footprint with existing access networks are still vital factors to be considered [1-4]. The optical filter at the optical distribution network (ODN) is a large cost-consumption for the whole optical fiber network; monolithic integration on InP is a way to lower footprint, and to facilitate the design of complex photonic circuits with multiple functions [4]. Recently, integrated semiconductor optical amplifier (SOA) and reflective-SOA (RSOA) are available for wavelength division multiplexed passive optical network (WDM-PON), reaching 10 Gb/s or more by means of wavelength reusing [5, 6] and seeding techniques [7]. Unfortunately, the Rayleigh backscattering (RB) and limited power budget, corresponding to the applications of wavelength reusing and seeding techniques respectively, can discourage their applications to λ-agnostic [2] bidirectional ultra-dense-WDM-PON

(UDWDM-PON). Also, WDM-PON or Dense WDM-PON (DWDM-PON) require optical filtering to select the wavelength for each final user. Furthermore, extending the number of accommodated users requires the ultra-dense WDM solutions, with the purpose of opening the way to the wavelength-to-the-user concept and provide the independent bit rate [2]. With the goal of implementing UDWDM-PON for the end-user, the low footprint integrated RSOA can be efficiently modulated and coherently detected for the configuration of the access network [8-12].

Considering the power source at the ONU, typical tunable distributed Bragg reflector laser (DBR) requires more controls, generally implies a complex electronics and a high cost as compared to the conventional single electrode distributed feedback laser (DFB) [13]. When using DFB with simple thermal tuning (2nm) and statistical initial wavelength distribution of non-preselected ONUs, a record of 256 wavelengths can be allocated in 14 nm with 99.9% availability [14].

Considering the power budget, there is a solution to employ coherent detection and an integrated laser (low footprint) at the optical network unit (ONU) to highly enhance the sensitivity and the total bandwidth. At the same time, phase modulation of the RSOA at the ONU is an advantageous approach for long reach UDWDM-PON [9-11].

The traditional UDWDM-PON scenario, which uses coherent detection, requires two lasers at the ONU [8, 9]. Hence, the stability is dependent by the wavelength drifts of both the two lasers. It is desired that the laser can be reduced to use only one laser at the ONU, for reducing the complexity and spectrum overlap [4].

3.2 General

The RSOA coherent ONU was first demonstrated in [10] in back-to-back, with the disadvantages of low modulating bandwidth and high modulating amplitude requirement. Unlike that To-can RSOA, in this letter a long cavity and polarization-independent RSOA chip, designed for this application, is used. The RSOA operation is optimized, with modulating bandwidth of 4.7 GHz for UDWDM-PON. Here, the key benefit of the proposed coherent ONU is that it uses only one single-DFB, as Local Oscillator Laser (LO) and as Transmitter (TX), with phase modulated RSOA, setting a cost efficient ONU implementation. Besides, at the optical line terminal (OLT), another DFB is used as LO, in polarization-diversity heterodyne detection, without employing any electronic equalization at the receiver (Rx).

The proposed system transmits downstream differential phase-shift keying (DPSK) data at the OLT using coherent detection at the ONU and coherently detects upstream DPSK

data at the OLT; the polarization diversity receivers with only two photo-detectors (PD) are exploited for both ONU and OLT. Both transmitter and receiver at the ONU can be integrated together in the future, with the purpose of low footprint component for the final users. The schematic of the proposed narrow channel spaced access network is shown in Figure 3.1. Between downstream and upstream, the wavelength deviation is twice the bit rate, for suppressing the Rayleigh Backscattering in the PON.

With the purpose of validating the proposed schematic given in Figure 3.1, the signal spectrum for multi-users bidirectional transmission for access network is taken. The 2-users DPSK-DPSK optical spectrum in Figure 3.2 shows the channel spacing of 12.5 GHz between two users, including down and upstream.

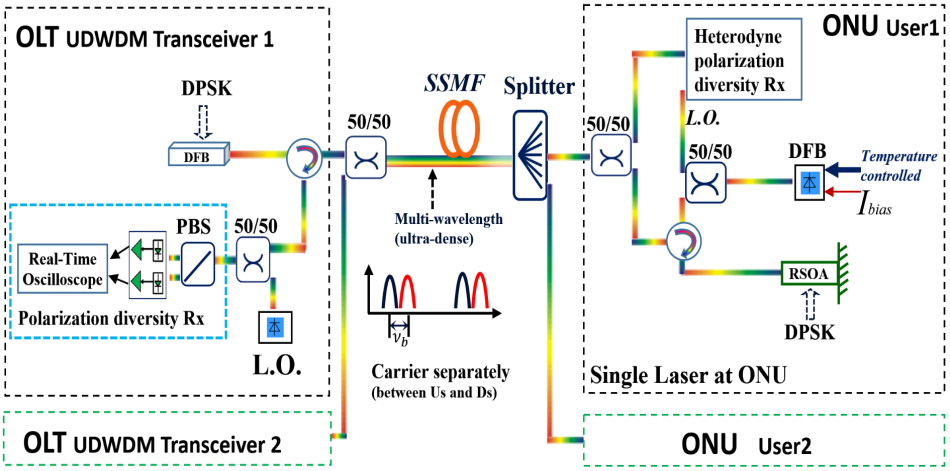

FIGURE 3.1: Bidirectional subsystem using heterodyne detection sharing one laser at ONU for UDWDM-PON using RSOA chip.

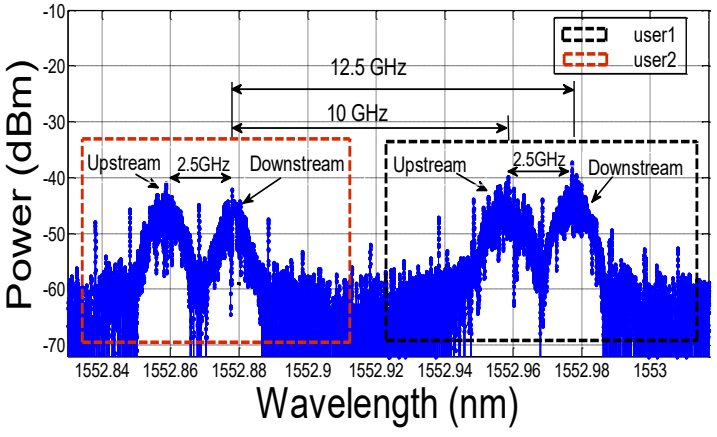

FIGURE 3.2: Optical spectrum for 1.25 Gb/s/user DPSK-DPSK bidirectional ultra-dense WDM.

3.3 Characterization

A RSOA chip has been implemented with relatively low optical confinement factor (Γ=20%) and relatively long active section (L=850 μm) which appears to be optimum for this application [10, 11, 15]. The RSOA has a polarization independent chip structure, which is discussed in detail in [16, 17]; and the test platform is shown in Figure 3.3.

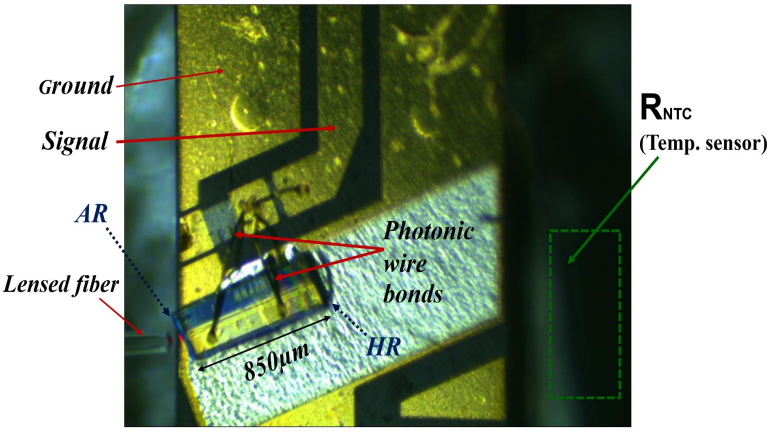

FIGURE 3.3: Polarization independent long cavity RSOA chip at ONU.

A resistor of 47 Ω is used in series, providing an effective matched impedance; and two wire bonds are used in the sub-mount to increase the modulating bandwidth. The amplified spontaneous emission (ASE) power spectrum of the RSOA chip (biased from 40 mA to 180 mA, 25 °C) displays an optical bandwidth from 20 nm to 50 nm as shown in Figure 3.4.

The test fixture of the RSOA chip performs stable coupled output power at room temperature (25 °C). The ASE ripple, corresponding to the gain ripple when injecting the optical signal into the RSOA, is influenced by the bias current, the temperature, the reflection and the wavelength [7]. There is a negligible ripple at 1550 nm around the Ibias=140 mA, and the chip can be operated at this wavelength and give a stable performance as shown in Figure 3.4.

The traditional colorless ONU based on RSOA with wavelength reusing, requires the injecting power around -10 dBm to -20 dBm. This limits the power budget because of the receivers capacity on sensitivity, besides, its 3-dB modulation bandwidth (BW) is about 3.5 GHz as shown in Figure 3.5. However, the BW increases to around 4.7 GHz at the higher input power (0 dBm). The bias current and temperature are maintained at 140 mA and 25 °C, respectively. It is an optimal condition for bandwidth, and also for reducing the IM residual components [7, 15], at 25 °C. For increasing the modulating bandwidth, the RSOA can add more bonding connections by the manufactory [18].

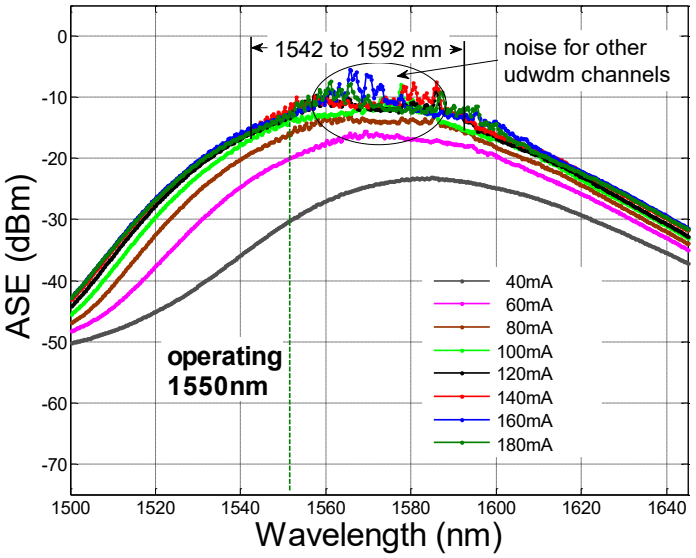

FIGURE 3.4: ASE spectrum at different bias condition.

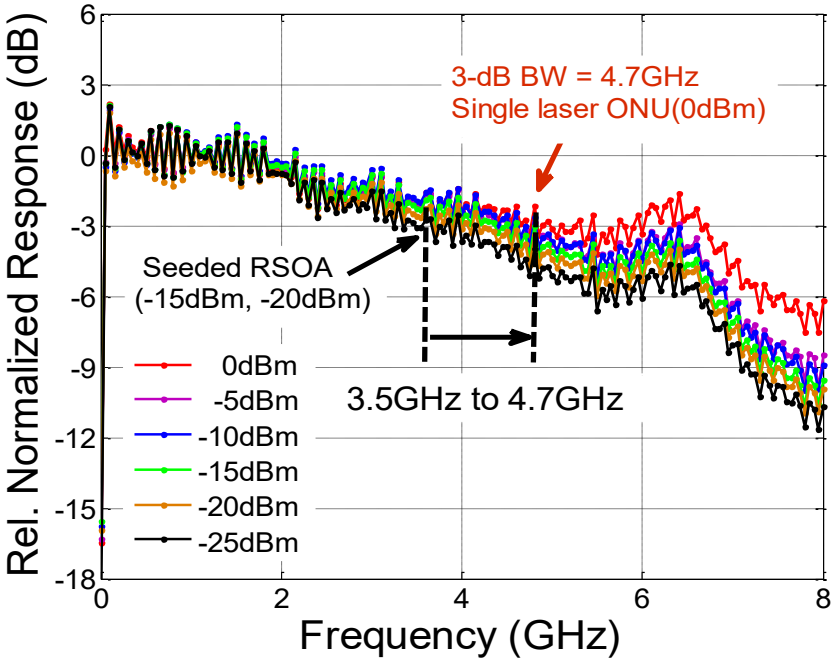

FIGURE 3.5: Frequency response as a function of the input powers of 0 dBm, -5 dBm, -10 dBm, -15 dBm, -20 dBm and -25 dBm at the injected current of 140 mA for RSOA chip.

3.4 Experimental setup

For the experiments, in order to evaluate the BER performances, we compare the long cavity RSOA with a traditional RSOA. On one hand, The optimal input signal amplitude at the long cavity 850 μm RSOA chip is V_{pp}=0.86 V and V_{pp}=1.47 V at 1.25 Gb/s and 2.5 Gb/s, respectively. On the other hand, the To-can packaged RSOA had been equalized using RC components in order to extend its modulation BW from 800 MHz to 1.5 GHz [5] and its input driving amplitude is 3V, both for 1.25 Gb/s and 2.5 Gb/s.

Insensitivity with respect to polarization fluctuations can be achieved in coherent optical communication if the receiver derives two demodulated signals stemming from two orthogonal polarizations of the received signal [19, 20], the schematic is shown in Figure 3.6.

A total of encoded 2^{18} bits consisting of non-return to zero (NRZ) binary sequences are differentially encoded and modulate the RSOA at 1.25 Gb/s and 2.5 Gb/s, for ECL-DFB and DFB-DFB Tx and LO combinations. The electrical data are amplified before modulation to obtain 180° phase variations, obtaining a DPSK signal. The optical signal, with 0 dBm input power from DFB at the ONU (5 MHz linewidth), through modulating RSOA, is then sent back-to-back and after 50km, together with an optical splitter at remote node for ultra-dense channels, and finally optical attenuator is used to change the received input power at receiver at the OLT.

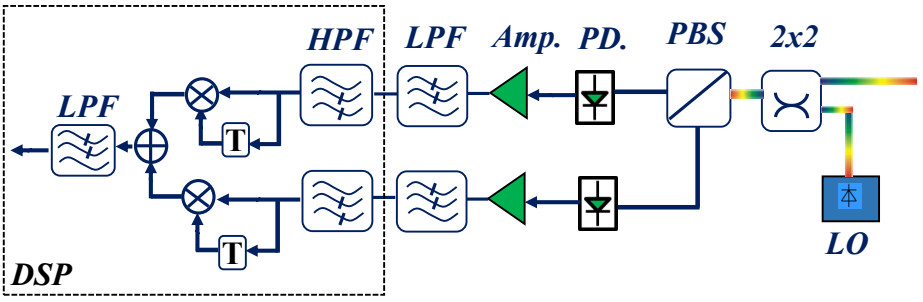

FIGURE 3.6: Polarization diversity heterodyne Rx.

The OLT receiver for upstream transmission is based on heterodyne detection and composed of a 50/50 coupler which mixes the received signal with the LO. The LO is firstly an external cavity laser (ECL) (100 kHz linewidth) and secondly a DFB (4 MHz) tuned at the emission frequency offset of 2.5 GHz (for 1.25 Gb/s) and of 5GHz (for 2.5 Gb/s) above the transmitted wavelength. A Polarization beam splitter (PBS) is included to resolve the polarization fluctuations, and only two single-ended PD [20, 21] are used for polarization diversity detection. The electrical signals are then sampled with a 50 G samples/s real-time oscilloscope (DPO71254B, limited at 12.5 GHz). The samples are

filtered with a high-pass filter (HPF) after the low pass filtering from the Oscilloscope, and passed through a 1-bit delay-and-multiply block for differential demodulation (Figure 3.6). Before bit decision, samples are filtered with a 4th order Butterworth low-pass filter (LPF).

For comparison, the To-can RSOA is mainly used for colorless ONU as the previous work [5]. As explained in the first paragraph, the RSOA is traditionally used as intensity modulation for WDM-PON. Here, we modulate the signal in phase, and use the polarization diversity receiver to coherently receive the signal without polarization controller.

3.5 Performances analysis

First, it is necessary to optimize the receiver in order to obtain the optimal condition for testing. In order to select the optimal operation point of the filters in the digital signal processing (DSP), we measure the BER for different cut-off frequencies for the 4th order low pass and high pass filters.

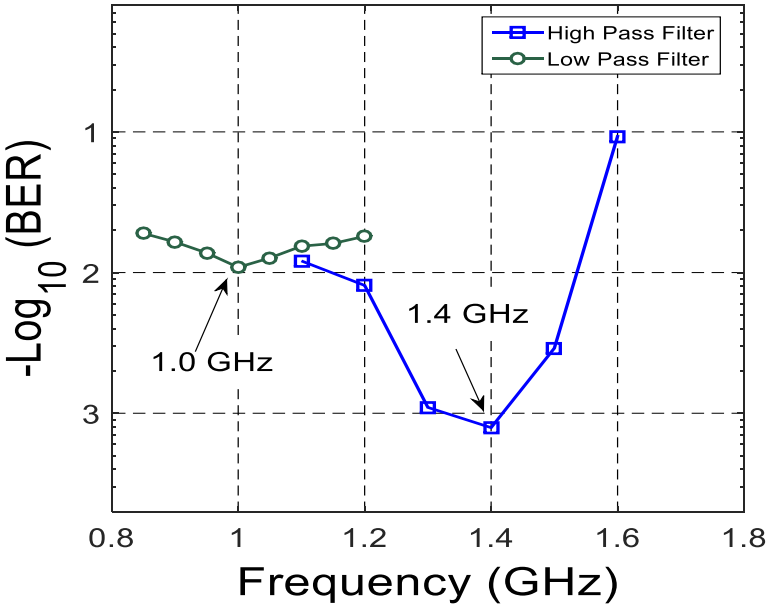

FIGURE 3.7: BER penalty against cut-off frequencies of the low pass (Rx input power at -50.6 dBm) and high pass (Rx input power at -47.5 dBm) filters at 1.25 Gb/s.

The transmitter source is a DFB laser, whose wavelength is influenced by the temperature controller, and as for the LO we compare DFB and ECL. For proper heterodyne detection, the two wavelengths should be precisely matched [4]. We investigate the BER penalty caused by the mismatch around the nominal intermediate frequency (IF), the

3.8 shows the IF margins of around 50 MHz and 100 MHz tolerable at 1.25 Gb/s, 2.5 Gb/s, respectively.

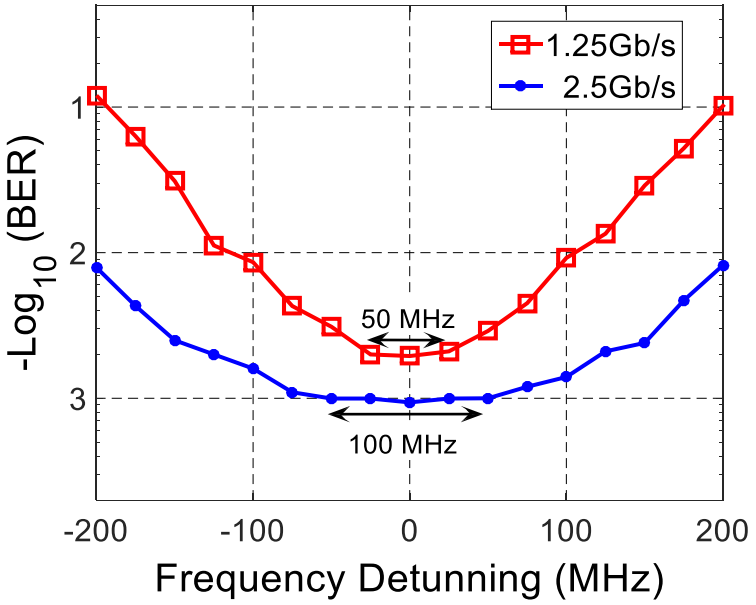

FIGURE 3.8: BER penalty versus frequency offset between Tx and LO (Rx input power at -46.6 dBm and -41.7 dBm for 1.25 Gb/s, 2.5 Gb/s, respectively).

At BER=10^{-3}, the measured Rx sensitivities are around -46 dBm and -41.8 dBm for 1.25 Gb/s and 2.5 Gb/s, respectively (Figure 3.9), first using the To-can RSOA. After 50 km, and with fluctuating polarization, the power penalty is limited to only 0.5∼0.8 dB (from -46 dBm to -45.2 dBm at 1.25 Gb/s, and from -41.8 dBm to -41.3 dBm at 2.5 Gb/s). Next, we apply DFB as Tx and another DFB as LO; the Rx sensitivity is then around -44.5 dBm for back to back, and -43.6 dBm after 50 km at 1.25 Gb/s (Figure 3.9). Compared to the DFB-ECL scheme, the 2 DFBs scheme presents low cost advantages and only around 1.5 dB (1.5 dB for back to back, 1.6 dB after 50 km) penalty, mostly caused by the increased phase noise and wavelength drifts; the influences of the wavelength drifts can be reduced via automatic wavelength controlling [22].

Now, using the RSOA chip for upstream modulation, and at the ONU, the DFB laser as emitter and as downlink LO, we also test it at 1.25 Gb/s, and 2.5 Gb/s at 25 °C. At BER=10^{-3}, the sensitivity reaches -47.3 dBm (1.25 Gb/s) and -42.8 dBm (2.5 Gb/s) as shown in Figure 3.10. The chip is designed with a relatively low value (confinement=20%), which appears to be the optimum one. In order to compare the performances between two kinds of chips, the To-can RSOAs performance in BtB condition are also added again in Figure 3.10. Compared with the To-can packaged RSOA, the 850 μm RSOA-chip improves around 1 dB of the Rx sensitivity at 1.25 Gb/s and 2.5 Gb/s (back to back, 25 °C). The optimal input driving amplitude is 0.86 V_{pp} (1.25 Gb/s)

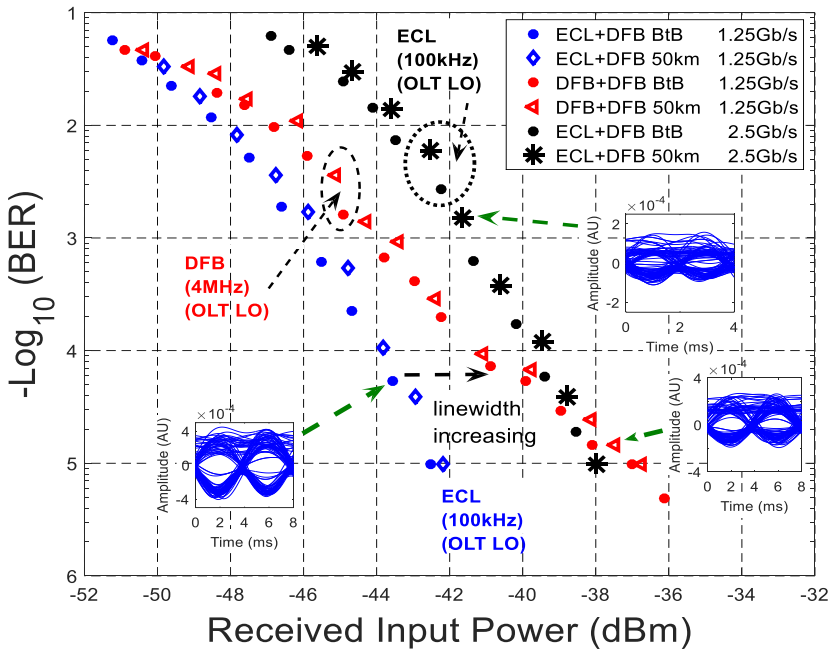

FIGURE 3.9: BER against Rx power back-to-back and after 50km at 1.25 Gb/s and 2.5 Gb/s (DFB as transmitter at ONU, and ECL as LO at OLT) together with 2 DFBs at 1.25 Gb/s.

and 1.47 V_{pp} (2.5 Gb/s). It is 10.9 dB (1.25 Gb/s) and 6.2 dB (2.5 Gb/s) lower than the case of the To-can RSOA, which highly benefits the electrical power requirements. The RSOA chip is also tested at the temperature of 22 °C as shown in Figure 3.10, for back to back transmission, the sensitivity reaches -48.2 dBm and -44.3 dBm for 1.25 Gb/s and 2.5 Gb/s, respectively. There is less than 1 dB penalty between back-to-back and 50 km transmission. Significantly, the RSOA chip could be integrated together with the laser as an integrated component which would be a simplified and low-footprint element for the ONU Tx and Rx.

Furthermore, the proposed system provides a total power budget of 52.2 dB for ODN loss at 1.25 Gb/s, and 48.3 dB at 2.5 Gb/s. It can be exploited to support a large splitting ratio and long reach PON. This is more than enough to support long reach operations [23] (up to 100 km length, corresponding nominally to 20 dB losses) and more than 28 dB [24] margin to allow for power splitting and other intrinsic ODN losses.

3.6 Conclusion

A simple, cost-effective, hardware-efficient, and high sensitivity scheme at the ONU is proposed, increasing the loss budgets and separating the wavelength between the

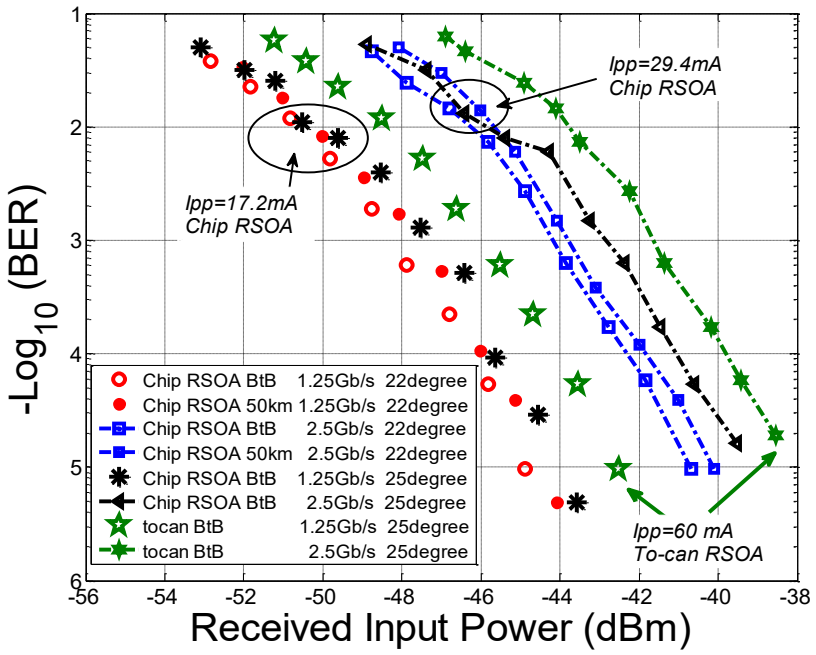

FIGURE 3.10: BER versus Rx power using RSOA chip compared with To-can RSOA (back to back, 25 °C), and RSOA chip at 22 °C.

downstream and upstream, which would improve the bidirectional systems performance significantly. A polarization insensitive heterodyne receiver is built at the OLT with minor penalty comparing ECL and DFB as LO that can be integrated as a low footprint and cost effective transceiver at the ONU [2, 12].

The high injected power unlike the traditional seeded RSOA ONUs significantly improves the modulating bandwidth and the power budget. Compared with the To-can packaged RSOA, the RSOA chip presents the advantages at bandwidth, sensitivity and power consumption. Furthermore, the schematic at the ONU can be integrated as a -agnostic ONU with a wavelength for each user, which is suitable for UDWDM-PON.

By optimizing the receiver both in terms of sensitivity, polarization independency and by optimizing the modulator, the work here enables a low cost UDWDM-PON [24, 25] with high channel number and a power budget in excess of 48 dB.

3.7 References

[1] F. Saliou, G. Simon, P. Chanclou, M. Brunero, L. Marazzi, P. Parolari, M. Martinelli, R. Brenot, A. Maho, S. Barbet, G. Gavioli, G. Parladori, S. Gebrewold, J. Leuthold, 125-km Long Cavity Based on Self-Seeded RSOAs Colorless Sources for 2.5-Gb/s DWDM Networks, IEEE/OSA J. Lightw. Technol., 33, 1602 (2015).

[2] J. Prat, I. Cano, M. Presi, I. Tomkos, D. Klonidis, G. Vall-llosera, R. Brenot, R. Pous, G. Papastergiou, A. Rafel, E. Ciaramella, Technologies for a Cost-effective udWDM-PON, IEEE/OSA J. Lightw. Technol., Nov. 2015. DOI: 10.1109/JLT.2015.2499381.

[3] J. Fabrega, M. Svaluto Moreolo, F. J. Vilchez, B. R. Rofoee, Y. ou, N. Amaya, G. Zervas, D. Simeonidou, Y. Yoshida, and K. Kitayama, Experimental Demonstration of Elastic Optical Networking utilizing Time-Sliceable Bitrate Variable OFDM Transceiver, in Proceedings of OFC, TU2G.8, San Francisco, (2014).

[4] G. Y. Chu, I. Cano, V. Polo, C. Kazmierski, R. Brenot, J. Prat, Monolithically integrated dual output DEML for full duplex DPSK-ASK and DPSK-SSB ONU in ultra-dense channel spaced access network, IEEE/OSA J. Lightw. Technol., Nov. 2015. DOI: 10.1109/JLT.2015.2501289.

[5] M. Omella, I. Papagiannakis, B. Schrenk, D. Klonidis, J. A. Lazaro, A. N. Birbas, J. Kikidis, J. Prat, and I. Tomkos, 10 Gb/s full-duplex bidirectional transmission with RSOA-based ONU using detuned optical filtering and decision feedback equalization, Opt. Express, 17, 5008 (2009).

[6] M. Morant, T. Quinlan, S. Walker, R. Llorente, Complete mitigation of brillouin scattering effects in reflective passive optical networks using triple-format OFDM radio signals, in Proceedings of OFC, JWA072, Los Angeles, (2011).

[7] J. Prat, Rayleigh Back-scattering reduction by means of Quantized Feedback Equalization in WDM-PONs, in Proceedings of ECOC, Th.10.B.3, (2010).

[8] Tomkos, I.; Miyamoto, Y.; Wellbrock, G.; Winzer, P.J., "Guest editorial: Spatially and spectrally flexible elastic optical networking," IEEE Comm. Magazine, 53, 20, (2015).

[9] J. Prat, V. Polo, P. Zakynthinos, I. Cano, J. A. Tabares, D. Klonidis, and I. Tomkos, Simple intradyne PSK system for UDWDM-PON, Opt. Express, 20, 28758 (2012).

[10] G. Y. Chu, A. Lern, I. N. Cano, V. Polo, J. A. Tabares, J. Prat, Exploiting RSOA for Uplink Transmission with Coherent Detection for Low Cost UDWDM-PON, in Proceedings of ACPC, AF2B.1, Shanghai, (2014).

[11] G. Y. Chu, V. Polo, A. Lern, J. Tabares, I. N. Cano, J. Prat, 1.25-3.125 Gb/s per user PON with RSOA as phase modulator for statistical wavelength ONU, Optics Communications, 357, 34-40, (2015).

[12] M. Presi, R. Corsini, M. Artiglia, and E. Ciaramella, Ultra-dense WDM-PON 6.25 GHz spaced 81 Gb/s based on a simplified coherent-detection scheme, Opt. Express, 17, 22706, (2015).

[13] M. Pantouvaki, Cyril C. Renaud, P. Cannard, M. J. Robertson, R. Gwilliam, A. J. Seeds, Fast Tuneable InGaAsP DBR Laser Using Quantum-Confined Stark-Effect-Induced Refractive Index Change, IEEE Sel. Topics Quan. Electron., 13, 1112, (2007).

[14] V. Sales, J. Segarra, V. Polo, and J. Prat, Statistical UDWDM-PONs Operating With ONU Lasers Under Limited Tunability, IEEE Photon. Technol.Lett., 27, 257, (2015).

[15] G. Y. Chu, A. Lerin, I. Cano, V. Polo, R. Brenot, C. Kazmierski, and J. Prat, Minimizing the Influences of Residual AM Component of RSOA for DPSK UDWDM-PON,, European Semicondictor Laser Workshop, SIV.3, Paris, (2014).

[16] C. Caillaud, G. Glastre, F. Lelarge, R. Brenot, S. Bellini, J. Paret, O. Drisse, D. Carpentier, and M. Achouche, Monolithic Integration of a Semiconductor Optical Amplifier and a High-Speed Photodiode With Low Polarization Dependence Loss, IEEE Photon Technol. Lett., 24, (2012).

[17] Ge de Valicourt, Next Generation of Optical Access Network Based on Reflective-SOA, Selected Topics on Optical Amplifiers in Present Scenario, Dr. Sisir Garai (Ed.), ISBN: 978-953-51-0391-2, InTech (2012).

[18] N. Lindenmann, G. Balthasar, D. Hillerkuss, R. Schmogrow, M. Jordan, J. Leuthold, W. Freude, and C. Koos, Photonic wire bonding: a novel concept for chip-scale interconnects, Opt. Express 20, 17667, (2012).

[19] L. G. Kazvoski, S. Benedetto, and A. E. Willner, Optical Fiber Communication Systems, 4th ed. London, U.K.: Artech House, 1996.

[20] I. Cano, A. Lern, V. Polo, and J. Prat, Simplified Polarization Diversity Heterodyne Receiver for 1.25 Gb/s Cost-Effective udWDM-PON, in Proceedings of OFC, W4G2, San Francisco, (2014).

[21] I. Cano, A. Lern, V. Polo, and J. Prat, Direct Phase Modulation DFBs for Cost-Effective ONU Transmitter in udWDM PONs, IEEE Photon. Technol. Lett., 26, 973-975 (2014).

[22] J. Tabares, V. Polo, I. Cano, and J. Prat, Automatic -Control with Offset Compensation in DFB Intradyne Receiver for udWDM-PON, IEEE Photon. Technol. Lett., 27, 443 (2015).

[23] M. Presi, F. Bottoni, R. Corsini, G. Cossu, E. Ciaramella, All DFB-Based Coherent UDWDM PON With 6.25 GHz Spacing and a ¿40 dB Power Budget, IEEE Photon. Technol. Lett., 26, 107, (2014).

[24] R. Gaudino, Advantages of Coherent Detection in Reflective PONs, in Proceedings of OFC, OM2A.1, Anaheim, (2013).

[25] J. Segarra, V. Sales, V. Polo, J. Prat, Dimensioning OLT architectures for UDWDM-PONs employing coherent transceivers, in Proceedings of ICTON, 2015.

Chapter 4

Dual output DEML for full duplex UDWDM-PON ONU

4.1 Introduction

In order to adapt for 5G Infrastructure Public Private Partnership, the optical communications, in particular optical access network, requires to be refreshed [1]. Compared with the standard 10-gigabit-capable passive optical network [2] and next-generation passive optical network 2 [NGPON2] networks [3]−[5], ultra dense wavelength division multiplexed passive optical network (UDWDM-PON) [1], [6] has advantages of increased capacity per user, inherent optical spectrum selectivity, providing a promising option of each user one wavelength. Hence, the UDWDM-PON becomes an interesting candidate for next generation PONs [1].

The key enabler for UDWDM-PON is coherent detection [1], [6], which implies that a light source is needed for the receiver (Rx) as local oscillator (LO). In order to reduce the complexity of the transceiver (TRx), in particular for the optical network unit (ONU), alternatives has been studied. Recently, colorless ONU with wavelength reuse scheme [9],

[10] and seeding techniques [11], [12] have been tested with optical multiplexing element. Differently, single laser based ONU [1], [7], [8] also can be a solution which shares the optical source for both upstream (US) and downstream (DS). Figure 4.1 shows a general scheme with an ONU having a laser that acts as DS LO and US carrier. Another factor to be considered for UDWDM-PONs is the TRx footprint [1], [7]. Unlike the traditional large footprint $LiNbO_3$ MachZehnder architecture, monolithic integration on InP lowers footprint, consumption, and facilitates the design of complex photonic circuits with multiple functions [13]. In recent years, integrated photonics components have been developed for WDM-PON [1], [7], such as reflective semiconductor optical amplifier [10], [14], binary phase shift keying electro-absorption modulated laser [13], and dual electro-absorption modulated laser (DEML) [15]. In order to simplify the ONU with integrated components and extend their applications for UDWDM-PON with coherent detection, the single integrated transmitter based ONU is desired.

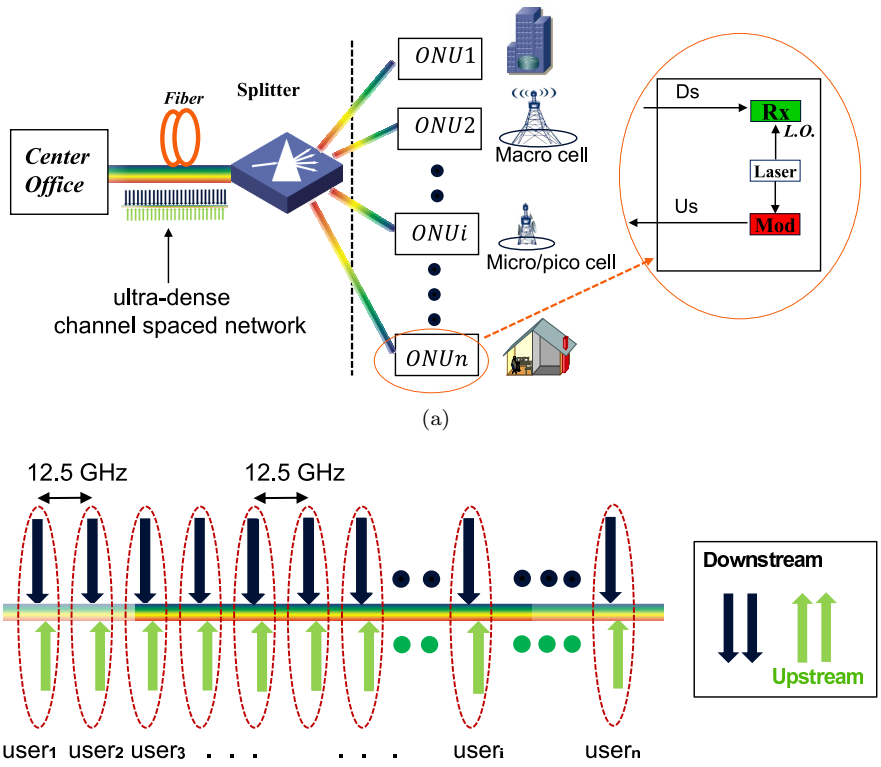

FIGURE 4.1: (a) The application scenario for single laser based UDWDM-PON ONU (b) The spectrum spacing of 12.5 GHz access network.

We have demonstrated the DEML as dual-output integrated chip for UDWDM-PON [16]. In this work, two scenarios are applied for 2.5 Gb/s full duplex transmission: the first one is differentially phase shift keying for downstream, while amplitude shift keying for US transmission (DPSK-ASK); the second one is DPSK for downstream, while single

side band for US transmission (DPSK-SSB). Single integrated transmitter at ONU with heterodyne detection are applied and tested; the ONU Rx uses only one photo detector (PD) and achieves a high sensitivity both at ONU and optical line terminal (OLT). The UDWDM-PON scenario for single integrated laser based ONU is shown in Figure 4.1, and a 12.5 GHz ultra-dense channel spacing spectrum is shown in Figure 4.1. The paper is organized as follows. In Section II, the dual output DEML is described. The full duplex transmission experiment is defined in Section III. The bidirectional DPSK-ASK system is shown in Section IV. In Section V, a full duplex DPSK-SSB system is presented. Finally, we summarize the study in Section VI.

4.2 Description of dual output DEML

The dual-output DEML is based on *AlGaInAs-QW* (quantum well) material due to its large electronic confinement which provides enhanced electro-absorption properties and reduced thermal carrier leakage. It emits in C-band at a wavelength of 1537 nm. The DEML consists of distributed feedback laser (DFB) and electro-absorption modulator (EAM), and the same active layer is used for both laser (DFB) and modulator (EAM) sections. The length of the DFB and EAM sections are around 470 and 75 μm respectively. A schematic representation of DEML chip is shown in Figure 4.2. The III-V epitaxial layers are grown on an InP substrate. Its intrinsic layer contains an *AlGaInAs* multiple-QW(MQW) stack sandwiched by two separate confinement heterostructures [17]. TheEAMis implemented by using a pin diode structure with the active MQW located inside the intrinsic layer. The bias applied to the pin diode adjusts the electrical field in the MQW region and results in the change of optical absorption due to the quantum-confined stark effect. In addition, the waveguide is selectively buried with a tandem layer of semiinsulating InP. The semi-insulating buried structure assures low EAM capacitance and low thermal resistance of the laser [18], [19].

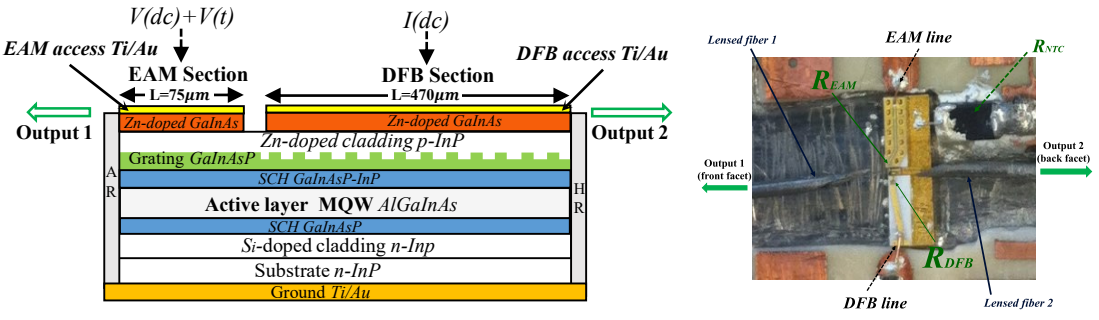

(a) (b)

FIGURE 4.2: (a) Side-view of DEML (b) Assembled two-output-DEML.

The DEML chip (size 0.25 mm×0.5 mm) assembled on a sub-mount (size 2 mm×6 mm×0.5 mm) with its radio frequency data access ceramics for DFB and EAM, the setup is shown in Figure 4.2. The DEML (linewidth, $\triangle\nu$ = 10 MHz) provides two output: one is the DFB output (back facet), another one for EAM output (front facet). In Figure 4.2, two lensed fiber can be seen at both sides, one for EAM and another for DFB. Since there are temperature constraints [17], [18], a temperature sensor (R_{NTC}) is placed beside of the chip and an external control is used to keep the DEML operating at 25 °C. Both the DFB and the EAM have resistors (R_{EAM} and R_{DFB}) of 50 for effective matched impedance. In order to modulate the EAM, we firstly measured the characteristics of the DEML in the front facet. A low-coupling-loss lensed fiber is used for the front facet of the chip. As shown in the Figure 4.3, the DFB has a threshold as low as 11 mA, and the coupled power could reach up to 3.2 mW when DFB is launched at 100 mA thanks to the benefit of low-coupling-loss. The DFB is operated at 70 mA, a balanced value of temperature stability, maximum bandwidth and output power. From Figure 4.3, the bias condition of 2.4 V for EAM (linear region) is chosen, providing -1 dBm output power.

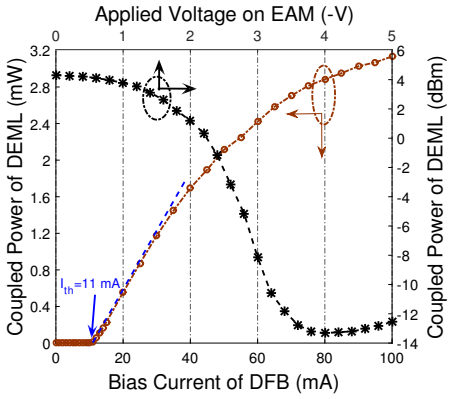

FIGURE 4.3: The characterization of theDEMLs front facet (The front facet coupled power versus DFB bias current (red color,VEAM = 0), and the front facet power versus EAM bias voltage (black color, IDFB = 70 mA)).

4.3 System Setup

The architecture of the proposed ultra-dense access network is shown in Figure 4.4. The OLT consists of several UDWDM TRx coupled, and each TRx corresponds to one ONU. For the ONU, a monolithically integrated dual-output-DEML is used both for DS LO and US optical source, which represents dramatically simplified ONU. As shown in Figure 4.1, the channel spacing in the UDWDM-PON is the standard 12.5 GHz. The backscattering effects are high when the US and DS are separated in frequency by only 1 GHz [20], differently here is 5 GHz. In a multilevel scenario, reflections caused by

many ONUs transmitting simultaneously could reduce the performance. Hence, some kinds of isolators are recommended in the outputs of the DEML. The signal are first generated from OLT. Then, after transmission over the feeder fiber, a power splitter distributes all wavelengths to the ONUs where heterodyne detection takes the benefits of the high sensitivity and the fine selection for thewavelength. It requires no optical filtering to select thewavelength for each ONU, thus being compatible with currently deployed PON distribution networks [21]−[23]. The polarization controller at ONU can be removed by following ways, such as the proposed common polarization scrambler [23] or using diversity [6].

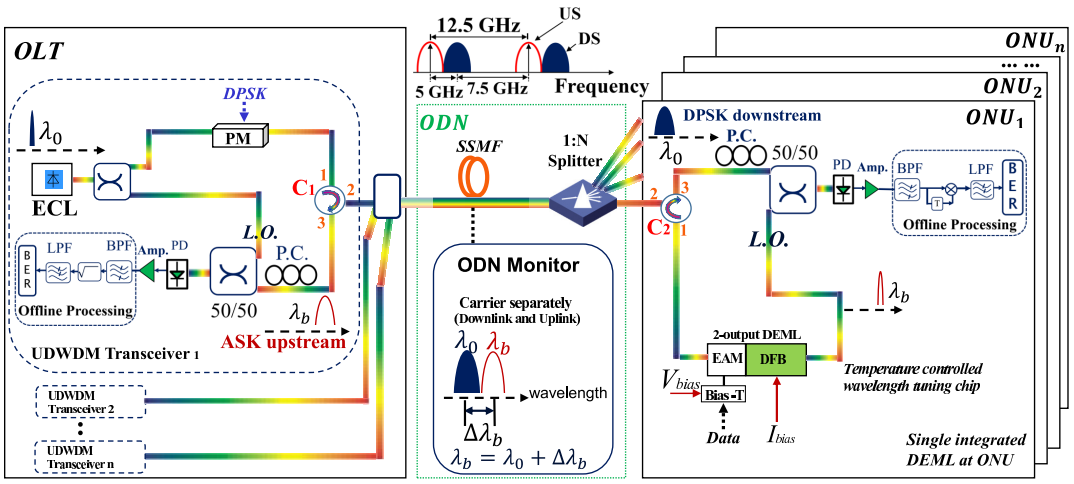

FIGURE 4.4: Monolithically integrated dual-output-DEML based ONU for 2.5 Gb/s bidirectional coherent UDWDM-PON (ODN. optical distribution network).

For DS, a total of 2^{18} bits consisting of non-return to zero (NRZ) binary sequences are differentially encoded and modulate the phase modulator (PM) at 2.5 Gb/s. The ECL output is divided with an optical coupler to reuse it for the Rx. The electrical data is amplified before modulation to obtain 180 ° phase variations, obtaining a DPSK signal. The DS optical signal is then sent through the optical distribution network which is composed of 50 km standard single mode fiber and a power splitter. At ONU, the DFB section of the integrated DEML is employed, in order to detect the signal, the ECL at OLT is tuned at 5 GHz shifted against the US carrier, which provides an intermediate frequency to perform the DPSK heterodyne detection. The DS and LO are mixed in a 3 dB coupler and one output is detected with 1 PD followed by a low-noise electrical amplifier. The electrical signal is band-pass filtered, decoded with a delay and multiply block and low-pass filtered. The bit error ratio (BER) is then calculated.

The US uses the same DFB in the integrated DEML at the ONUas optical carrier. TheEAMsection of theDEMLis modulated with 2.5 Gb/s NRZ data to generate an ASK optical signal. After the distribution network, at the OLT the US signal is detected with a heterodyne Rx with the ECL optical output as LO. As in the ONU, only 1 PD is used

for detection. Afterwards, the electrical signal is amplified and band-pass filtered. An envelope detector followed by a low-pass filter is then employed to decide the Rx bit and finally compute the BER.

4.4 Bidirectional DPSK-ASK transmission

4.4.1 Unidirectional transmission for DPSK DS

The DS is a DPSK signal modulated with the $LiNbO_3$ phase modulator (PM) at the OLT and detected with a heterodyne Rx in the ONU. The DFB section of the DEML is used as LO. It has a threshold as low as 11 mA, and the back facet provides -9 dBm optical power for DS LO. This power is restricted by the high reflection (Figure 4.2) coating on the back facet. The BER against received input power is shown in Figure 4.5; the sensitivity for 2.5 Gb/s at $BER = 10^{-3}$ reaches -35 dBm and -34.2 dBm for back-to-back (BtB) and 50 km transmission, respectively. There is a BER floor appearing around $BER = 10^{-5}$. This is caused by the phase noise in the Rx which is not completely compensated. The 2.5 Gb/s signal spectrum from electrical spectrum analyser (ESA) is shown in the inset. The output power of DEMLs back facet can be increased later by reducing the coating reflection, A 6 dB sensitivity improvement would be expected when 0 dBm is provided, according to simulations.

4.4.2 Unidirectional transmission for ASK US

For US, an ASK signal is produced by modulating the EAM section of the DEML. The EAM section is modulated at the bias condition of -2.4 V with a peak-to-peak signal amplitude of 1 V. At the OLT, a heterodyne Rx reusing the Tx LO detects the signal. The frequency offset between the signal and the LO is 5 GHz. Figure 4.6 shows the BER against the received optical power in the OLT in BtB and with 50 km fiber link. Negligible penalty is observed between two conditions as the Rx sensitivities at $BER = 10^{-3}$ are -40.5 dBm and -39.7 dBm for BtB and 50km, respectively. The eye diagram and the signal spectrum are also shown in the inset of Figure 4.6. Compared with DS, the Rx sensitivities are improved. The reason is because the LO at the OLT has an optical power of 0 dBm which is 9 dB higher than the LO at the ONU. Furthermore, the coherent ASK can allow more phase noise tolerance than coherent DPSK [24-28] which explains that there is no BER floor in Figure 4.6.

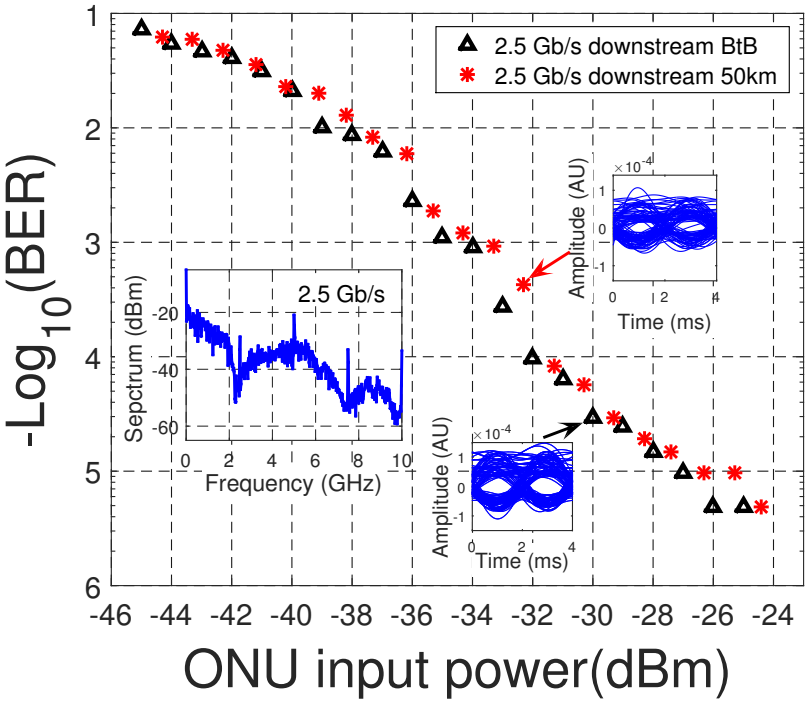

FIGURE 4.5: DS BER versus received input power for BtB and 50 km transmission (the insets. heterodyne spectrum from ESA and eye diagram).

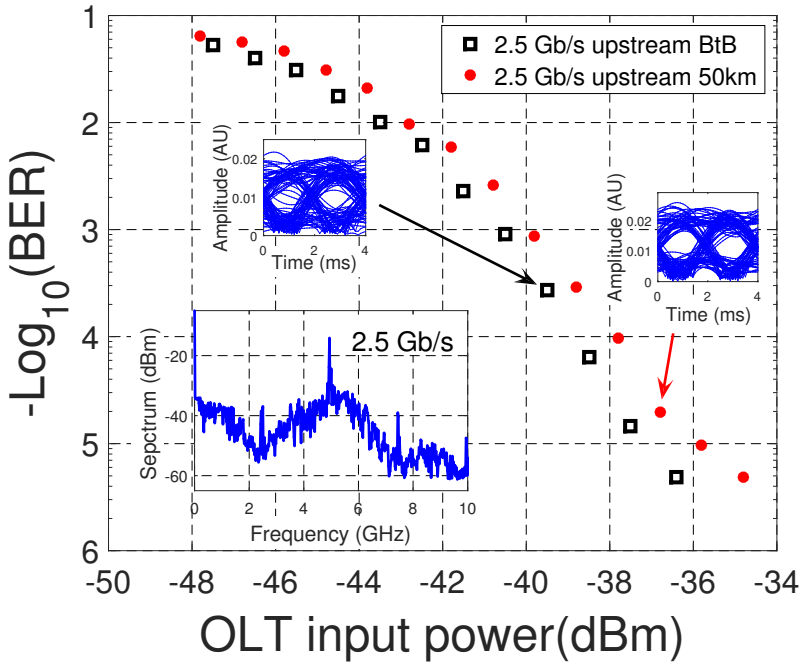

FIGURE 4.6: US BER versus received input power for BtB and 50 km transmission (the insets. heterodyne spectrum from ESA and eye diagram).

4.4.3 Full duplex DPSK-ASK transmission

After the proper detection of DS and US separately, both systems are put into operation simultaneously with 5 GHz spectral separation. The results are plotted in Figure 4.7. The coherent ASK can allow more phase noise tolerance than coherent DPSK [24], which explains that the DS presents more influences on the BER floor. Furthermore, as expected the US performance is better than DS because of the limited LO power in the ONU.

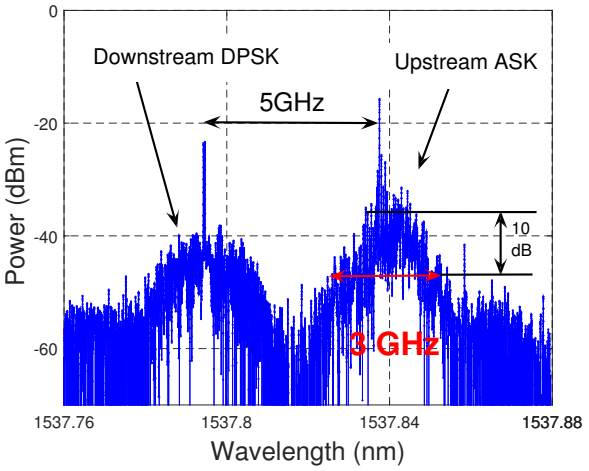

(a)

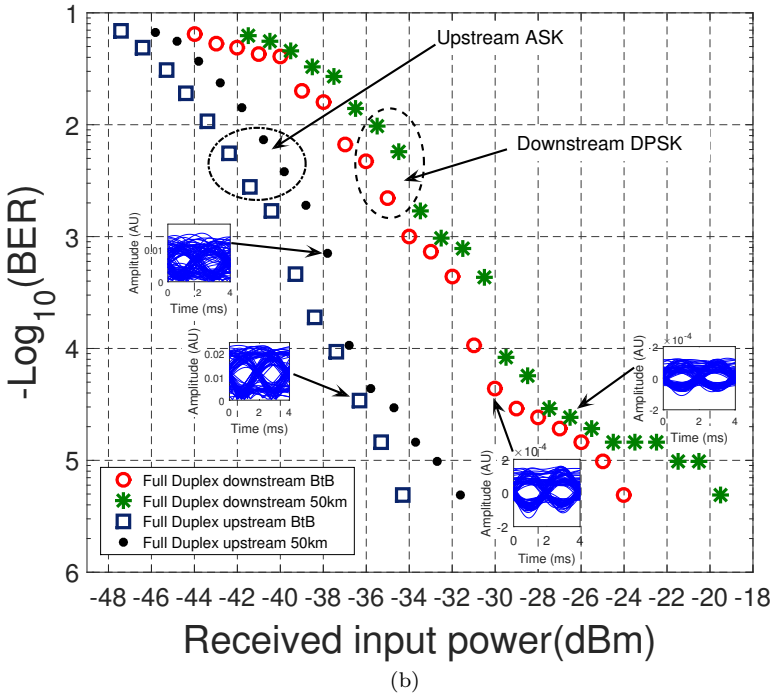

(b)

FIGURE 4.7: (a) DPSK-ASK bidirectional spectrum (b) DPSK-ASK bidirectional transmission performances and the insets show eye diagrams.

At $BER = 10^{-3}$, the DS Rx sensitivity is -34.1 dBm and -32.4 dBm at BtB and with 50 km fiber transmission. There is approximately 1.7 dB penalty between BtB and 50 km fiber transmission, which is 0.9 dB larger than the case of unidirectional transmission. Less than 1 dB penalty is found compared with unidirectional transmission (Figure 4.5) for BtB, and 50 km transmission has a BER floor from the backscattering effects.

The upstream transmission, the sensitivity reaches -39.8 dBm and -38 dBm for BtB and 50 km transmission, respectively. Compared with unidirectional case, there is 0.7 dB and 1.7 dB penalty for BtB and 50 km at $BER = 10^{-3}$. The higher penalty for the 50 km case is because part of the spectrum overlapped causing backscattering and degrading the performance. In BtB, the penalty is mainly due to some reflections that appear in the bidirectional system [29], [30]. However, both US and DS are successfully detected.

The optical spectrum is monitored using a high resolution optical spectrum analyser (HR-OSA) as the Figure 4.7 upper, which shows a 5 GHz channel spacing between DPSK DS and ASK US. The spectrum 10-dB bandwidth for upstream is 3 GHz. The eye diagrams are shown in the inset of Figure 4.7 bottom. When more users transmit simultaneously, the crosstalk due to fiber nonlinearities can degrade the performance. In addition, a high level of noise in the Rx is expected because of the PDs detecting a high signal power. The nonlinearities effects could be reduced by limiting the optical power in the fiber, however further tests are required to evaluate the penalty for multiuser bidirectional transmission.

4.5 Bidirectional DPSK-SSB transmission

4.5.1 Single side band generation with DEML for US

The available spectrum must be used in an efficient way to serve more users in an UDWDM-PON. The ultra-narrow channel spacing requires the signal spectral bandwidth to be as compact as possible. We thus investigate the generation of an optical single side band (OSSB) signal with the DEML.

For SSB generation, it was first performed with laser as early as 1994, for the case of low adiabatic chirp [31]. The method called FM-AM was firstly proposed by *H. Kim et al.* in [32]. The DEML for SSB was performed in [17] by matching AM and FM, for the applications for high bit-rate dispersion compensating transmission.

By modulating the EAM with a proper value also can generate a SSB. In order to prove the concept, we firstly employ an electrical sinusoidal signal at 500 MHz to modulate

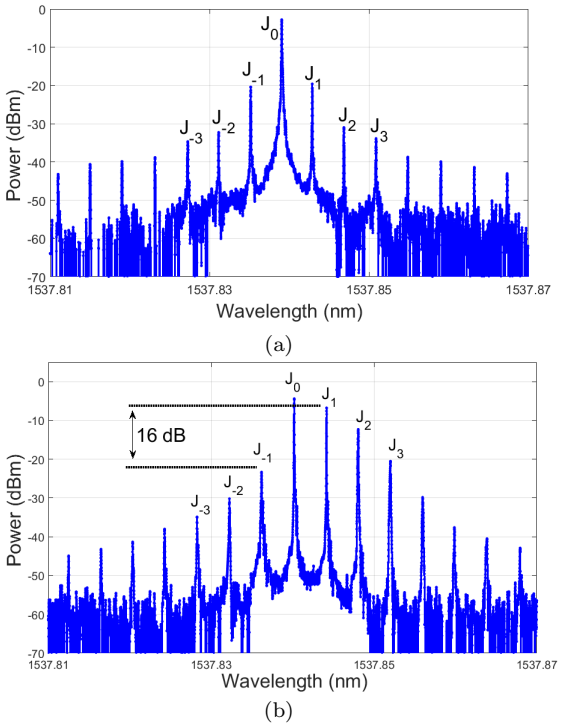

FIGURE 4.8: (a) Discrete-time signal for ASK mode with signal amplitude of 1 V_{pp} (b) discrete-time signal for ASK mode with signal amplitude of 2.4 V_{pp}.

the EAM and the signal spectra are captured with a HR-OSA as shown in Figure 4.8. When injecting with a signal amplitude of 1 Vpp (corresponding to the previous measurements), the spectrum has a slight asymmetries: less than 2 dB. This is explained by the fact that part of the modulating current from EAM is reflected towards to the DFB, hence some optical phase modulation is produced by the DFB due to its clamped operation [33], [34]. This reflection increases when signal amplitude of EAM is increased. Hence, the phase modulation of DFB together with the amplitude modulation of the EAM produce the OSSB [17], [34]. As observed in Figure 4.8, with a data signal peak-to-peak amplitude of 2.4 Vpp, the power of J_{-1} is 16 dB lower than J_1, producing an almost OSSB signal.

We hence modulate the EAM with a 2.4 Vpp electrical data at 2.5 Gb/s. The EAM bias condition is the same as in the previous sections (-2.4 V). The Rx at the OLT is identical to the one employed in section IV. We test firstly unidirectional transmission for the US. The BER against the received optical power is plotted in Figure 4.9. At $BER = 10^{-3}$, the Rx sensitivities are -43.6 dBm and -42.4 dBm for BtB and 50 km fiber link respectively.

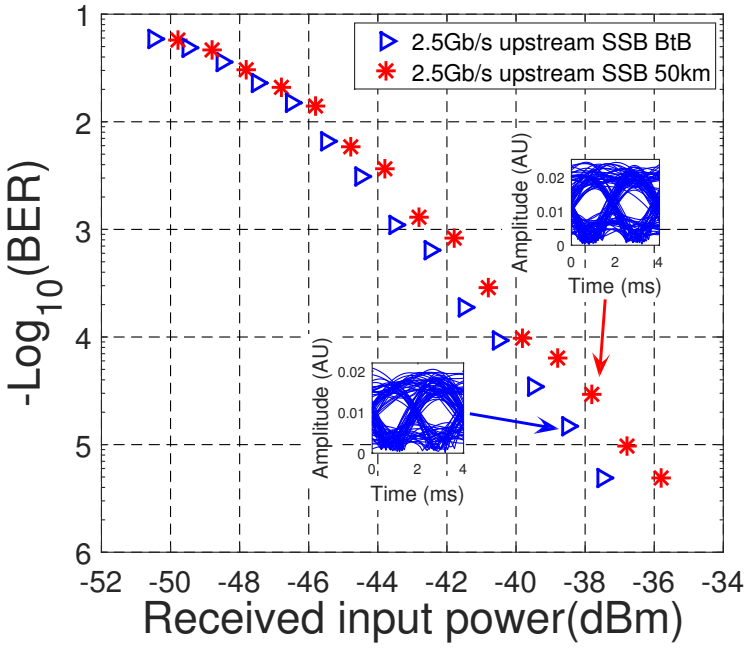

FIGURE 4.9: US SSB BER versus Rx power and the insets show eye diagrams.

4.5.2 Full duplex DPSK-SSB transmission

We then test the OSSB in a bidirectional transmission keeping a 5 GHz separation between US and DS. The Rx in the OLT and ONU are identical to the ones described in the section IV - C part. The results are shown in Figure 4.10.

For the full duplex DS, the sensitivity for 2.5 Gb/s at $BER = 10^{-3}$ reaches -33 dBm and -31.5 dBm for BtB and 50 km transmission, respectively. Compared with unidirectional transmission (previous section IV, Figure 4.5), there is only around 2 dB penalty for back-to-back, and 50 km transmission, and it tanks to the wavelength separation between US and DS. The BER penalty comes from the backscattering effects for full duplex transmission.

For US, the Rx sensitivity at the OLT is -42.7 dBm and -41.6 dBm at BtB and 50 km fiber correspondingly. The penalty compared with unidirectional transmission is reduced to 1 dB indicating that the backscattering has a lower effect than in the double side band (DSB) case. This is because the DS/US spectra do not overlap as much as with the DSB (section IV) as can be noticed in Figure 4.10. Besides, the BW is 1.75 GHz, the occupancy for the spectrum is reduced. Furthermore, the difference in the Rx sensitivities between US and DS are due to the dissimilar LO powers in the ONU and OLT.

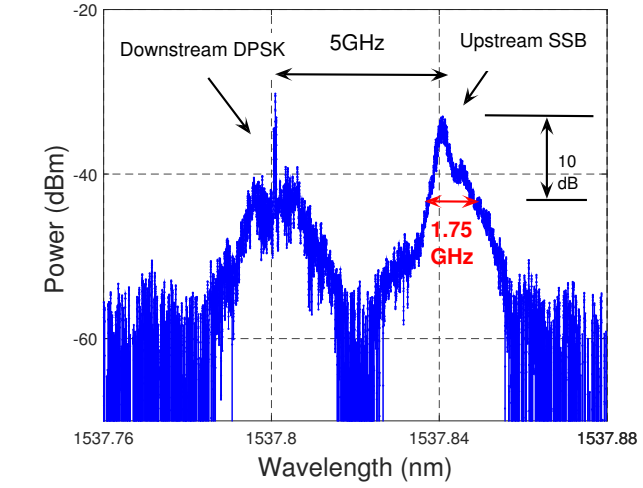

(a)

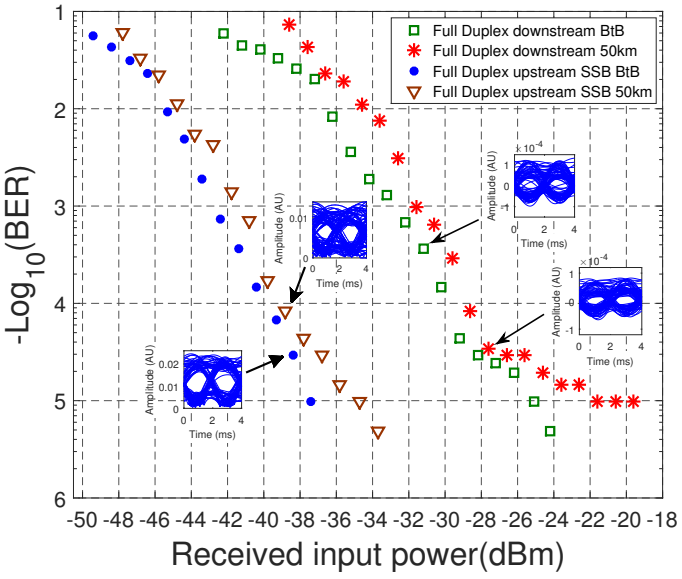

(b)

FIGURE 4.10: (a) DPSK-SSB bidirectional spectrum (b) DPSK-SSB bidirectional transmission performances and the insets show eye diagrams.

4.6 Conclusion

We demonstrate a dual output DEML as TRx in an UDWDM-PON ONU. The DEML is a single integrated chip consisting of a DFB and an EAM. The DEML is both Tx and LO in the Rx for a low footprint and simplified coherent ONU. The ONU is experimentally tested in a bidirectional link at 2.5 Gb/s DS/US with 5 GHz separation between them. The DS is a DPSK signal, whereas the US is ASK produced by modulating the EAM. The Rx at the ONU and OLT is a heterodyne detector with only 1 PD. In a 50 km fiber link, sensitivities of -32.4 dBm and -38 dBm are achieved for DS and US respectively. The penalty on the DS are because of the low power in the LO. In addition, penalties of almost 2 dB are observed in the bidirectional transmission because of backscattering. By

modulating the EAM with a higher amplitude signal, part of the current leaked into the DFB causing a chirped signal which has the opposite sign in the first harmonic. Hence, an OSSB signal is generated. When testing the bidirectional link with the OSSB, the back scattering effect is reduced to just 1 dB, indicating that potentially the channel spectral separation could be reduced. The proper detection and transmission of data with the dual output DEML suggests it can be employed in a simplified ONU for a future UDWDM-PON.

4.7 Experimental setup for lab measurement

The experimental setup in lab is shown in Figure 4.11.

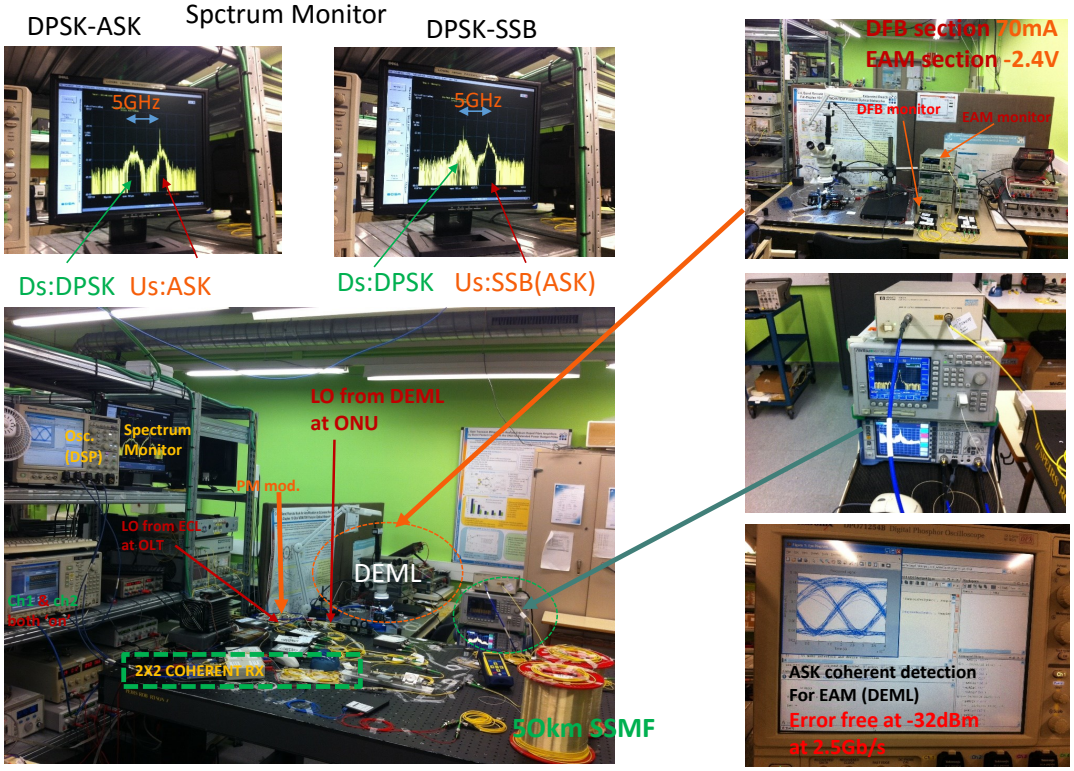

FIGURE 4.11: Experimental setup for dual output DEML.

4.8 References

[1] J. Prat, Technologies for a cost-effective coherent udWDM-PON, presented at the Optical Fiber Communication Conf. Exhibition, Los Angeles, CA, USA, 2015, Paper Th3I.

[2] 10-Gigabit-Capable Passive Optical Network (XG-PON), ITU-T G.987 Series Recommendations.

[3] 40-Gigabit-Capable Passive Optical Networks (NG-PON2), ITU-T G.989 Series Recommendations.

[4] D. Nesset, NG-PON2 technology and standards, IEEE J. Lightw. Technol., vol. 33, no. 5, pp. 11361143, Mar. 2015.

[5] Y. Luo, X. Zhou, F. Effenberger, X. Yan, G. Peng, Y. Qian, and Y. Ma, Time- and wavelength-division multiplexed passive optical network (TWDM-PON) for next-generation PON stage 2 (NG-PON2), IEEE J. Lightw. Technol., vol. 31, no. 4, pp. 587593, Feb. 2013.

[6] M. Presi, R. Corsini, M. Artiglia, and E. Ciaramella, Ultra-denseWDMPON 6.25 GHz spaced 81 Gb/s based on a simplified coherent-detection scheme, Opt. Exp., vol. 23, no. 17, pp. 2270622713, Aug. 2015.

[7] G. Y. Chu, V. Polo, A. Lern, J. Tabares, I. N. Cano, and J. Prat, 1.25 3.125 Gb/s per user PON withRSOA as phase modulator for statistical wavelength ONU, Opt. Commun., vol. 357, pp. 3440, Dec. 2015.

[8] G. Y. Chu, A. Lern, I. N. Cano, V. Polo, J. A. Tabares, and J. Prat, Exploiting RSOAfor uplink transmission with coherent detection for low cost UDWDM-PON, presented at the Asia Communications Photonics Conf., Shanghai, China, 2014, Paper AF2B.1.

[9] M. Omella, A. Jimenez, G. Bosco, P. Poggiolini, and J. Prat, Non-linear function for aGaussian photo-reception in standard IM/DD systems, Opt. Quantum Electron., vol. 42, no. 3, pp. 165178, Feb. 2010.

[10] E. Kehayas, B. Schrenk, P. Bakopoulos, J. A. Lazaro, A. Maziotis, J. Prat, and H. Avramopoulos, All-optical carrier recovery with periodic optical filtering for wavelength reuse in RSOA-based colorless optical network units in full-duplex 10Gbps WDM-PONs, presented at the Optical Fiber Communication Conf. Exhibition, San Diego, CA, USA, 2010, Paper OWG4.

[11] R. Brenot, Demystification of Self-Seeded WDM Access, presented at the Optical Fiber Communication Conf. Exhibition, Los Angeles, CA, USA, 2015, Paper W1J1.

[12] F. Saliou, G. Simon, P. Chanclou, M. Brunero, L. Marazzi, P. Parolari, M. Martinelli, R. Brenot, A. Maho, S. Barbet, G. Gavioli, G. Parladori, S. Gebrewold, and J. Leuthold, Self-seeded RSOAs WDM PON field trial for business and mobile front haul applications,

presented at the Optical Fiber Communication Conf. Exhibition, Los Angeles, CA, USA, 2015, Paper M2A2.

[13] C. Kazmierski, D. Carrara, K. Lawniczuk, G. Aubin, J. Provost, and R. Guillamet, 12.5GB operation of a novel monolithic 1.55m BPSK source based on prefixed optical phase switching, presented at the Optical Fiber Communication Conf. Exhibition, Anaheim, CA, USA, 2013, Paper OW4J8.

[14] G. Y. Chu, V. Polo, A. Len, I. Cano, and J. Prat, Optimizing reflective semiconductor optical amplifier as phase modulator for low cost colorless ONU with 3x3 homodyne detection, presented at the Asia Communications Photonics Conf., Shanghai, China, 2014, Paper AF2B.5.

[15] A. Lern, G. Y. Chu, V. Polo, I. Cano, and J. Prat, Chip integrated DFB-EAM for directly phase modulation performance improvement in UDWDM-PON, presented at the Eur. Conf. Optical Communication, Valencia, Spain, 2015, Paper P.7.10.

[16] G. Y. Chu, I. N. Cano, C. Kazmierski, R. Brenot, and J. Prat, First demonstration of monolithically integrated dual output DEML for full-duplex UDWDM-PON ONU, presented at the Eur. Conf. Optical Communication, Valencia, Spain, 2015, Paper Th.1.3.1.

[17] D. Erasme, T. Anfray, M. E. Chaibi, K. Kechaou, J. Petit, G. Aubin, K. Merghem, C. Kazmierski, J. Provost, P. Chanclou, and C. A. Berthelemot, The dual-electroabsorption modulated laser, a flexible solution for amplified and dispersion uncompensated networks over standard fiber, IEEE J. Lightw. Technol., vol. 32, no. 21, pp. 40684078, Nov. 1, 2014.

[18] C. Kazmierski, Electro-absorption-based fast photonic integrated circuit sources for next network capacity scaling, IEEE/OSA J. Opt. Commun. Netw., vol. 4, no. 9, pp. A8A16, Sep. 2012.

[19] W. S. C. Chang, RF Photonic Technology in Optical Fiber Links. Cambridge, U.K.: Cambridge Univ. Press, 2002, Ch. 6, pp. 166170.

[20] H. Rohde, E. Gottwald, P. Alves, C. Oliveira, I. Dedic, and T. Drenski, Digital multi-wavelength generation and real time video transmission in a coherent ultra-dense WDM PON, presented at the Optical Fiber Communication Conf. Exhibition, Anaheim, CA, USA, 2013, Paper OM3H3.

[21] I. N. Cano, A. Lern, V. Polo, and J. Prat, Direct phase modulation DFBs for cost-effective ONU transmitter in udWDM PONs, IEEE Photon. Technol. Lett., vol. 26, no. 10, pp. 973975, May 15, 2014.

[22] V. Polo, P. Borotau, A. Lerin, and J. Prat, DFB laser reallocation by thermal wavelength control for statistical udWDM in PONs, presented at the Eur. Conf. Optical Communication, Cannes, France, 2014, Paper P.4.1.3.

[23] I. N. Cano, A. Lern,V. Polo, and J. Prat, Polarization Independent Single- PD Coherent ONU Receiver with Centralized Scrambling in udWDMPONs, presented at the Eur. Conf. Optical Communication, Cannes, France, 2014, Paper P.7.12.

[24] L. G. Kazovsky, S. Benedetto, and A. E.Willner, Optical Fiber Communication Systems, 4th ed. London, U.K.: Artech House, 1996, pp. 388390.

[25] J. Prat, V. Polo, P. Zakynthinos, I. Cano, J. A. Tabares, J. M. F'abrega, D. Klonidis, and I. Tomkos, Simple intradyne PSK system for udWDM-PON, Opt. Exp., vol. 20, no. 27, pp. 2875828763, Dec. 2012.

[26] J. M. Fabrega and J. Prat, Homodyne receiver prototype with timeswitching phase diversity and feedforward analog processing, Opt. Lett., vol. 32, no. 5, pp. 463465, Mar. 2007.

[27] J. M. Fabrega and J. Prat, Experimental investigation of channel crosstalk in a time-switched phase diversity optical homodyne receiver, Opt. Lett., vol. 34, no. 4, pp. 452454, Feb. 2009.

[28] M. Presi, M. Artiglia, and E. Ciaramella, Electrical filter-based and lowcomplexity DPSK coherent optical receiver, Opt. Lett., vol. 39, no. 21, pp. 63016303, Nov. 2014.

[29] R. Gaudino, Advantages of coherent detection in reflective PONs, presented at the Optical Fiber Communication Conf. Exhibition, Anaheim, CA, USA, 2013, Paper OM2A1.

[30] J. W. Simatupang and S. L. Lee, Transfer matrix analysis of backscattering and reflection effects on WDM-PON systems, Opt. Exp., vol. 21, no. 23, pp. 2756527577, Nov. 2013.

[31] J. Binder and U. Kohn, 10 Gb/s Dispersion optimized transmission at 1.55mwavelength on standard singlemode fiber, IEEE Photon. Technol. Lett., vol. 6, no. 4, pp. 558560, Apr. 1994.

[32] H. Kim, S. K. Kim, H. Lee, S. Hwang, and Y. Oh, A novel way to improve the dispersion-limited transmission distance of electroabsorption modulated lasers, IEEE Photon. Technol. Lett., vol. 18, no. 8, pp. 947949, Apr. 2006.

[33] C. Kazmierski, A. Konczykowska, F. Jorge, F. Blache, M. Riet, C. Jany, and A. Scavennec, 100 Gb/s operation of an AlGaInAs semi-insulating buried heterojunction

EML, presented at the Optical Fiber Communication Conf. ExhibitionOThT7, San Diego, CA, USA, 2009, Paper OThT7.

[34] C. Kazmierski, N. Chimot, F. Blache, J. Decobert, F. Alexandre, J. Honecker, C. Leonhardt, A. Steffan, O. Bertran-Pardo, H. Mardoyan, J. Renaudier, and G. Charlet, 56Gb/s PDM-BPSK experiment with a novel InP monolithic source based on prefixed optical phase switching, presented at the Int. Conf. Indium Phosphide Related Material, Kobe, Japan, 2013, Paper TuD42.

Chapter 5

Mitigating residual AM using DEML

5.1 Introduction

The explosive growth of telecommunications services, has continued to fuel the deployment of optical access networks [1, 2]. Ultra-dense wavelength division multiplexing (UDWDM) with coherent detection provides a promising option for a wavelength-to-the-user access network [2]. However, the cost and footprint are still vital factors that have to be considered [1-5]. With this purpose, integrated modulators are an interesting option for transmitters (Tx), particularly at the user side. Unlike LiNbO3, monolithic integration on InP presents lower footprint, cost, consumption, and facilitates the design of complex photonic circuits with multiple functions [6]. In recent years, integrated chips are available for WDM passive optical network (WDM-PON) [1-3], such as semiconductor optical amplifier (SOA), reflective-SOA (RSOA) [4, 7-10], binary phase shift keying electro-absorption modulated laser (BPSK-EML) [11], and dual electro-absorption modulated laser (DEML) [3, 11]. The DEML combines a distributed feedback laser (DFB) and an electro-absorption modulator (EAM). It can be easily integrated and fabricated

[11], thus, it is attractive for Tx at the optical network unit (ONU) [3, 11]. Normally, the DEML uses the DFB as the optical carrier source and the EAM for data modulation in intensity. Recently, a method called balanced FM-AM [11, 12] was developed for DEML with the purpose of compensating the fiber dispersion by spectrum sculpting [11, 13]. The DEML also can be directly modulated in phase by equalizing the signal as done with DFBs [14, 15]. Unfortunately, there is a residual amplitude modulation (AM), causing a penalty in the performance [14, 16, 17]. For the receiver (Rx) side, coherent detection presents better performance compared with the direct detection [18-20]. More importantly, it gives the benefit of wavelength selection for ultra-dense channel spaced network without the demand of optical filters. We have demonstrated, in [21], a differential phase-shift keying (DPSK) transmission by means of a DEML. In this work, we explain the assembly for DEML, discuss the effect of mitigation and extend the measurements to 2.5 Gb/s and even 5 Gb/s with intradyne detection. The EAM is employed to mitigate the residual AM produced when directly phase modulating the DFB. An intradyne coherent Rx is tested for detecting the signal. An enhancement of 2.5 dB is achieved when compared with a directly phase modulated DFB, showing that the residual AM is mitigated effectively. This paper is organized as follows: in section 2, the monolithic DEML is introduced and the characteristics on the phase modulating efficiency (PME) are measured. The experimental setup is described in section 3. Then, in section 4, the mitigated residual AM effect and BER performances at 2.5 Gb/s and 5Gb/s are shown. Finally, a conclusion is in section 5.

5.2 Monolithically integrated DEML

The integrated DEML is designed for temperature-stable, energy-efficient, and high-bit rate operation, at an emitting wavelength of 1537 nm. The same active layer is used for both laser (DFB) and modulator (EAM) sections. The length of the DFB and EAM sections is around 470m and 75m respectively. A schematic representation of the DEML chip is shown in Figure 5.1(a). The III-V epitaxial layers are grown on an InP substrate. Its intrinsic layer contains an InGaAlAs multiple-quantum well (MQW) stack sandwiched by two separate confinement heterostructures (SCH). The EAM is implemented by using a pin diode structure with the active MQW located inside the intrinsic layer [13]. The bias applied to the pin diode adjusts the electrical field in the MQW region and results in the change of optical absorption due to the quantum-confined stark effect (QCSE). In addition, the waveguide is selectively buried with a tandem layer of semi-insulating InP [11].

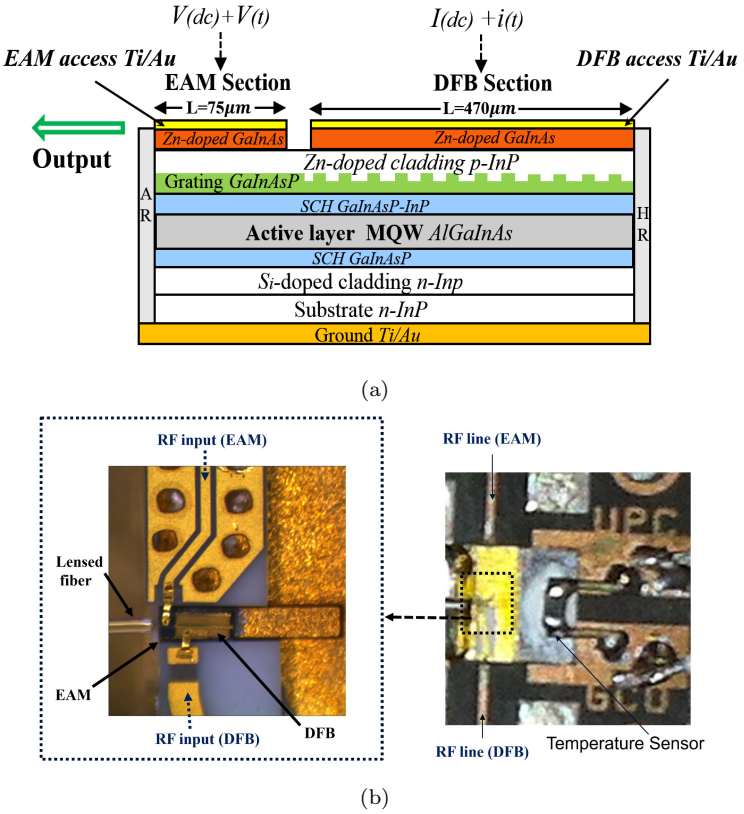

FIGURE 5.1: (a) Side-view of DEML chip structure. (b) DEML chip on a sub-mount showing RF input for DFB and EAM access ceramics.

The semi-insulating buried structure assures a low EAM capacitance and low thermal resistance of the laser [13]. The DEML chip (size 0.25 mm × 0.5 mm) is on a sub-mount (size 2 mm × 6 mm × 0.5 mm) and RF data access ceramics for DFB and EAM are shown in Figure 5.1(b). Both the DFB and the EAM have resistors of 50 for matching the impedance. A microchip circuit board is used to provide the RF access to DFB and EAM. The substrate of circuit board is RO-Duroid-5880 with 0.127 mm thickness, supporting the propriety of maximum bandwidth for the chip assembly [22].

The temperature is controlled by a peltier at an operating condition of 25 °C with the help of a temperature sensor, in order to avoid high wavelength drifts. The DFB threshold is as low as 10 mA as shown in Figure 5.2(a). In the same figure, the output DEML power against the bias voltage of the EAM is plotted. The DFB is adjusted at a bias condition of 50 mA, a balanced value for temperature stability, maximum bandwidth and output power. From Figure 5.2(a), the bias condition of -2 V for EAM is chosen, providing around 0 dBm output power. The linewidth for the DEML is measured at 10 MHz.

Two effects occur when modulating DFB: a variation in the power and a frequency deviation due to the lasers chirp [23]. The frequency deviation is related with phase

modulation (PM) by a derivative term. We firstly obtained the AM and PME of the DFB in this integrated DEML following the procedure described in [23]. A high pass filter based on a simple RC network equalizer is required to obtain the PM. The PME and AM response are shown in Figure 5.2(b). It is observed that the 3-dB modulating bandwidth is around 8 GHz. The PME presents a flat response at low frequencies after using the equalizer (Figure 5.2(b)), reducing phase distortions when it is modulated by the driving current.

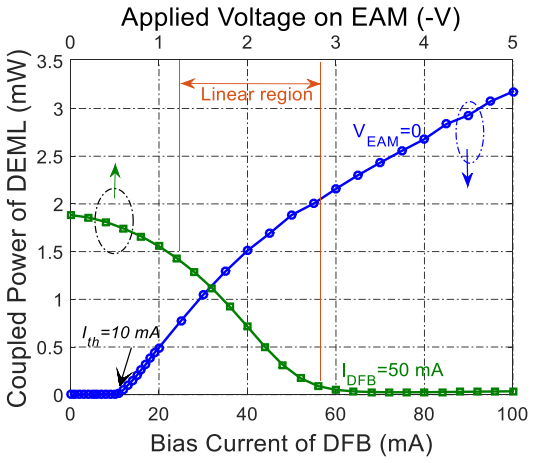

(a)

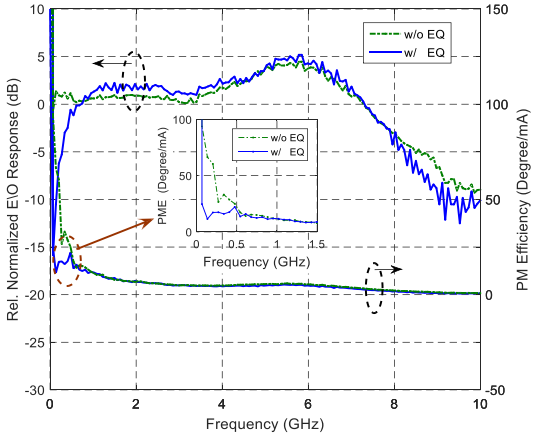

(b)

FIGURE 5.2: (a) DEML characterization. (b) Normalized Frequency Responses.

5.3 Experimental setup

The DEML is modulated with 218 non-return to zero (NRZ) differentially coded bits. The data is generated to modulate the DFB and the EAM as shown in Figure 5.3. Two electrical amplifiers are used to introduce appropriate signal power into the chip [11].

A phase shifter ($\Delta\phi$) is used to adjust the delay of the driving signals to the DFB and EAM [11, 13].

With the purpose of modulating the DFB in phase instead of frequency, the data signal is equalized. Correspondingly, a second equalizer is used for providing a coordinated RF signal to the EAM. After the two equalizers, the signals are injected into the two sections of the DEML. An isolator is used for minimizing the optical reflections introduced from the link. After 50 km standard single mode fiber (SSMF) link, the signal is coherently detected with an intradyne Rx. The local oscillator (LO) is an external cavity laser (ECL) with 0 dBm optical power. A polarization controller (PC) is employed for compensating fluctuations in the state of polarization (SOP) in the fiber. A polarization scrambler [24] or polarization diversity receiver could be used to avoid the PC.

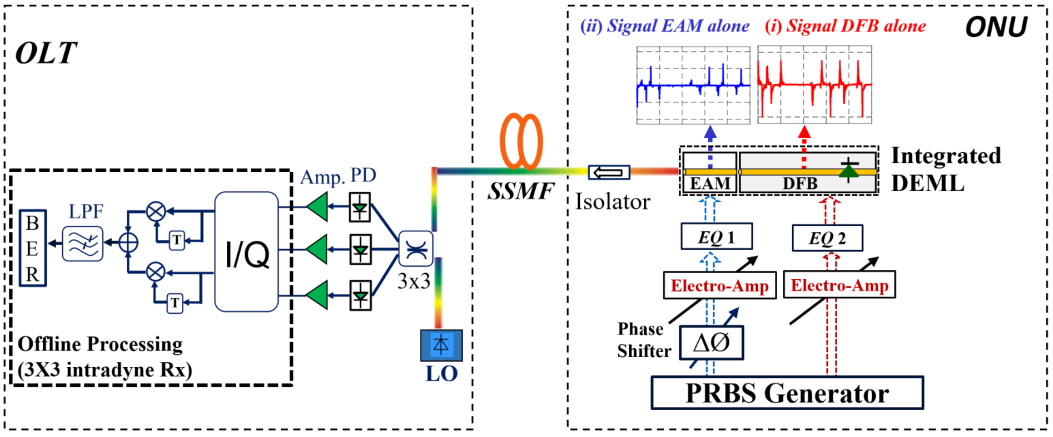

FIGURE 5.3: DPSK with integrated DEML with coherent detection (The inset (i) shows the signals injecting DFB and EAM).

The received data signal is mixed with the LO by means of a 120 optical coupler. The outputs are detected with 3 photo-diodes (PDs) followed by low noise electrical amplifiers. The electrical signals are sampled and digitally processed with a 50GSa/s real time oscilloscope. The I and Q components are computed and filtered, then the samples pass through a 1-bit delay and multiply block for differential demodulation. Before bit decision, samples are filtered with a 4 order butterworth low-pass filter (LPF). Finally, the BER is computed.

5.4 Minimizing residual AM of DEML

With the purpose of minimizing the AM component, the EAM can be modulated with the data that drives the DFB of the DEML. By adjusting the electrical amplifiers and phase shifter, the appropriate amplitude and delay are produced. Figure 5.4 shows the

amplitudes before mitigating residual AM and after the mitigation. The amplitude of the PM signal is around 315 mVpp before mitigating AM. Whereas, after the mitigation by EAM, the amplitude is reduced at almost 40% to 197 mVpp.

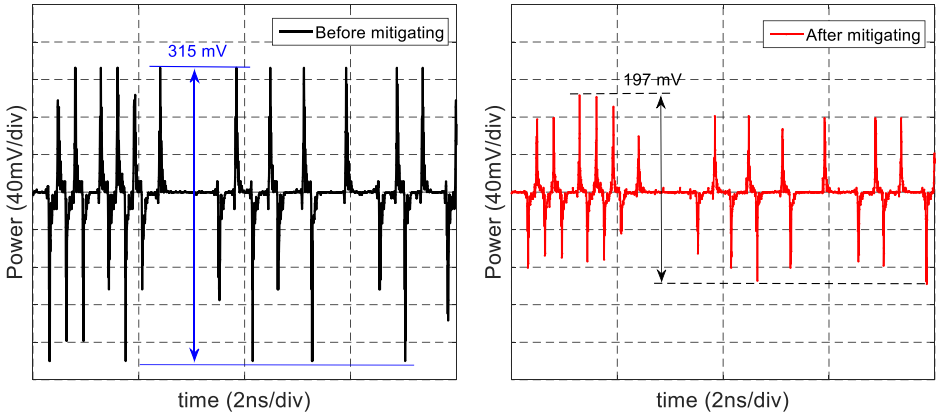

(a)

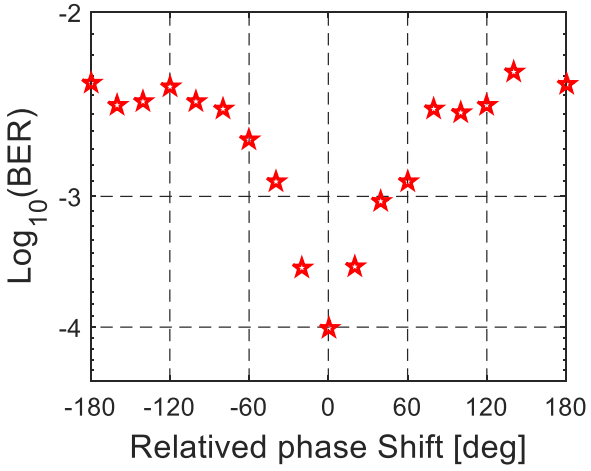

(b)

FIGURE 5.4: (a) The detected 2.5 Gb/s signal amplitudes. (b) BER versus phase shift of the signal between DFB and EAM.

In order to minimize the residual AM, both signals modulating the DEML are synchronized. To guarantee this, a phase shifter ($\Delta\phi$) is introduced (Figure 5.3). The effect on the BER produced by varying the phase shift between the DFB and EAM signals is plotted in Figure 5.4(b). The received power is left constant for a BER of 10^{-4} in the optimal delay. A phase shift of $\pm 20°$ is tolerated with less than 1 dB penalty.

Validating tests are firstly carried out at a data speed of 2.5 Gb/s. The DEML is measured in the following conditions: modulating DFB alone (back-to-back (BtB)); both DFB and EAM are dual driven (BtB), with the signal amplitude for EAM of 0.5 Vpp; and, dual driven (BtB and 50 km transmission) with signal amplitude for EAM

of 2 Vpp. For all the measurements, the signal amplitude for DFB is maintained at 20 mApp. The results are shown in Figure 5.5. For DFB alone, the Rx sensitivity reaches -44 dBm for BtB at BER=10^{-3} (corresponding to a 7% Forward Error Correction, FEC [24, 25]). When the signal amplitude of the EAM only reaches 0.5 Vpp, the sensitivity improves to -44.7 dBm. When minimizing the residual AM by the EAM with 2 Vpp, the Rx sensitivity reaches -46.5 dBm for BtB transmission. There is a marginal penalty for 50km fiber transmission lower than 2 dB. Hence, for intradyne Rx a 2.5 dB enhancement of the sensitivity is obtained when minimizing the residual AM.

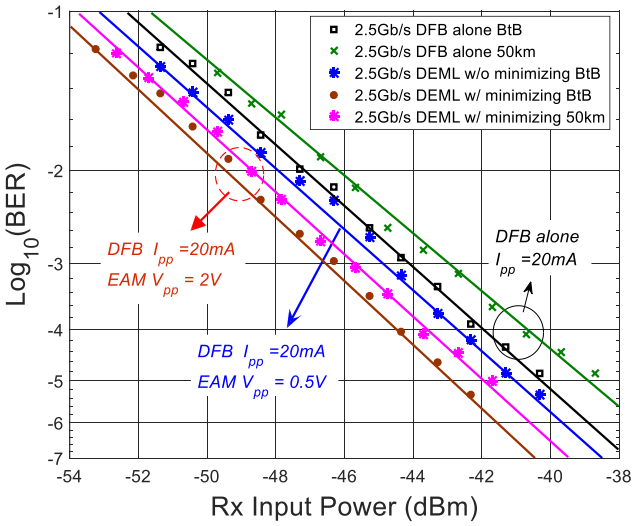

FIGURE 5.5: BER versus Rx input power for 2.5 Gb/s.

Then, in order to extend the bit rate for each user, the case of 5 Gb/s is also measured at the same mitigating condition. The signal amplitudes for DFB and EAM are 20 mApp and 2 Vpp as shown in the Figure 5.6. At BER, the sensitivity reaches -35.3 dBm and -33.2 dBm for BtB and fiber transmission when modulating DFB alone, respectively; and -39.4 dBm, -37.5 dBm for BtB and fiber transmission when dual driven. For the benefit of the mitigating residual AM, there is 4 dB improvement now at the data speed of 5 Gb/s. The BER performances are shown in Figure 5.6.

5.5 Conclusion

A simple, cost-effective ONU Tx based on a novel DEML integrated device with PSK modulation is demonstrated. An approach for mitigating the residual AM of integrated DEML is proposed and experimentally tested, at 2.5 Gb/s and 5 Gb/s.

The synchronization between the DFB and EAM is critical, showing a tolerance of just 20 for maintaining BER=10^{-4}. An improvement of 2.5 dB and 4 dB on the sensitivity

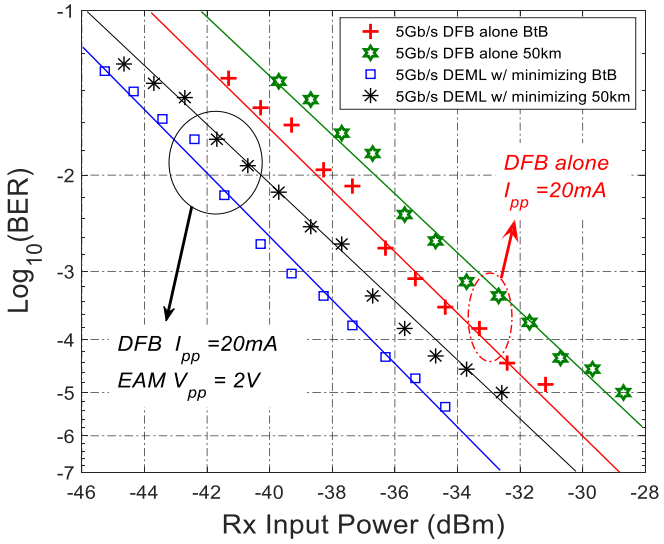

FIGURE 5.6: BER versus Rx input power for 5 Gb/s.

are obtained for 2.5 Gb/s and 5 Gb/s when the residual AM is mitigated. This can potentially help on producing multilevel formats and thus increase the bitrate. Furthermore, DEML promises an economic-efficient solution because both DFB and EAM could be easily integrated in large-scale production.

5.6 References

[1] Y. Luo, X. Zhou, F. Effenberger, X. Yan, G. Peng, Y. Qian, and Y. Ma, Time and wavelength division multiplexed passive optical network (TWDM-PON) for next-generation PON stage 2 (NG-PON2), J. Lightw. Technol., 31(4), 587593, Feb. (2013).

[2] J. Prat, I. Cano, M. Presi, I. Tomkos, D. Klonidis, G. Vall-llosera, R. Brenot, R. Pous, G. Papastergiou, A. Rafel, E. Ciaramella, Technologies for a Cost-effective udWDM-PON, J. Lightw. Technol., (2015).

[3] G. Y. Chu, I. Cano, V. Polo, C. Kazmierski, R. Brenot, J. Prat, Monolithically integrated dual output DEML for full duplex DPSK-ASK and DPSK-SSB ONU in ultra-dense channel spaced access network, J. Lightw. Technol., 34(8), (2016).

[4] R. Brenot, Demystification of Self-Seeded WDM Access, Proc. OFC, W1J1, Los Angeles, 2015.

[5] M. Presi, R. Corsini, M. Artiglia, and E. Ciaramella, Ultra-dense WDM-PON 6.25 GHz spaced 81 Gb/s based on a simplified coherent-detection scheme, Opt. Express, 23(17), 22706, Aug. (2015).

[6] C. Kazmierski, D. Carrara, K. Lawniczuk, J. Provost, and R. Guillamet, 12.5GB Operation of a Novel Monolithic 1.55m BPSK Source Based on Prefixed Optical Phase Switching, Proc. OFC, OW4J8, Anaheim, (2013).

[7] G. Y. Chu, V. Polo, A. Lerín, J. Tabares, I. N. Cano, J. Prat, 1.25-3.125 Gb/s per user PON with RSOA as phase modulator for statistical wavelength ONU, Opt. Comm., 357, 34-40, (2015).

[8] G. Y. Chu, A. Lerín, I. N. Cano, V. Polo, J. A. Tabares, J. Prat, Exploiting RSOA for Uplink Transmission with Coherent Detection for Low Cost UDWDM-PON, Proc. ACPC, AF2B.1, Shanghai, (2014).

[9] F. Saliou, G. Simon, P. Chanclou, M. Brunero, L. Marazzi, P. Parolari, M. Martinelli, R. Brenot, A. Maho, S. Barbet, G. Gavioli, G. Parladori, S. Gebrewold, J. Leuthold, Self-seeded RSOAs WDM PON field trial for business and mobile front haul applications, Proc. OFC, M2A2, Los Angeles, (2015).

[10] M. Omella, I. Papagiannakis, B. Schrenk, D. Klonidis, J. A. Lazaro, A. N. Birbas, J. Kikidis, J. Prat and I. Tomkos, 10 Gb/s full duplex bidirectional transmission with RSOA-based ONU using detuned optical filtering and decision feedback equalization," Opt. Express, 17, 5008-5013 (2009).

[11] C. Kazmierski, Electro-Absorption-Based Fast Photonic Integrated Circuit Sources for Next Network Capacity Scaling, IEEE/OSA J. Opt. Commun. Netw., 4, A8-A16, (2012).

[12] J. Binder and U. Kohn, 10 Gbits/s-Dispersion Optimized Transmission at 1.55 m Wavelength on Standard Single Mode Fiber, IEEE Photon. Technol. Lett., 6(4), (1994).

[13] C. Kazmierski, A. Konczykowska, F. Jorge, F. Blache, M. Riet, C. Jany, and A. Scavennec, 100 Gb/s operation of an AlGaInAs semi-insulating buried heterojunction EML, Proc. OFC, OThT7, San Diego, (2009).

[14] I. N. Cano, A. Lerín, V. Polo, J. Tabares, J. Prat, Simple ONU transmitter based on direct-phase modulated DFB laser with heterodyne detection for udWDM-PON, Proc. ECOC, We.2.F.4, London, (2013).

[15] I. N. Cano, A. Lerín, V. Polo, J. Prat, Simplified polarization diversity heterodyne receiver for 1.25Gb/s cost-effective udWDM-PON, Proc. OFC, W4G.2, San Francisco, (2014).

[16] Y. C. Chung, Recent Advancement in WDM PON Technology, Proc. ECOC, Th.11.C.4, Geneva, (2011).

[17] S. P. Jung, Y. Takushima and Y. C. Chung, Transmission of 1.25Gb/s PSK signal generated by using RSOA in 110-km coherent WDM PON, Opt. Express, 18, 14871-14877, Jul., (2010).

[18] J. Prat, V. Polo, P. Zakynthinos, I. Cano, J. A. Tabares, J. M. Fbrega, D. Klonidis, and I. Tomkos, Simple intradyne PSK system for UDWDM-PON, Opt. Express, 20(27), 28758, (2012).

[19] J.M. Fabrega and J. Prat, Homodyne receiver prototype with time-switching phase diversity and feedforward analog processing, Opt. Lett., 32(5), (2007).

[20] J.M. Fabrega and J. Prat, Experimental investigation of channel crosstalk in a time-switched phase diversity optical homodyne receiver, Opt. Lett., 34(4), (2009).

[21] A. Lerín, G. Y. Chu, V. Polo, I. Cano, J. Prat, Chip Integrated DFB-EAM for directly phase modulation performance improvement in UDWDM-PON, Proc. ECOC, P.7.10, Valencia, (2015).

[22] F. H. Wee, F. Malek, A. U. Al-Amani and Farid Ghani, Effect of Two Different Superstrate Layers OnBismuth Titanate (BiT) Array Antennas, Sci. Reports, 4, 3709, Jan., (2014).

[23] K. Sato, S. Kuwahara, and Y. Miyamoto, Chirp Characteristics of 40-Gb/s Directly Modulated Distributed-Feedback Laser Diodes IEEE/OSA J. Lightw. Technol., 23(11), 3790, (2005).

[24] M. Presi, M. Artiglia, and E. Ciaramella, Electrical filter-based and low-complexity DPSK coherent optical receiver, Opt. Lett., 39(21), 6301-6303, 2014.

[25] I. N. Cano, A. Lerín, V. Polo, and J. Prat Polarization Independent Single-PD Coherent ONU Receiver with Centralized Scrambling in udWDM-PONs, Proc. ECOC, P.7.12., Cannes, 2014.

Chapter 6

Bidirectional DPSK-DPSK transmission with single-DFB ONU

6.1 Introduction

Optical access networks (OANs) based on ultra dense wavelength division multiplexing technology have been demonstrated as potential candidate to increase the network capacity with improved spectral efficiency [1, 2], in order to improve the sensitivity, coherent detection are applied [3-7]. In this chapter, the Polarization independent integrated RSOA are applied for bidirectional transmission subsystem.

In this chapter, we propose and validate a low cost efficient solution for bidirectional coherent transmission with the purpose of avoiding the Rayleigh Backscatterings influences, and we use circulators to avoid the reflections from the transmission link. The structure can be successfully tested because there is a wavelength deviation between

downstream and upstream. We focus on the bidirectional transmission implementations based on RSOA as a phase modulator and DFB laser for both uplinks carrier and downlinks L.O. at ONU. They constitute a potentially integrable solution for the ONU.

6.2 Optimization on operating RSOA as phase modulator

In order to be operated at the best condition for the phase modulation, the gain, the optical-signal-to-noise-ratio (OSNR), amplified spontaneous emission (ASE) noise and the polarization dependent factors are required to be considered [8-20]. Different with Chapter2, here the RSOA is an polarization independent type. Then, the operation is simplified. The method for optimizing phase region consists of tuning both input power and bias current to achieve the minimum residual AM component and the polarization sensitivity. The optimal condition should have a better performance of phase modulating efficiency (PME). The setup is shown in Figure 6.1.

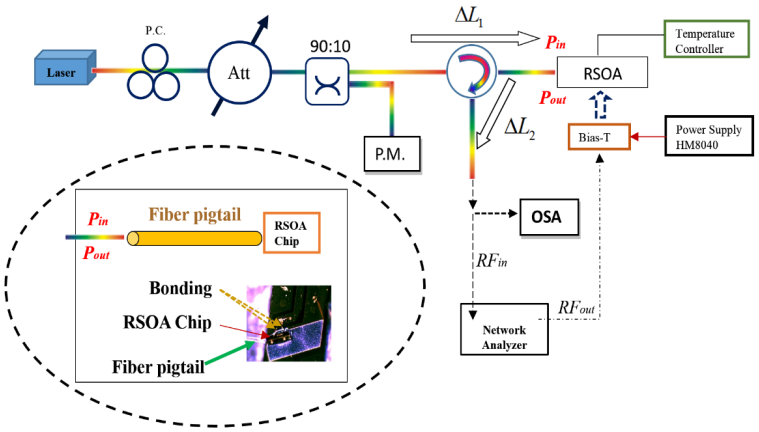

FIGURE 6.1: Experimental setup for measuring the RSOA's characterization.

The equation for gain measurement is as follows:

$$G = 10lg\frac{P^s_{out}}{P^s_{in}} = 10lg\frac{P_{out} - P_N}{P_{in} - P_{sse}} \tag{6.1}$$

where P^s_{out} and P^s_{in} are the pure output power and input power of RSOA, respectively. P_{out} and P_{in} are the measured output and input powers, P_N represents the noise power, P_{sse} is the source spontaneous emission power of the laser in the experiment.

The RSOA is operated at 25 °C with temperature controller. Measured gain and OSNR are shown in Figure 6.2. The maximum gain of the RSOA is about 28.5 dB, and the modulation region is between -10 dBm and 0 dBm. OSNR factor would be increased

by injecting more optical power. The output power of the RSOA influences the signal quality at the receiver side, the increasing power goes to the linear region from -30 dBm to -10 dBm, and nearly flat region between -10 dBm and 0 dBm. The output power which directly influences the received performance of modulation, is increased by the input power and the injected current as shown in Figure 6.2. At the same time, with a laser after amplifier, the ASE power (P_{ASE}) of RSOA is the main noise for RSOA [16]. From Figure 6.3, the ASE would be limited by increasing the input power [17, 18].

$$P_{ASE} = P_N - G \cdot P_{sse} \tag{6.2}$$

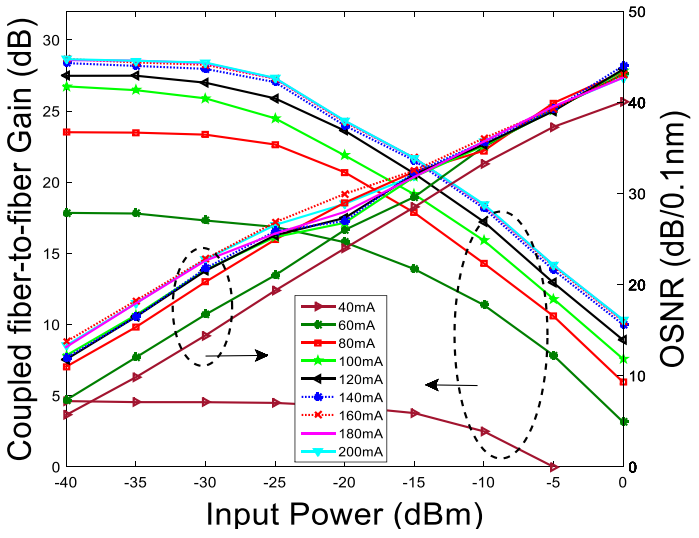

FIGURE 6.2: Measured Fiber-to-fiber Gain and OSNR against input power at different bias conditions.

Considering both the noise and output power of the RSOA, 0 dBm presents the optimal condition that minimizes the residual AM. While, for higher than 0 dBm of input power, the laser has a high consumption and it is not suitable for low cost ONU. It is because that we need the laser at ONU, and split the power both for RSOA and coherent detection at ONU for colorless ONU, all the component is required monolithic integrated chip.

As previously mentioned, when directly modulating the RSOA, the AM component would degrade the performance of DPSK detection. Hence, besides input power, we also need to select the bias current for RSOA in order to limit the tiresome AM component [21-26]. The measured output power under different bias condition is shown in Figure 6.4. Clearly, the 140 mA current is the ideal condition for phase modulation which the amplitude component would maintain the same value, and it would give a stable performance when the signal is introduced to the RSOA.

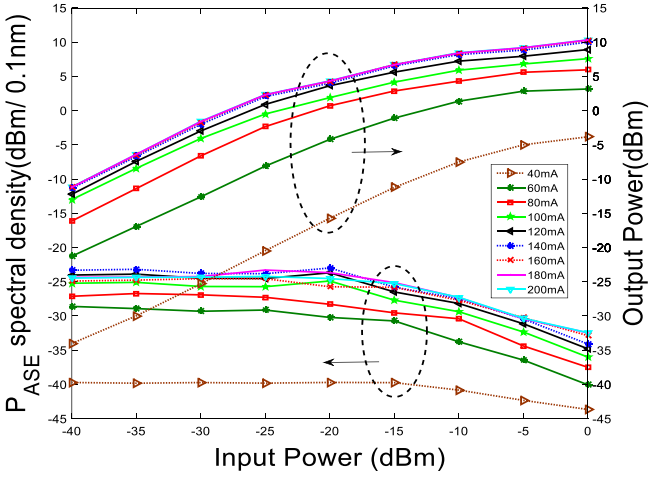

FIGURE 6.3: Measured ASE spectrum density and output power against input power at different bias conditions.

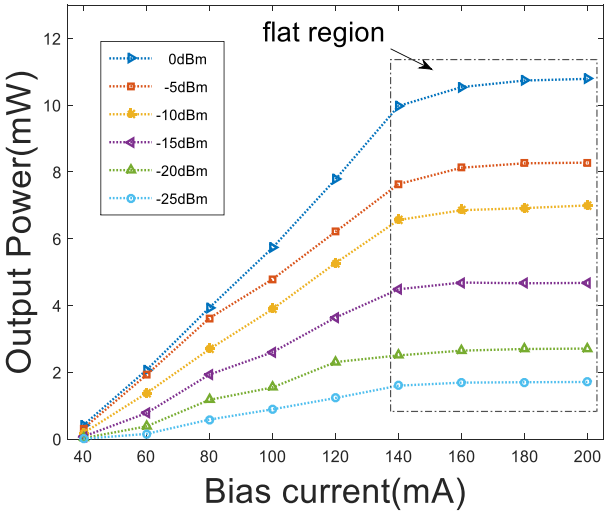

FIGURE 6.4: Measured output power against bias current at different input powers.

6.3 Principal

The architecture of the proposed ultra-dense access network is shown in Figure 6.5. The OLT consists of several UDWDM TRx coupled, and each TRx corresponds to one ONU. For the ONU, a DFB is used both for DS LO and US optical source, which represents dramatically simplified ONU. The channel spacing considered in this chapter in the UDWDM-PON is the standard 6.25 GHz and 12.5 GHz. The backscattering effects are high when the US and DS are separated in frequency by only 1 GHz [21], differently here is 1.25, 2.5, 3.75 and 5 GHz for 1.25Gb/s. In a multilevel scenario, reflections caused

by many ONUs transmitting simultaneously could reduce the performance. Hence, the isolators are added in the outputs of the DFB and the RSOA. The signal are first generated from OLT. Then, after transmission over the feeder fiber, a power splitter distributes all wavelengths to the ONUs where heterodyne detection takes the benefits of the high sensitivity and the fine selection for thewavelength. It requires no optical filtering to select thewavelength for each ONU, thus being compatible with currently deployed PON distribution networks [21]−[28].

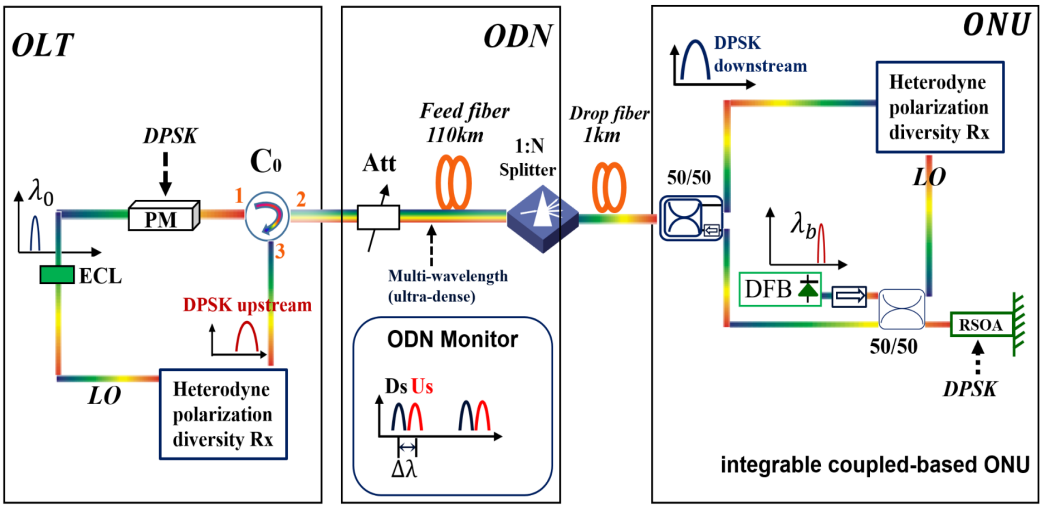

FIGURE 6.5: Bidirectional subsystem for colorless UDWDM-PON.

6.4 US unidirection performance

In order to analyze for the bidirectional transmission's performances, the low pass and high pass filters are optimized and selected for different intermediate frequency (IF), and the ESA spectra are shown in Figure 6.6. At BER=10^{-3}, the receiver sensitivity is around -46.8 dBm (1.25 Gb/s) for back to back (BtB) and -44.3 dBm for 110 km fiber transmission.

The BER performances with different IF are shown in Figure 6.7.

6.5 DS unidirection performance

The DS is a DPSK signal modulated with a phase modulator at OLT and detected with a heterodyne Rx at the ONU. The ESA spectra are shown in Figure 6.8. The BER performances with different IF are shown in Figure 6.9.

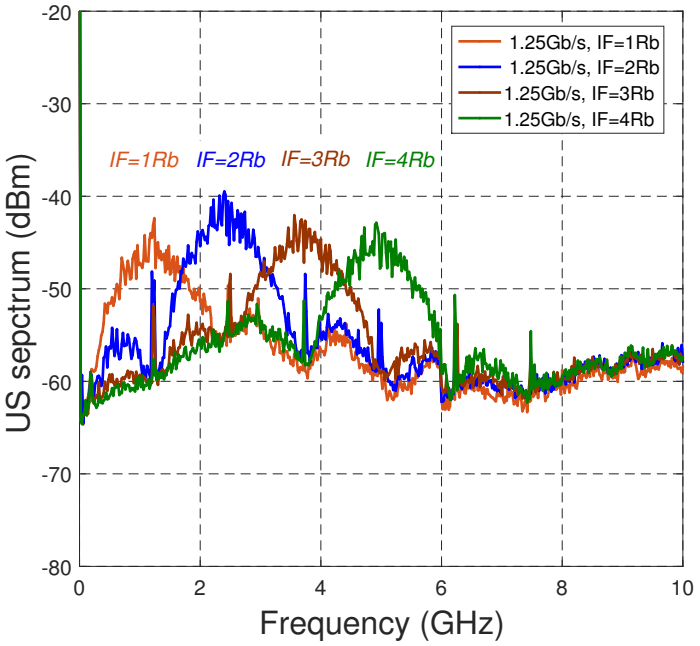

FIGURE 6.6: US heterodyne spectra from ESA with different IF.

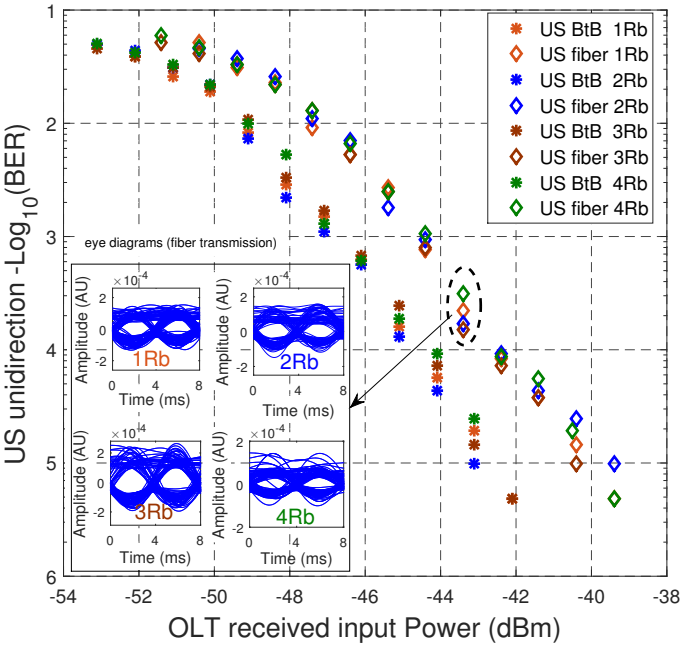

FIGURE 6.7: US BER versus received input power for BtB and fiber transmission with different IF (the insets. eye diagrams at same input power of -43.4 dBm).

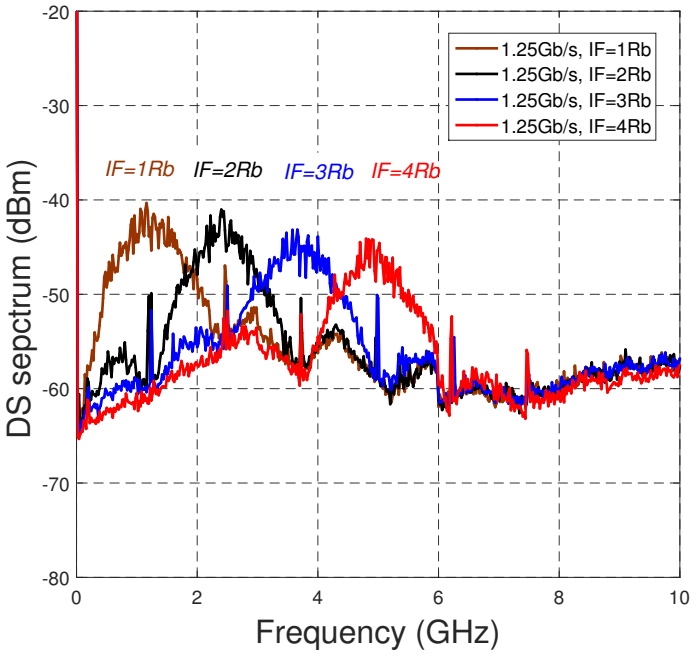

FIGURE 6.8: DS heterodyne spectra from ESA with different IF.

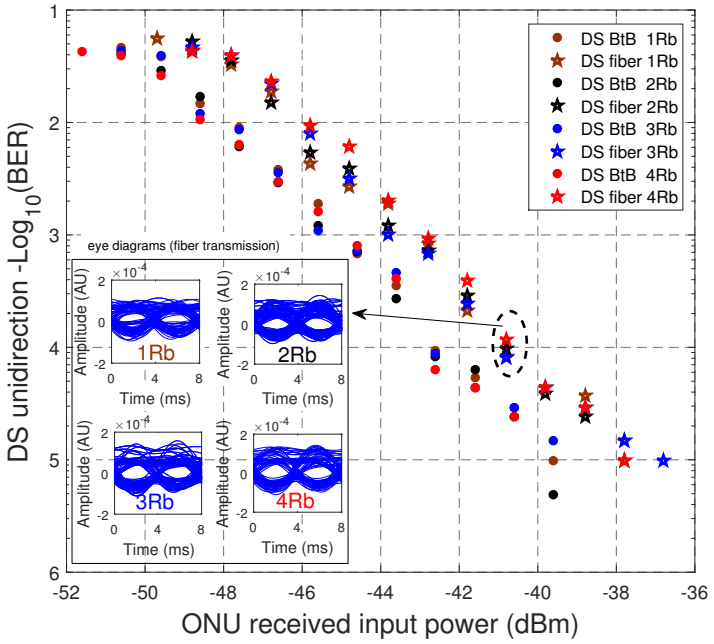

FIGURE 6.9: DS BER versus received input power for BtB and fiber transmission with different IF (the insets. eye diagrams at same input power of -40.8 dBm).

6.6 Conclusion

5G infrastructure requires the access network to be refreshed, especially the access network. Compared with the traditional 2 laser based coherent ONU, in this paper, the single-DFB based coherent ONU presents a good performance. With this simplified structure, we investigate the integrated RSOA and modulating with phase modulation instead of the traditional intensity modulation, furthermore, 1.25 and 2.5 Gb/s/user full duplex transmission with different channel spacing between uplink and downlink are measured. This is useful for further research with the optimal design. The channel spacing for the UDWDM network are also investigated and optimized in this paper. The optical distribution network power budget of this system is evaluated. Finally, the 12.5 GHz based UDWDM network are presented and tested.

We minimize the influences of residual AM component of RSOA for phase modulation via selecting the appropriate operation point according to the measured characteristics, then propose the schematics of bidirectional transmission for UDWDM-PON, finally optimize the RSOA as a phase modulator and finish the bidirectional transmission experiment at 1.25Gb/s with validating tests. Compared with channel spacing of for 2.5GHz, 3.75GHz, and 5GHz for downstream and upstream. We select the optimal channel spacing at 3.75GHz, and propose the new schematic for UDWDM-PON.

6.7 Experimental setup for lab measurement

The experimental setup in lab is shown in Figure 6.10.

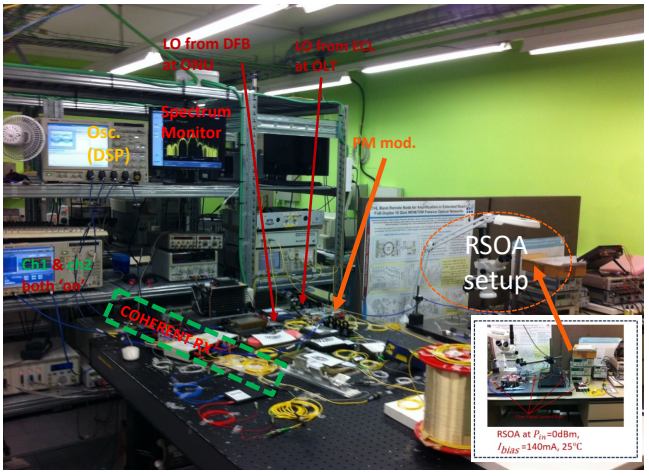

FIGURE 6.10: Experimental setup for bidirectional DPSK-DPSK transmission.

6.8 References

[1] J. Prat, I. Cano, M. Presi, I. Tomkos, D. Klonidis, G. Vall-llosera, R. Brenot, R. Pous, G. Papastergiou, A. Rafel, E. Ciaramella, Technologies for a Cost-effective udWDM-PON, IEEE/OSA J. Lightw. Technol., 2015. DOI: 10.1109/JLT.2015.2499381.

[2] Ferreira, R.M.; Reis, J.D.; Rossi, S.M.; Amado, S.B.; Guiomar, F.P.; Shahpari, A.; Oliveira, J.R.F.; Pinto, A.N.; Teixeira, A.L., "Coherent Nyquist UDWDM-PON with Digital Signal Processing in Real-Time," IEEE/OSA J. Lightw. Technol., 2015. DOI: 10.1109/JLT.2015.2493207.

[3] Shahpari, A.; Ferreira, R.M.; Guiomar, F.P.; Amado, S.B.; Ziaie, S.; Rodrigues, C.; Reis, J.D.; Pinto, A.N.; Teixeira, A.L., "Real-Time Bidirectional Coherent Nyquist UDWDM-PON Coexisting with Multiple Deployed Systems in Field-Trial," IEEE/OSA J. Lightw. Technol., 2015. DOI: 10.1109/JLT.2015.2508378.

[4] G. Y. Chu, I. Cano, V. Polo, C. Kazmierski, R. Brenot, J. Prat, Monolithically integrated dual output DEML for full duplex DPSK-ASK and DPSK-SSB ONU in ultra-dense channel spaced access network, IEEE/OSA J. Lightw. Technol., 2015. DOI: 10.1109/JLT.2015.2501289.

[5] M. Omella, I. Papagiannakis, B. Schrenk, D. Klonidis, J. A. Lazaro, A. N. Birbas, J. Kikidis, J. Prat and I. Tomkos, 10 Gb/s full duplex bidirectional transmission with RSOA-based ONU using detuned optical filtering and decision feedback equalization," Opt. Express, 17, 5008-5013 (2009).

[6] J.M. Fabrega and J. Prat, Homodyne receiver prototype with time-switching phase diversity and feedforward analog processing, Opt. Lett., 32(5), (2007).

[7] J.M. Fabrega and J. Prat, Experimental investigation of channel crosstalk in a time-switched phase diversity optical homodyne receiver, Opt. Lett., 34(4), (2009).

[8] F. Saliou, G. Simon, P. Chanclou, M. Brunero, L. Marazzi, P. Parolari, M. Martinelli, R. Brenot, A. Maho, S. Barbet, G. Gavioli, G. Parladori, S. Gebrewold, J. Leuthold, Self-seeded RSOAs WDM PON field trial for business and mobile front haul applications, Proc. OFC, M2A2, Los Angeles, (2015).

[9] J. Prat, V. Polo, P. Zakynthinos, I. Cano, J. A. Tabares, J. M. Fbrega, D. Klonidis, and I. Tomkos, Simple intradyne PSK system for UDWDM-PON, Opt. Express, vol. 20, no. 27, pp. 28758, 2012

[10] M. Presi, G. Cossu, R. Corsini, F. Bottoni, E. Ciaramella., A 1.25Gb/s low-cost coherent PON in Proc. of ECOC, London, UK, Sept. 2013, pp. 13,paper We.3.F.5.

[11] V. Sales, J. Segarra, V. Polo, and J. Prat, Statistical UDWDM-PONs Operating With ONU Lasers Under Limited Tunability, IEEE Photon. Technol. Lett., vol. 27, no. 3, 257-260, 2015.

[12] I. N. Cano, Adolfo Lern, Victor Polo, and Josep Prat, Direct Phase Modulation DFBs for Cost-Effective ONU Transmitter in udWDM PONs, IEEE Photonics Technol. Letters, vol. 26, no. 10, May, 2014

[13] Z. Al-Qazwini, M. Thollabandi, and H. Kim, Colorless optical transmitter for upstream WDM PON based on wavelength conversion, J. Lightwave Technol., vol. 31, no. 6, pp. 896-902, Mar. 2013.

[14] H. K. Shim, H. Mu, U. H. Hong, and Y. C. Chung, A Practical 10-Gb/s Ultra-dense WDM PON, Optoelectronics and Communications Conference (OECC), MR2.4, Melbourne, Austrailia, July, 2014.

[15] K. Y. Cho, U. H. Hong, A. Agata, T. Sano, Y. Horiuchi, H. Tanaka, M. Suzuki, and Y. C. Chung, "10-Gb/s, 80-km reach RSOA-based WDM PON employing QPSK signal and self-homodyne receiver," Optical Fiber Communication Conference 2012, paper OW1B, Los Angeles, USA, Mar. 2012.

[16] B. Schrenk, J.A. Lazaro, J. Prat, Employing feed-forward downstream cancellation in optical network units for 2.5G/1.25G RSOA-based and 10G/10G REAM-based passive optical networks for efficient wavelength reuse, ICTON, Azores, Portugal, Th.B3.4, July, 2009

[17] J. Prat, V. Polo, P. Zakynthinos, I. Cano, J. A. Tabares, J. M. Fbrega, D. Klonidis, and I. Tomkos, Simple intradyne PSK system for UDWDM-PON, Opt. Express, vol. 20, no. 27, pp. 28758, 2012

[18] J. Prat, M. Angelou, C. Kazmierski, R. Pous, M. Presi, A. Rafel, G. Vallosera, I. Tomkos, E. Ciaramella., Towards ultra-dense wavelength-to-the-user: The approach of the COCONUT project, in Proc. ICTON, Cartagena, Spain, Jun. 2013, pp. 14, paper Tu.C3.2

[19] B. Schrenk, F. Bonada, M. Omella, J.A. Lazaro, J. Prat, Enhanced Transmission in Long Reach WDM/TDM Passive Optical Networks by Means of Multiple Downstream Cancellation Techniques, ECOC, Vienna, Austria, We.8.5.4, 2009

[20] M. Presi, G. Cossu, R. Corsini, F. Bottoni, E. Ciaramella., A 1.25Gb/s low-cost coherent PON in Proc. of ECOC, London, UK, Sept. 2013, pp. 13,paper We.3.F.5.

[21] H. Rohde, E. Gottwald, P. Alves, C. Oliveira, I. Dedic, and T. Drenski, Digital multi-wavelength generation and real time video transmission in a coherent ultra-dense

WDM PON, presented at the Optical Fiber Communication Conf. Exhibition, Anaheim, CA, USA, 2013, Paper OM3H3.

[22] I. Cano, A. Lern, V. Polo, J. Tabares, J. Prat, Simple ONU transmitter based on direct-phase modulated DFB laser with heterodyne detection for udWDM-PON, in Proc. ECOC, 2013, paper We.2.F.4

[23] V. Polo, P. Borotau, A. Lern, J. Prat, DFB laser reallocation by thermal wavelength control for statistical udWDM in PONs, in Proc. ECOC, 2014, paper P.4.13.

[24] I. N. Cano, Adolfo Lern, Victor Polo, and Josep Prat, Direct Phase Modulation DFBs for Cost-Effective ONU Transmitter in udWDM PONs, IEEE Photonics Technol. Letters, vol. 26, no. 10, May, 2014

[25] V. Sales, J. Segarra, V. Polo, and J. Prat, Statistical UDWDM-PONs Operating With ONU Lasers Under Limited Tunability, IEEE Photon. Technol. Lett., vol. 27, no. 3, 257-260, 2015.

[26] G. Y. Chu, V. Polo, A. Lern, J. Tabares, I. N. Cano, J. Prat, 1.25-3.125 Gb/s per user PON with RSOA as phase modulator for statistical wavelength ONU, Optics Communications, vol. 357, pp. 34-40, Dec. 2015.

[27] G. Y. Chu, A. Lern, I. N. Cano, V. Polo, J. A. Tabares, J. Prat, Exploiting RSOA for Uplink Transmission with Coherent Detection for Low Cost UDWDM-PON, Proc. ACPC, AF2B.1, Shanghai, 2014.

[28] G. Y. Chu, A. Lerin, I. Cano, V. Polo, R. Brenot, C. Kazmierski, and J. Prat, Minimizing the Influences of Residual AM Component of RSOA for DPSK UDWDM-PON,, European Semicondictor Laser Workshop, SIV.3, Paris, (2014).

Chapter 7

Ultra fast λ jumping and adjustment using FML

7.1 Introduction

At present, the access networks are being improved for adapting the near future 5G public private partnership (5G-PPP)[1]. As one of the most promising candidates for next generation access networks (NGANs), long-reach ultra-dense wavelength division multiplexing passive optical networks (LRUDWDM-PON) takes the advantages of wavelength selectivity and enhanced power budget, providing the capability of high splitting ratio and compatibility with legacy infrastructure [1],[2]. Monolithic integration on InP is a way to lower footprint, cost, and consumption [3]. Recently, integrated components have been implemented for WDM-PON, and are being implemented for UDWDM-PON [4]. The ONUs for ultra-dense NGAN and latest NGPON standard are switched using thermal effect at present [1]. Traditionally, it requires 1 minute or even more time for the wavelength jumping and adjusting. Unluckily, during this time, neighbor users can be interfered. This disadvantage would seriously impact the users demand, especially on the network expected quality. Hence, Fast wavelength jumping and adjustment are quite

desirable for multi-user ONU, either for WDM-PON or for next generation UDWDM-PON. Based on these reasons, in this paper, we demonstrate for the first time the fast wavelength jumping and adjustment with an monolithically integrated Frequency Modulating Laser (FML) for coherent LRUDWDM-PON.

7.2 General concept

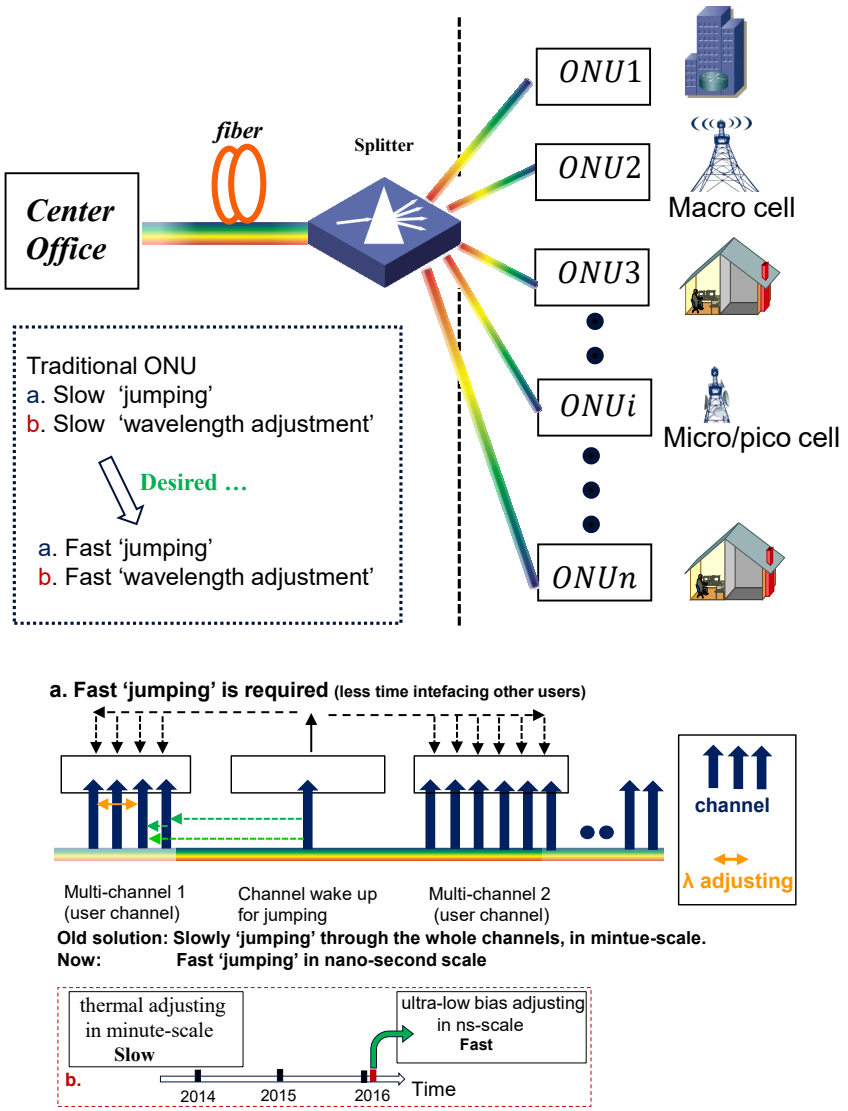

FIGURE 7.1: UDWDM-PON schematic and its challenge at ONU.

Figure 7.1 shows the high level system concept. The optical core network is divided by a power splitter. When adding a user for ultra-dense access network (UDAN), firstly the wavelength is required to be wake up in wake-up region as shown in Figure 7.1; then the wavelength need to be jumped to the desired channel; hence, this jumping must be fast enough to avoid interfacing other users. Besides, after jumping, wavelength

adjustment is also desired to be the same function like tunable laser, however tunable laser for each ONU is a high cost implementation. Hence, we propose both jumping and adjustment in nano-second scale by bias controlling. The significant benefit of the wavelength adjustment is under ultra-low bias condition (less than 7 mA), it presents temperature independence.

7.3 Characterization and assembly for FML

The FML is designed for pure frequency modulation by modulating the phase section (Ps) [5], [6]. However, unlike the frequency modulation, it is desired to be modulated by the gain section (Gs) and take the benefit of fast tuning for wavelength jumping and adjustment. The overview of the FML is shown in Figure 7.2(a) and (b), and it consists of Gs with 470 m cavity and 75 m grating phase adjustment section. In order to avoid the electro-interfacing, the space between the two sections is kept. Traditionally, the Ps is injected with DC signal and data, now in order to modulate the Gs, we put a 43 resistor in series to provide an effective matched impedance. After the assembly, the Gs shows a 3-dB bandwidth of 9 GHz. The wavelength at different bias conditions as shown in Tab. 1 and Tab. 2. There is 4.2 nm wavelength range from Igs=30 mA to Igs=130 mA as shown in Tab. 1, while for Tab. 2, with as low as 6 mA (from 1 mA to 7 mA) can adjust 1.31 nm. Unlike the Distributed Bragg reflector (DBR) laser with multi-sections [5], the FML with only two section provide enough jumping range for Ultra-dense access networks channels. The ice on the cake is, less section chip provides the possibility for lower footprint and simplified ONU with less controlled. For adjusting, the varying the bias condition of Ps can adjust the wavelength drift inside the desired channel quickly.

7.4 Proof of fast λ jumping and adjustment

Dynamic characterization of the FML is carried out using the configuration of Figure 7.3. Two types of experiments are performed, the first using a step pulse injecting Gs to measure the jumping time between two lasing wavelengths, while the second is the same except injecting Ps instead of Gs. During the wavlength jumping measurement, the Ps is kept at fixed bias condition to simplify the measurement. On the contrary, the Gs is fixed for the wavelength adjustment measurement. The resulting optical pulse output from the FML pass through an optical filter of 0.3 nm bandwidth and the rise time is measured on a sampling oscilloscope with a 20 GHz photodiode. As rise time, we refer to the time required for transition between 10% and 90% power at the desired

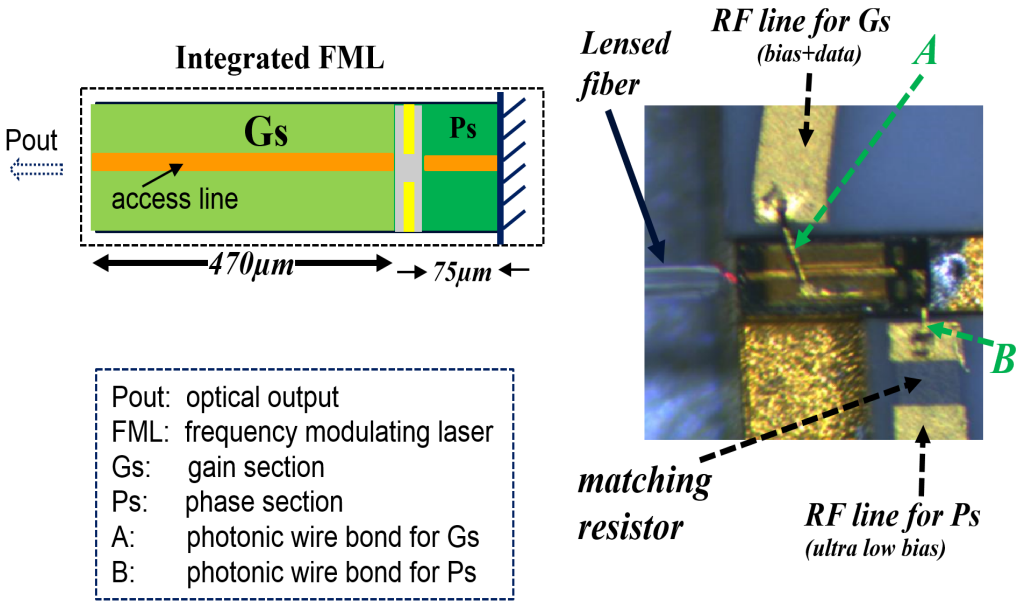

FIGURE 7.2: FML based on grating phase adjustments consists of gain and phase sections.

wavelength. The FML laser is operated at 298.15 K in pulsed mode with a 5 μs duration of switching pulse.

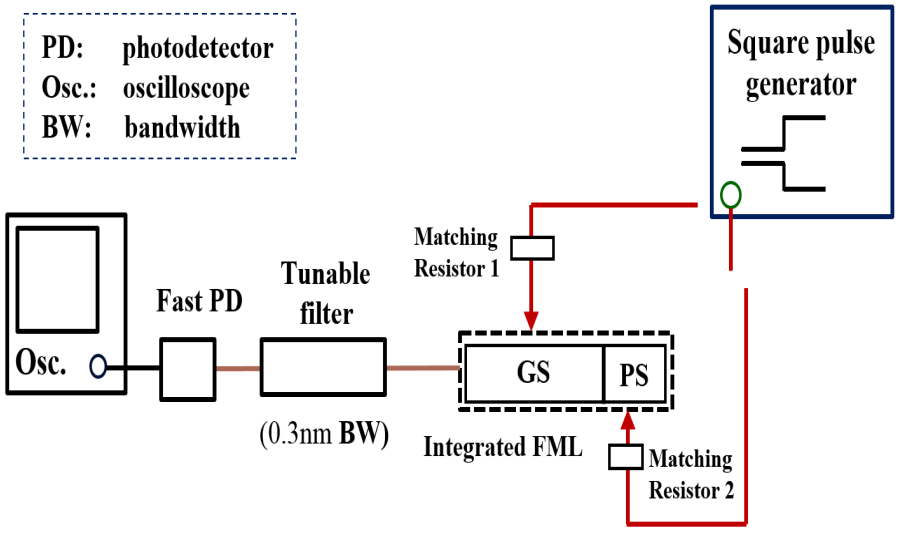

FIGURE 7.3: Experimental setup for time calculation of wavelength jumping and adjusting.

Carrier effects occur within a few nanoseconds, however a temperature change is simultaneously produced by the heat generated by the current injection. Therefore, relatively slow wavelength variations also appear like the thermal drift. The wavelength jumping time is defined as the time [7,8-12] taken for one wavelength (1) to the allowable wavelength (2).

For the wavelength jumping measurement, the bias for Ps is kept at 1 mA, and the Gs is kept at 30 mA. However the filter is set at the wavelength of 1534.24 nm, which corresponds the case of Igs=50 mA. The amplitude of the pulse is selected at Ipp=20 mA, exactly equal the difference between the two gain sections condition. The time with an allowable range, it is 2.7 ns.

The other side, for the wavelength adjustment test, the Gs is fixed at 30mA, the bias for Ps is previously set at 1 mA, and the filter is set at 1532.96 nm now. Then after introducing Ipp=4 mA of square signal, the filed wavelength is passed by the filter when the pulse at the upper level. The wavelength adjustment is applied with an ultra-low signal amplitude and ultra-low bias, which makes the thermal effects wake. here, the tuning time in 1.8 ns.

7.5 Performances

The coherent amplitude shift keying (ASK) can allow more phase noise tolerance than coherent differential phase-shift keying (DPSK) [4], which providing the possibility to detect the signal with a good stability. Here, a 5 Gb/s 2^{18} non-return-zero (NRZ) binary sequences is generated and modulate in Gs after adding matching resistor. After 110 km standard single mode fiber (SSMF) distribution, the signal is coherently detected using heterodyne detection with a single PD at the center office as shown in Figure 7.4.

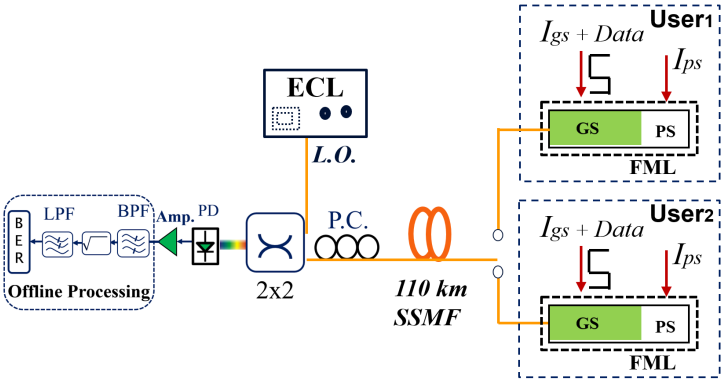

FIGURE 7.4: Integrated FML transmission experimental setup.

The Gs signal amplitude is as low as 10 mA, and as talked in previous section, the bias condition are Igs=30 mA, Ips=1 mA for $user_1$, and Igs=50 mA, Ips=1 mA for $user_2$. It corresponding the same condition of wavelength jumping. With the purpose of maintaining the injecting power into the remote node (RN) like the $user_1$, a property optical attenuator is introduced for the $user_2$.

For $user_1$, at the standard forward error correction (FEC) level11 of BER=1.2×10^{-3}, the sensitivity is -31.3 dBm (back-to-back, BtB), and -29.4 dBm (110 km). There is 1.9 dB penalty between BtB and fiber transmission as shown in Figure 7.5.

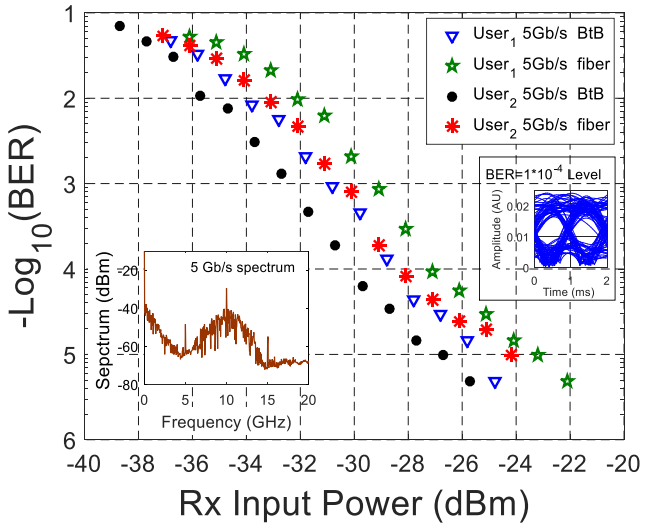

FIGURE 7.5: BER versus received input power for user$_1$ and user$_2$.

For $user_2$, the sensitivity now reaches -32.8 dBm and -30.6 dBm for BtB and 110 km fiber transmission, respectively. Compared with the $user_1$, the $user_2$ has 1.5 dB, 1.2 dB sensitivity improvement for BtB and fiber transmission, it is because that Igs=50mA for $user_2$ is near the linear region compared with Igs=30mA for $user_1$ even though they are located in different wavelengths. An eye diagram with $BER = 10^{-4}$ level is shown, and the signal spectrum from electrical spectrum analyzer (ESA) is shown in the inset of Figure 7.5. The results show the successfully validated transmission for the users located at the fast jumped channel.

7.6 Conclusions

We demonstrate an ultra-fast -tuning integrated laser, directly modulated at 5 Gb/s for UDWDM-PON. It is obviously that that reconfiguring the wavelength of the laser at ONU is slowly with temperature, the wavelengths drift by temperature would interfere other ultra-dense channels. Based on these, in this paper, wavelength jumping in ns-scale is presented, it provides much better performance than the traditional effect in minutes scale. Furthermore, after jumping the required channel, the stability of the transceiver here is provide by FMLs phase section also in ns-scale. Compared with the traditional way, it attracts more attentions.

7.7 References

[1] J. Prat, Technologies for a Cost-effective Coherent udWDM-PON, Proc. OFC, Th3I, Los Angeles (2015).

[2] D. Shea et al., Long Reach Optical Access Technologies,IEEE networks, Vol. 21, no. 5, p. 5 (2007).

[3] C. Kazmierski et al., 12.5GB Operation of a Novel Monolithic 1.55m BPSK Source Based on Prefixed Optical Phase Switching, Proc. OFC, OW4J8, Anaheim (2013).

[4] G. Y. Chu et al., First demonstration of monolithically integrated dual output DEML for full-duplex UDWDM-PON ONU, Proc. ECOC, Th1.3.1, Valencia (2015).

[5] M. Pantouvaki et al., Fast Tuneable InGaAsP DBR Laser Using Quantum-Confined Stark-Effect-Induced Refractive Index Change, IEEE J. Sel. Topics Quantum Electron., Vol.13, no. 5, p. 1112 (2007).

[6] R. Corsini et al., 1.4 mA (70 mV) Peak-to-Peak Drive of 1.25 Gb/s Frequency Modulated Laser for WDM Coherent Access Networks, Proc. OFC, M2A.22, Los Angeles (2015).

[7] R. Phelan et al., A Novel Two-Section Tunable Discrete Mode Fabry-Prot Laser Exhibiting Nanosecond Wavelength Switching, IEEE Photon. Technol. Lett., Vol. 44, no. 4, p. 331 (2008).

[8] K. Nozaki et al., Ultralow-power all-optical RAM based on nanocavities, Nat. Photon., Vol. 6, p. 248 (2012).

[9] N. Nunoya et al., Tunable Distributed Amplification (TDA-) DFB Laser with Asymmetric Structure, IEEE J. Sel. Topics Quantum Electron., Vol.17, no. 6, p. 1505 (2011).

[10] M. T. Hill et al., A fast low-power optical memory based on coupled micro-ring lasers, Nat. Vol. 432, p. 206 (2004).

[11] M. Presi et al., Ultra-dense WDM-PON 6.25 GHz spaced 8x1 Gb/s based on a simplified coherent-detection scheme, Opt. Express, Vol. 23, no. 17 (2015).

[12] G. Y. Chu, *et al.*, Monolithically integrated dual-output DEML for full duplex DPSK-ASK and DPSK-SSB ONU in ultra-dense channel spaced access network, IEEE/OSA J. Lightw. Technol., vol.34, no.8, 2016.

Chapter 8

Conclusions

Different techniques for access network have been discussed and developed in this thesis, covering a wide range of topics such as electro-optical modulation, single-laser ONU, full duplex ultra dense channel spacing network, multi-user full duplex UDWDM-PON transmission.

What remains is to draw a set of rules for photonic integrated transceiver for the end-user. Before an outlook for the future is given, a short technical conclusion is made in the following section.

8.1 Technical conclusion

Traditional UDWDM-PON requires two laser at ONU, one for DS LO, another for US optical source.

Simple devices such as the RSOAs, which provide first of all a low cost solution, have been shown to be capable for phase modulating with coherent detection. Meanwhile, unlike the DFB lasers, the RSOAs do not have the requirement of controlling the wavelength. Therefore, the RSOAs reduce the consumption. Based on this reason, the local

RSOA is optimized, analyzed, and modulated in phase instead of the traditional intensity modulation. As we have known, after characterization, the RSOA has a relationship with the polarization, hence, it is important to put a polarization independent RSOA at the ONU in order to reduce the component consumption. Finally, coupler-based ONU for full duplex DPSK-DPSK transmission with coherent PON are analyzed and the wavelength spacing for DS and US is optimized.

The monolithcally integrated DEML are first demonstrated for full duplex DPSK-ASK, and DPSK-SSB transmission, with the benefit of dual output power. The designed dual output chip serve both as DS LO, and US source.

The DEML also serves for mitigating the residual AM. By means of injecting signal into EAM, the residual AM component of phase modulating on DFB is mitigated successfully.

The FML is used for fast jumping and ultra fast wavelength adjustment for ultra dense access network.

Based on the explanation in this thesis, a last but not unimportant aspect is including DFB-SOA based elements in the ONU.

8.2 Future outlook

Looking closer at the investigation presented in the previous chapters, there are several ideas and thoughts hidden between the lines, which can be further developed.

Considering the low footprint for final users, the integrated coherent transceiver (including Tx and Rx) is required, especially with the single laser type.

Besides, the integrated laser's linewidth require to be reduced, which could provide a high possibility for multi-level modulation, such as 16 QAM using monolithically integrated photonic devices. It would be interesting for long reach PON together with an outstanding sensitivity.

Finally, the wavelength shift with more than 10 GHz by photonic devices is also desired. For avoiding the spectrum overlap between DS and US, it could be an efficient solution for single-laser based ONU with homodyne coherent detection.

Appendix A

Pulication list

A.1 Publications in International, Peer-Reviewed Journals

[1] G. Y. Chu, V. Polo, A. Lerín, J. Tabares, I. N. Cano, J. Prat, 1.25-3.125 Gb/s per user PON with RSOA as phase modulator for statistical wavelength ONU, *Optics Communications,* vol. 357, pp. 34-40, Dec., 2015.

Impact factor 2015: 1.449 (Q3 in Optics)

[2] G. Y. Chu, I. N. Cano, V. Polo, C. Kazmierski, R. Brenot, J. Prat, Monolithically integrated dual-output DEML for full duplex DPSK-ASK and DPSK-SSB ONU in ultra-dense channel spaced access network, *IEEE/OSA Journal Lightw. Techonol. (invited review),* vol. 34, no. 8, Nov., 2015.

Impact factor 2015: 2.965 (Q1 in Telecommunications, Optics, and Engineering)

[3] G. Y. Chu, I. Cano, V.Polo, J. Prat, Monolithically Integrated DEML for Mitigating Residual AM for DPSK UDWDM-PON ONU, *Submitted to Opt. Express*, Sept., 2016.

Impact factor 2015: 3.488 (Q1 in Optics)

[4] G. Y. Chu, A. Lerín, I. Cano, V. Polo, J. Prat, Coherent ONU based on 850 um Long Cavity Reflective Semiconductor Optical Amplifier for Next Generation Ultra-dense Access Network, *Submitted to Chinese Optics Letters (Minor revision)*, Sept. 2015.

Impact factor 2015: 1.851 (Q2 in Optics)

[5] G. Y. Chu, I. N. Cano, J. Prat, Demonstration on full duplex DPSK-DPSK Coherent LR-UDWDM-PON shared single-DFB based integrable ONU, *Submitted to Opt. Express*, 2016.

Impact factor 2015: 3.488 (Q1 in Optics)

[6] G. Y. Chu, V. Polo, I. Cano, J. Prat, Ultra-fast wavelength jumping and wavelength adjustment with low current using integrated FML for 110 km LRUDWDM-PON, *Submitted to Opt. Lett.*, 2016.

Impact factor 2015: 3.292 (Q1 in Optics)

[7] G. Y. Chu, et al., First demonstration and field trial of multi-user full duplex DPSK-DPSK, DPSK-DPSK with single DFB, single monolithically integrated HP-EMLSOA based LR-UDWDM-PON ONUs, *to be submitted to Journal lightwave technology*, 2016.

Impact factor 2015: 2.965 (Q1 in Telecommunications, Optics, and Engineering)

[8] G. Y. Chu, et al., 10 Gb/s EML-SOA negative chirp transmission, *to be submitted to Optics Communications*, 2016.

Impact factor 2015: 1.449 (Q3 in Optics)

A.2 Publications in Scientific Conferences

1) G. Y. Chu, V. Polo, A. Lerín, I. N. Cano, J. Prat, Optimizing Reflective Semiconductor Optical Amplifier as Phase Modulator for Low Cost Colorless ONU with 3x3 Homodyne Detection, OSA/ACP,AF2B.5, Shanghai, 2014.

2) G. Y. Chu, A. Lerín, I. N. Cano, V. Polo, J. A. Tabares, J. Prat, Exploiting RSOA for Uplink Transmission with Coherent Detection for Low Cost UDWDM-PON, OSA/ACP, AF2B.1, Shanghai, 2014.

3) G. Y. Chu, A. Lerín, I. N. Cano, V. Polo, R. Brenot, C. Kazmierski, J. Prat, Minimizing the Influences of Residual AM Component of RSOA for DPSK UDWDM-PON, European Semiconductor Laser Workshop, SIV3, Paris, 2014.

4) G. Y. Chu, I. N. Cano, C. Kazmierski, R. Brenot, J. Prat, First demonstration of monolithically integrated dual output DEML for full-duplex UDWDM-PON ONU, IEEE ECOC, Th.1.3.1, Valencia, 2015.

5) I. Cano, A. Lerín, G. Y. Chu, V. Polo, J. Prat, Performance comparison between direct phase modulated DFB and RSOA for cost effective user transmitter in udWDM-PONs, IEEE ICTON, Budapest, Mo.D2.2, 2015.

6) A. Lerín, G. Y. Chu, V. Polo, I. Cano, J. Prat, Chip Integrated DFB-EAM for Directly Phase Modulation Performance Improvement in UDWDM-PON, IEEE ECOC, P.7.10, Valencia, 2015.

Biography

Guang Yong Chu was born in China, in 1986. He holds the MSc (2012) in Optical Engnieering in Zhengzhou University (ZZU), Henan, China.

The work presented in this Ph.D. thesis was performed from Oct. 2012 to Jan. 2016 at the Department of Signal Theory and Communications at the Polytechnic University of Catalonia (UPC) in Barcelona, Spain. The research topics cover a wide range of novel techniques for optical network units in high data rate Fiber-to-the-Home applications and their impact on the overall transmission performance within long-reach and highsplit access networks. The work was carried out within the European Union FP7 ICT COCONUT project, China Scholarship Council fellowship, and Spanish Ministry of Science and Innovation ROMULA project.